Zentime

Perioperative Precision Medicine

Volume 2, Number 3; Sept. 30, 2024

ISSN: 2957-5443
Editor-in-Chief: Lize Xiong
Published by ZENTIME PUBLISHING CORPORATION

Perioperative Precision Medicine
ISSN: 2957-5443

Zentime

Review Article https://doi.org/10.61189/313377zqjuff

Progress in heatstroke-induced multiple organ damage

Ruilong Li[1,2*], Dezhi Guo[1,2*], Tianying Li[1,2], Panpan Hu[1,3], Tianying Xu[1]

[1]Department of Anesthetic Pharmacology, School of Anesthesiology, Second Military Medical University/Naval Medical University, Shanghai 200433, China. [2]College of Basic Medicine, Second Military Medical University/Naval Medical University, Shanghai 200433, China. [3]National Key Laboratory of Immunity & Inflammation, Second Military Medical University/Naval Medical University, Shanghai 200433, China.
[*]The authors contribute equally.

Corresponding authors: Tianying Xu and Panpan Hu.

Acknowledgement: This work was supported by the Basic Medical Research Fund of Naval Medical University (2023QN034). The authors would like to thank all the guest editors and anonymous reviewers for their constructive comments.

Received January 23, 2024; Accepted April 29, 2024; Published September 30, 2024

Highlights

- Patients with heatstroke often suffer from multiple organ dysfunction and have a high fatality rate.
- The molecular mechanisms underlying multiple organ damage in heatstroke are complex.
- This review outlines the manifestations of multiple organ dysfunction caused by heatstroke and explores the possible molecular mechanisms involved.

Abstract

Heatstroke is a life-threatening acute condition characterized by dysregulated temperature control, resulting in high core temperature and multi-organ dysfunction. Despite extensive research, the molecular mechanisms underlying heatstroke-induced organ damage have not been fully elucidated. This review aims to summarize recent advancements in the field of heatstroke, focusing on etiological factors, organ damage, and molecular mechanisms. By exploring the intricate interplay between heat-related cytotoxicity, inflammatory response, and tissue dysfunction, this review offers insights for future research and clinical practice in managing heatstroke patients. Further investigations are warranted to elucidate the specific mechanisms of organ damage and improve treatment strategies for heatstroke.

Keywords: Heatstroke, organ damage, molecular mechanisms

Introduction

Heatstroke is a heat-related disease characterized by hyperthermia (core body temperature greater than 40 °C) and delirium [1]. It can be classified into exertional heatstroke (EHS), caused by excessive heat production during physical activity in hot and humid environments, and classic heatstroke, more prevalent in the elderly or those with underlying health conditions affecting heat dissipation [2]. Heatstroke often leads to multiple organ dysfunction, initially impacting the cardiovascular system, followed by the central nervous, digestive, urinary, and respiratory systems [3]. To maintain a relatively stable body temperature and prevent heatstroke, the human body primarily relies on the hypothalamus, which receives heat information from sensors in the skin, spinal cord, and internal organs. The hypothalamus regulates heat production and dissipation accordingly. Additionally, it is crucial to avoid excessively high environmental temperatures, as they can directly damage cells, induce oxidative stress, and compromise cell membrane stability, ultimately contributing to multiple organ dysfunction. Epidemiological data indicate an increasing incidence of heatstroke, exacerbated by extreme heatwaves and climate change [4, 5]. In short, heatstroke can occur when the body's temperature regulation function is im-

Address correspondence to: Tianying Xu, Department of Anesthetic Pharmacology, School of Anesthesiology, Second Military Medical University/Naval Medical University, 800 Xiangyin Road, Shanghai 200433, China. Tel: +86 021 81872029, E-mail: xutianying@smmu.edu.cn; **Panpan Hu**, Department of Anesthetic Pharmacology, School of Anesthesiology, National Key Laboratory of Immunity & Inflammation, Second Military Medical University/Naval Medical University, 800 Xiangyin Road, Shanghai 200433, China. Tel: +86 021 81872029, E-mail: hpp510@smmu.edu.cn.

paired or when environmental temperatures are excessively high, affecting various bodily systems.

Etiological and risk factors for the occurrence of heatstroke

Heat imbalance

Heat imbalance is a key pathogenic mechanism of heatstroke, characterized by excessive heat production and limited heat dissipation in the body. Risk factors include high ambient temperatures, food intake, fever elevate metabolic heat production in a resting state, etc. Additionally, increased heart rate and pulmonary ventilation raise energy demands, further augmenting metabolic heat production. Skeletal muscles primarily contribute to the elevated basal metabolic rate [6]. During intense physical activity, skeletal muscle excitation-contraction coupling sharply increases the rate of metabolic heat production, reaching levels up to 15-20 times higher than at rest [7].

The excitation-contraction coupling mechanism of skeletal muscles proceeds as follows: Action potentials propagate along the sarcolemma and T-tubules, activating L-type calcium channels on the sarcolemma [8]. This activation induces a conformational change, opening calcium release channels in the sarcoplasmic reticulum, allowing calcium ions to be released into the cytoplasm along the concentration gradient [8]. The increased cytoplasmic calcium concentration initiates muscle contraction through binding to muscle calcium-binding protein C [9]. Subsequently, the majority of cytoplasmic calcium ions are recaptured into the sarcoplasmic reticulum via the activated calcium pump in the sarcolemma [10]. Both muscle contraction and calcium reuptake by the pump require ATP for energy supply. Skeletal muscle contraction consumes approximately 20% of metabolic energy, with the remaining 80% released as heat, contributing to excessive heat production. Elevated heat from excessive production can promote the leakage of calcium ions from the sarcoplasmic reticulum, further enhancing skeletal muscle metabolic heat production and potentially triggering heatstroke [11].

When body temperature rises, a cascade of pathophysiological responses occurs to maintain normothermia. This includes an increase in heart rate and cardiac output. Simultaneously, there is a redistribution of circulatory blood volume, with decreased flow to internal organs like the intestines and kidneys, and increased flow to the skin, reaching up to 50% of cardiac output. Heat carried by the bloodstream to the skin prompts vasodilation of skin blood vessels, while sweat glands actively secrete sweat to facilitate heat dissipation [12]. Dysregulation in sweat gland function can reduce overall sweat rate, significantly impairing the body's ability to dissipate heat.

When skin temperature exceeds ambient temperature, the body can still dissipate heat effectively through dry mechanisms like conduction and convection. However, when ambient temperature equals or exceeds skin temperature, evaporation becomes the primary heat loss avenue. In humans, evaporative heat dissipation occurs primarily through the conversion of sweat, secreted by skin sweat glands, into a gaseous state. Approximately 580 kcal of heat can be carried away per liter of evaporated sweat. Excessive evaporation leading to significant sweat loss may reduce blood volume, particularly organ blood flow, diminishing heat transport to the skin via circulation. This can rapidly elevate core body temperature, ultimately culminating in heatstroke. Moreover, in humid environments that hinder evaporation, sweat may accumulate on the skin surface, compromising the evaporative heat dissipation pathway and increasing heatstroke risk.

Heat adaptation disorder

Heat adaptation is a physiological phenomenon widely observed in mammals [13]. It refers to the adaptive response of individuals residing in hot environments for extended periods to heat exposure. Compared to individuals exposed to high temperatures for shorter durations, those living in such environments long-term typically exhibit increased heat tolerance. For instance, protein-carbohydrate supplementation during a 5-day training period enhanced plasma volume expansion and thermoregulatory adaptation, thereby reducing heat and cardiovascular strain in young men [14]. It is indicated that heat adaptation is closely associated with genetic factors, potentially involving enhanced physiological functions facilitated by heat-tolerant genes or their products [15]. These functions play a significant role in maintaining cell membrane stability under conditions of elevated temperatures [15].

Under normal physiological conditions, the interaction between environmental temperature and signals transmitted from effector organs to the hypothalamic temperature regulation center, along with changes in the number and excitation levels of thermo-sensitive neurons, lowers the threshold for heat dissipation by or-

gans and raises the threshold for heat damage. This broadens the adaptive range of dynamic body temperature regulation [15]. Clinical signs of heat adaptation include a lower core temperature, decreased heart rate, and increased sweating responses during activities in high temperatures. While repeated elevation of core temperature is recognized as a primary stimulus for promoting heat adaptation, recent years have brought debate over the optimal method to induce such adaptation [16]. It is important to note that individuals lacking heat adaptation capability are more susceptible to heatstroke, thus facing an increased risk of heat stress.

Preexisting diseases diminish heat tolerance

The "multiple hit hypothesis" suggests that the immune system, once "primed" by initial stimuli such as mild diseases, infections, skin allergies, or blisters, becomes more susceptible to subsequent impacts of exercise-induced heat stress [17]. There is substantial evidence supporting this hypothesis. For example, an experiment with rats injected with lipopolysaccharide from Salmonella enteritidis, a gram-negative bacterial cell wall product triggering a reaction similar to that induced by live bacteria, showed a rapid increase in body temperature at a lower heat exposure temperature compared to rats injected with isosmotic saline without a heat source [18]. This suggests that concurrent or pre-existing inflammation or infection may increase the risk of heatstroke. In addition, these preexisting conditions can exacerbate the progression of heatstroke, leading to increased mortality. An in vitro experiment demonstrated that pretreatment with tumor necrosis factor (TNF) and interferon (IFN) can enhance the heat stress-induced death of microvascular endothelial cells [19].

In a study where participants engaged in brisk walking in high temperatures for four consecutive days and developed mild cellulitis due to foot blisters on the third day, their core temperature was higher despite maintaining the same exercise intensity and duration as on the other days [20]. Moreover, the research indicates that mild diseases or inflammation can increase susceptibility to heat injury or hyperthermia in both soldiers and volunteers [20]. Animal studies further support this, suggesting that mice with a prior history of disease, even if showing no overt clinical symptoms during heat exposure, experience increased severity of heatstroke [21].

Genetics and epigenetics alterations

Current research highlights EHS as a potentially life-threatening condition with long-term epigenetic implications observed in female mice. These studies suggest that EHS can induce epigenetic changes in monocytes, enhancing the production of robust immune cells characterized by altered heat shock protein (HSP) responses and immunosuppression [22].

Additionally, epigenetics plays a critical role in regulating cellular heat adaptation, involving chromatin remodeling, particularly through post-transcriptional modifications of histones H3 and H4, such as phosphorylation and acetylation. During the consolidation phase of heat adaptation "memory," short-term heat stress triggers phosphorylation of histone H3, crucial for heat shock factor (HSF)1 binding to heat shock elements and subsequent transcription of HSPs like HSP70, irrespective of H3 acetylation status. The heat adaptation phenotype is characterized by abundant reserves of HSP72 and HSP90, with HSP90 playing a pivotal role in regulating various proteins, including facilitating HIF-1α nuclear translocation. Studies have indicated involvement of histone expression changes in the H1 cluster, multiple microRNAs, and other epigenetic markers in this process [15].

The susceptible gene ryanodine receptor (RyR) may play a role in the pathogenesis of heatstroke. Type 1 RyR (RyR1) serves as a calcium release channel in skeletal muscle, and mutations in RyR1 can lead to channel overactivation, triggering malignant hyperthermia (MH). RyR1 selective inhibitors, such as the oxyquinoline acid derivative (Compound 1), have shown potential in rescuing animals from EHS-induced heat stress [23]. Moreover, MH-related mutations in the RyR1 gene have been reported in some cases of heatstroke [24]. Research indicates that at high temperatures (41 °C), calsequestrin-1 undergoes oligomerization, reducing its interaction with RyR1/2 and increasing RyR2 activity in ventricular muscle [25]. This regulation affects calcium release from ventricular muscle cells, influencing MH and arrhythmias induced by environmental heatstroke [25]. Therefore, variations in RyR genes may contribute to heatstroke pathogenesis.

EHS has been linked to specific gene mutations, particularly those at the g.31829044 locus of the HSPA1B gene. HSPA1B, a subtype of HSP72, is highly induced and promotes positive heat adaptation and cellular responses during exercise [26]. Participants with a history of EHS and heat tolerance often possess the AG genotype at the HSPA1B single nucleotide

polymorphism g.31829044 locus, suggesting it may serve as a protective marker against heat stress [27]. Animal studies have shown a positive correlation between HSPA1B expression and primate heat stress severity [28]. Additionally, HSPA1B expression is upregulated in individuals with a history of EHS [29]. However, due to limited current evidence, further research is necessary to elucidate the functional role of the HSPA1B single nucleotide polymorphism in the HSPA1B gene and its impact on heatstroke.

Manifestations of organic injury in heatstroke

Central nervous system injury

Neurological injury is a frequent and serious outcome of heatstroke, especially in cases of sudden exposure to high temperatures. Cooling interventions typically result in substantial neurological improvement in 70% to 90% of heatstroke patients. However, those who do not regain consciousness after cooling or initial treatment often develop seizures or focal motor disorders. Histological examinations of the central nervous system in heatstroke patients reveal notable injuries such as white matter demyelination, significant reduction in Purkinje cells, and progressive degeneration of cortical neurons [30]. Autopsy findings commonly show congestion, edema, and microhemorrhages alongside these histopathological changes [31].

Animal models of heatstroke demonstrate increased intracranial pressure and decreased arterial blood pressure, leading to reduced cerebral perfusion pressure [32]. Heatstroke-induced intracranial hypertension may be attributed to cerebral edema, and lowering cerebral perfusion pressure below the self-regulating threshold can result in cerebral ischemia and neuronal damage in affected animals. Studies have investigated the survival of cortical and hippocampal neurons under high temperature conditions, as well as their effects on DNA degradation and nuclear morphology, highlighting the critical role of cell culture duration in heat stress-induced necrosis or apoptosis [33]. Neuronal damage due to high temperatures involves endoplasmic reticulum stress, nuclear damage, and cytoskeletal damage from protein denaturation [34]. Neurons show significant activation within 24 hours of heat stress, leading to apoptosis, indicating that the impact of high temperatures is not only irreversible but also persists beyond the cessation of heat stress.

Clinically, some patients develop trunk ataxia, orientation disorders, and weakness following heatstroke. Brain diffusion-weighted magnetic resonance imaging reveals high signal intensity and decreased apparent diffusion coefficient values in the bilateral cerebellar hemispheres and globus pallidus [35]. Dysfunction in the globus pallidus contributes to disorientation and malaise, while dysfunction in the cerebellar hemispheres leads to trunk ataxia [36, 37]. Elevated temperatures can damage the anterior and lateral horns of the spinal cord, resulting in quadriplegia and degeneration of Purkinje cells in the cerebellum. During heatstroke, increased release of catecholamines, particularly dopamine, serotonin, and interleukin-1β (IL-1β), contributes to neuronal degeneration and necrosis, accompanied by significant down-regulation of γ-aminobutyric acid B receptors and inhibition of the high-affinity γ-aminobutyric acid uptake system [38]. Studies have shown that high temperatures adversely affect the autonomic nervous system, impacting axonal conduction and synaptic transmission velocity, particularly in laryngeal reflexes and sudden infant death [34].

Rhabdomyolysis (RM)

RM is characterized by the breakdown of muscle fibers, often triggered by high temperatures. The incidence of RM due to hyperthermia ranges from 4% to 8%. Evidence suggests that individuals with a predominance of type II muscle fibers are not only at higher risk of RM but also more prone to EHS [39].

Following RM, activated neutrophils are the first responders to the site of muscle damage, where they clear cellular debris. Subsequently, monocytes migrate to the inflamed area and differentiate into macrophages, which possess superior phagocytic capabilities compared to neutrophils within days or weeks, becoming the primary phagocytes. Both neutrophils and macrophages contribute to tissue degradation by releasing reactive oxygen and nitrogen species, exacerbating injury, increasing membrane permeability, and facilitating the release of intracellular proteins (such as myoglobin and creatine kinase) into the systemic circulation. Additionally, damaged muscle fibers, leukocytes, and other resident inflammatory cells contribute to cytokine production at the injury site. The substantial release of free radicals and intracellular toxic substances is a crucial factor contributing to the systemic inflammatory response (**Figure 1**).

Myoglobin released from RM can be cleaved into myosin, which plays a critical role in the coagulation cascade, including factors involved in both coagulation and fibrinolysis [40]. Post-RM,

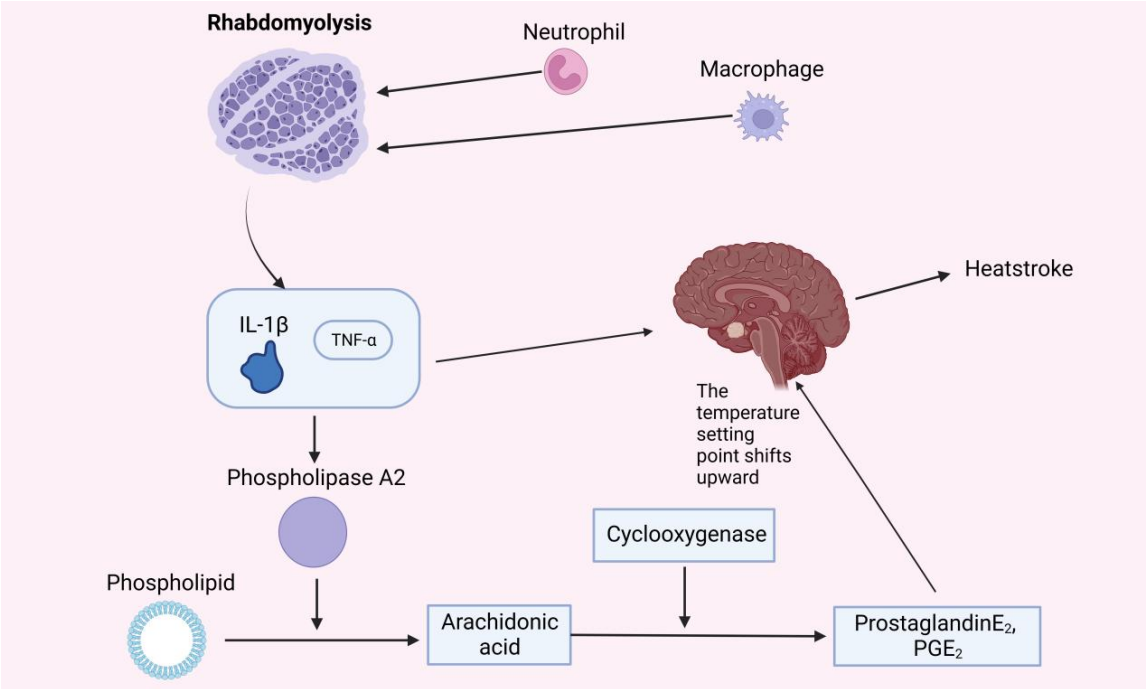

Figure 1. Rhabdomyolysis exacerbates the occurrence of heatstroke. After rhabdomyolysis, neutrophils and macrophages will sequentially reach the damaged area, exacerbating the damage, and helping the production of pro-inflammatory cytokines at the damaged site, including interleukin-1β and tumor necrosis factor-α. These inflammatory factors can directly act on the hypothalamic temperature regulation center to produce a fever response after entering the blood, or promote the release of phospholipase A2. Phospholipase A2 can cleave membrane phospholipids, release arachidonic acid, and generate PGE_2 under the action of cyclooxygenase. PGE_2 can increase the set point of body temperature, thus exacerbating the development of heatstroke. IL-1β, interleukin 1β; TNF-α, tumor necrosis factor α; PGE_2, Prostaglandin E_2.

there is a significant influx of sodium and potassium ions, leading to blood hyperconcentration and an increased thrombotic risk. Furthermore, the release of nuclear proteins (such as histone 3 and high-mobility group protein B1) from damaged muscle cells activates platelets, contributing to disseminated intravascular coagulation. Pro-inflammatory cytokines like IL-1β, TNF-α, and IFN-α enter the bloodstream, mediating the febrile response via the hypothalamic temperature regulation center. These cytokines also stimulate phospholipase A2, which cleaves membrane phospholipids to release arachidonic acid. Arachidonic acid is converted to prostaglandin E_2 (PGE_2) by cyclooxygenase, increasing the body's temperature set point and leading to fever, ultimately contributing to heatstroke [41].

Several studies have investigated ultrastructural changes in muscle tissue following EHS [42]. Imaging has shown rupture of the outer mitochondrial membrane, loss of cristae, and an increase in markers of cell ferroptosis, such as malondialdehyde, 12-hydroxyeicosatetraenoic acid, and prostaglandin endoperoxide synthase 2. Ferroptosis, characterized by iron-dependent lipid peroxidation and specific mitochondrial alterations, is considered a crucial pathway of cell death in RM post-EHS [43]. The mechanism involves EHS-induced Yes-associated protein upregulating ACSL4 through TEAD1/TEAD4, promoting lipid peroxidation and subsequent ferroptosis of skeletal muscle cells, contributing to muscle cell loss and subsequent RM [43].

Intestinal barrier dysfunction

Studies indicate that, while high temperatures can induce heatstroke, the primary driving force for the progression of heatstroke is the systemic inflammatory response mediated by various cytokines [44]. The gut is recognized as the body's largest reservoir of bacteria and toxins. When enteric microbial products, such as endotoxin, flagellin, and bacterial DNA, enter the bloodstream, they trigger the production of numerous cytokines, including PGE_2, TNF-α, IL-1β, IL-6, and IFN-γ [45]. This cascade of events ultimately results in a systemic inflammatory response, leading to disseminated intravascular coagulation, multiple organ failure, and other critical conditions. In scenarios where high temperatures lead to a sustained elevation in core body temperature, blood flow is redirected to the skin and active skeletal muscles, consequently diminishing blood flow to internal organs. This redirection reduces the transfer of heat from internal organs to the skin, allowing

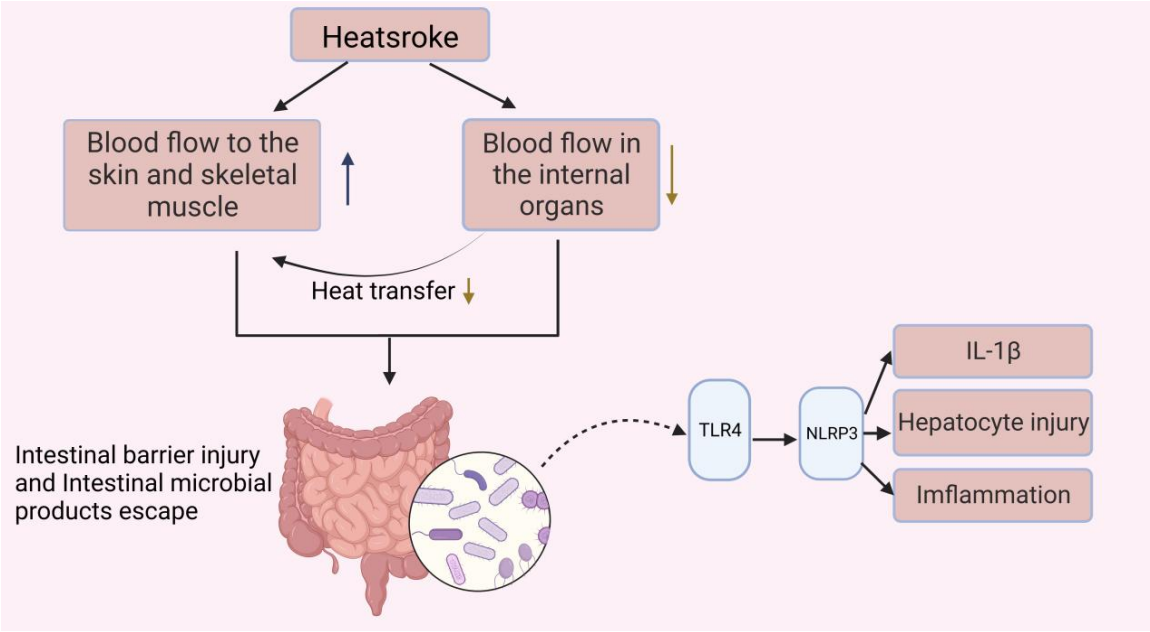

Figure 2. The impact of high temperature on intestinal barrier dysfunction. In cases of a continuous rise in core temperature due to elevated external temperatures, blood preferentially flows to the skin and active skeletal muscles, consequently diminishing blood flow to internal organs. As a result, the heat transferred from internal organs to the skin is also reduced, triggering a rapid increase in core temperature and leading to organ dysfunction, including intestinal ischemia. This sequence of events results in tissue hypoxia, acidosis, and damage to the intestinal barrier, facilitating the escape of microbial products from the intestine. These products then interact with Toll-like receptor 4, activating the inflammasome and further promoting the release of IL-1β, liver cell apoptosis, and sterile inflammation. TLR4, Toll-like receptor 4; NLRP3, NOD-like receptor family pyrin domain containing 3; IL-1β, interleukin 1β.

for a rapid increase in core temperature. Such an escalation may result in dysfunction of vital organs, including intestinal ischemia and liver cell injury. Intestinal ischemia fosters tissue hypoxia, acidosis, and a sequence of alterations disrupting the structure and function of the intestinal mucosa, ultimately increasing intestinal permeability [46]. Additionally, cell culture experiments have demonstrated that even a slight elevation in ambient temperature (1.3 °C) can swiftly and transiently alter the integrity of the intestinal epithelial barrier, a change that persists for up to 24 hours [47].

The gut barrier serves as both a physical and biochemical defense, crucial for preventing commensals and pathogens from crossing into the bloodstream [48]. High temperatures can compromise this barrier, allowing intestinal microbial products to escape and bind to Toll-like receptors (TLRs). TLRs play a key role in immune signaling by recognizing pathogen-associated molecular patterns. Interaction between TLR4 and advanced glycation end products activates the NOD-like receptor family pyrin domain containing 3 (NLRP3) inflammasome, triggering the release of IL-1β, liver cell apoptosis, and sterile inflammation (**Figure 2**) [49]. This cascade leads to functional liver cell loss, impairing the liver's ability to clear endotoxins from the body [50]. Consequently, inhibiting gut microbial translocation becomes challenging, perpetuating elevated body temperature.

The liver's reticuloendothelial system, comprising monocytes, macrophages, and Kupffer cells, monitors pathogens, activates the complement cascade, locally produces PGE_2, and transmits this signal to the hypothalamic ventral preoptic area via the vagus nerve. This process induces norepinephrine production, alters preoptic PGE_2 levels, and reduces the firing rate of temperature-sensitive neurons, disrupting temperature regulation, heat dissipation, and further elevating core body temperature [51]. Research exploring bovine colostrum, rich in growth factors, suggests it may modulate these responses. Studies indicate colostrum can mitigate temperature-induced increases in Baxα and decreases in Bcl-2 levels, potentially enhancing exercise performance and reducing heatstroke risk [52].

Recent research has highlighted the pivotal role of CCAAT enhancer binding protein homologous protein (CHOP) in mediating heatstroke-induced cell apoptosis and barrier dysfunction in intestinal epithelial cells by regulating the expression of Bcl-2 and Bax [53]. Studies indicate that 4-phenylbutyrate can effectively modulate this process by inhibiting the PERK-CHOP pathway, thereby decreasing the levels of pro-apoptotic

Bax and increasing anti-apoptotic Bcl-2 proteins [53]. This intervention has shown promise in reducing cellular morphological changes and apoptosis induced by heatstroke, suggesting potential utility for 4-phenylbutyrate as a therapeutic approach in managing heatstroke [53]. Furthermore, recent findings suggest that intestinal microbes can bypass the liver and enter the systemic circulation through the mesenteric lymph nodes [54]. Once in circulation, microbial products encounter various host defense mechanisms, including binding by natural antibodies such as immunoglobulin G and M, leukocyte granule proteins like lactoferrin and lysozyme, and interactions with high-density lipoproteins [55]. These pathways help neutralize microbial products, mitigate excessive cytokine production, and potentially delay the progression of heatstroke.

In summary, the liver's detoxification function and the presence of immune antibodies in the systemic circulation are two crucial mechanisms for detoxifying gastrointestinal microbial products in humans. However, these mechanisms become impaired at core body temperatures exceeding 41-42 °C, exacerbated by strenuous exercise. Consequently, excessive heat production during exercise compromises both detoxification processes, allowing pathogen-associated molecular patterns in the gastrointestinal tract to bind to TLRs on cell membranes, triggering the transcription of activator protein-1 and nuclear factor kappa-B (NF-κB) [12, 56]. This leads to heightened production of pro-inflammatory mediators including PGE_2, TNF-α, IL-1β, IL-6, IFN-γ, and acute-phase C-reactive protein [45]. This inflammatory cascade perpetuates a positive feedback loop, driving continuous microbial product and cytokine production, which activates systemic inflammation. This inflammatory response is a key driver of disseminated coagulation, tissue necrosis, and organ failure, ultimately precipitating conditions conducive to sepsis and potentially fatal shock.

Cardiovascular system disorders

Cardiovascular diseases remain the leading cause of morbidity and mortality in the developed world, accounting for over 30% of deaths in the United States. Several studies have demonstrated a significant correlation between high temperatures and cardiovascular mortality, arrhythmias, sudden cardiac arrest, and the incidence of coronary heart disease [57]. High temperatures can increase myocardial oxygen consumption, potentially leading to fatal arrhythmias, with sinus tachycardia being the most common [57]. Sinus tachycardia promotes heat dissipation by increasing cardiac output. Additionally, high adrenaline stress due to elevated temperatures can trigger myocardiopathy and even result in circulatory failure or death [58]. High temperatures can also induce microcirculatory disorders, primarily due to increased expression of endothelial damage biomarkers (such as von Willebrand Factor and thrombomodulin), elevated release of cell adhesion molecules (such as ICAM-1), and an imbalance in the release of vasoactive substances involved in regulating local vascular relaxation and contraction (such as NO and endothelin). These changes can lead to tissue edema, damage to organ vascular endothelial cells, microthrombosis, extensive hemorrhage, and necrosis, causing heatstroke and multiple organ damage [59]. Specifically, patients with EHS exhibit a higher incidence of cardiovascular disease, myocardial infarction, ischemic heart disease, and acute ischemic stroke as early as 14 years following the initial heatstroke event [60].

Calcium Calsequestrins are expressed in the heart and regulate heart rate by controlling Ca^{2+} release from the sarcoplasmic reticulum. Heat stress can induce arrhythmias in rats by causing calsequestrin-1 oligomerization, which alleviates its inhibitory effect on RyR -2-mediated Ca^{2+} release. Additionally, calsequestrin-1 deficiency can independently lead to MH and EHS-like ventricular arrhythmias, revealing a new genetic mechanism for arrhythmias and MH/EHS arrhythmic occurrences [25].

Platelet damage

Heatstroke is often accompanied by coagulation disorders, with the incidence of disseminated intravascular coagulation reported to be as high as 48% [61]. The mechanisms of platelet damage caused by heatstroke may include the following:

1. Apoptosis mechanism triggered by high fever: High temperatures can directly damage platelets by inducing their apoptosis.

2. Inflammatory mediators causing platelet damage: Different inflammatory mediators can damage platelets through various pathways, primarily by activating platelets to release proteins and small molecules, inducing platelet apoptosis and necrosis.

3. Damage by reactive oxygen species (ROS): Due to ischemia and hypoxia in heatstroke patients, neutrophils are activated, leading to a respiratory burst and the production of a large

amount of ROS under the catalysis of reduced nicotinamide adenine dinucleotide.

4. Effects of vascular endothelial damage on platelets: Substances released by vascular endothelial cells can cause platelet aggregation and adhesion [62].

5. Direct activation of platelets by heat: Heat can directly promote platelet aggregation. Excessive aggregation caused by high temperatures can lead to platelet damage [63]. The specific pathway may involve elevated extracellular high mobility group box protein 1 (HMGB1) inducing high levels of ROS through platelet TLR4 and receptor for advanced glycation end product (RAGE), thereby participating in the activation of the NLRP3 inflammasome, resulting in platelet reduction during heatstroke [64].

The reduction in platelets and the release of inflammatory mediators and cytokines further damage vascular endothelial cells, promote coagulation reactions, form thrombi, block organ perfusion, and create a vicious cycle, leading to multiple organ dysfunction syndrome.

Liver function failure

The liver is the main organ involved in the production and response to cytokines during inflammation. In recent years, examinations of heatstroke patients have revealed that widened liver lymphocyte gap, thinner or spherical microvilli liver cells, and increased levels of enzymes such as glutamic pyruvic transaminase and lactate dehydrogenase, which are indicators of liver function [38]. Additionally, due to hypoxia, ischemia, and metabolic acidosis, there is local neutrophil infiltration in the liver, formation of local microthrombosis in the liver sinusoids, rupture of the liver cell membrane, balloon-like lesions, and even necrosis of liver cells, resulting in liver function failure [38, 65]. Some reports have indicated that heatstroke patients present with severe hypophosphatemia at the time of admission [66]. Hypophosphatemia may be related to respiratory alkalosis induced by hyperthermia, which causes phosphorus to shift from the extracellular to the intracellular compartment, resulting in reduced ATP synthesis and 2,3-diphosphoglycerate in red blood cells. This reduction diminishes the oxygenation function of the liver, impairs liver perfusion, and ultimately leads to acute liver failure [67].

Studies have shown that after heatstroke, the expression level of PINK1 in mitochondria increases, and the translocation of Parkin from the cytoplasm to the mitochondria also increases [68]. This indicates that heatstroke stabilizes PINK1 at the outer mitochondrial membrane, thereby recruiting more Parkin to eliminate damaged mitochondria. In heatstroke-induced acute liver injury (HS-ALI), the upregulation of p53 is involved in triggering HS-induced cell apoptosis [69]. Cytoplasmic p53 inhibits the translocation of Parkin to damaged mitochondria, preventing the removal of these damaged mitochondria. The lack of mitophagy subsequently increases cell apoptosis and oxidative stress response in HS-ALI [68]. In summary, cytoplasmic p53 binds to Parkin and inhibits mitophagy by preventing Parkin's translocation from the cytoplasm to the mitochondria, thereby reducing mitophagy activation and causing liver cell apoptosis in HS-ALI. Therefore, pharmacological inhibition of p53 to induce mitophagy may be a novel therapeutic approach for HS-ALI treatment. Additionally, research has found that angiotensin II-induced ROS activation leads to liver injury after heatstroke [44]. The angiotensin-(1-7) receptor agonist AVE 0991 can alleviate liver injury by inhibiting the ROS-NLRP3 inflammatory signaling pathway, indicating that the angiotensin-(1-7) receptor may be a potential target for treating liver injury following heatstroke [70].

Kidney injury

An increased death toll from chronic kidney disease among agricultural workers in Africa, India, the Middle East, and Central America has been reported, which is related to heat exposure and dehydration [71]. Heatstroke is often accompanied by acute kidney injury (AKI), characterized by renal tubular cell degeneration and apoptosis, resulting in symptoms such as hematuria and proteinuria, which may rapidly progress to acute renal failure with high mortality [72]. The pathogenesis of heatstroke-induced AKI involves multiple mechanisms, including renal ischemia, RM, and heat damage [73]. Hyperthermia can lead to disorders of the human anticoagulation system. Studies have shown that under hyperthermic conditions, there is glomerular swelling, inflammatory cell infiltration, vacuolar degeneration of endothelial cells, and renal tubular erythrocytes, which are characteristic signs of congestion, indicating a high risk of hemorrhage [74]. As a coagulation-related marker, the risk of AKI increases by 5.4 times with every 1 mg/L increase in D-dimer levels [75]. Other studies have shown that enhanced mitochondrial uncoupling protein 2 expression can improve mitochondrial dynamics in AKI [76].

Heatstroke-induced AKI is not only due to de-

hydration or reduced renal blood flow but also related to tubular injury caused by heat stress itself and the inflammatory immune response [77]. Some studies have shown that neutrophil infiltration in the kidney increases immediately after heat exposure and significantly increases 24 hours after heat stress [78]. A retrospective study on EHS patients in intensive care units also showed that increased neutrophils and decreased lymphocytes were risk factors for AKI [79]. Other studies have also shown that a decreased lymphocyte count is associated with an increased 90-day mortality rate and AKI incidence in heatstroke patients [80]. A reduction of macrophages in the kidney can inhibit renal recovery from AKI and exacerbate renal fibrosis. Additionally, due to heat damage, the release of myoglobin from RM in EHS gradually increases. Trials have revealed that muscle damage induced by exercise prior to high-temperature running can result in a more pronounced inflammatory response and increased renal stress compared to exercises without muscle damage [81]. Consequently, muscle damage should be recognized as a potential risk factor for AKI during physical activity in hot conditions [81]. Experimental models have shown that myoglobin may be a pathogenic factor for human renal proximal tubular cells after heat stress, exacerbating cell ferroptosis and endoplasmic reticulum stress response [82].

Lung Injury

The respiratory system is often affected during the initial attack of heatstroke. Acute lung injury (ALI) is a common complication in heatstroke patients, clinically characterized by acute pulmonary congestion and edema. Severe cases can develop into acute respiratory distress syndrome [83]. Microscopically, ALI is manifested by interstitial vasodilation and congestion caused by increased capillary permeability, widening of the interstitial spaces, blurred alveolar structure, injured epithelial cells, and pulmonary injury due to tissue infiltration of inflammatory cells [84].

The malignant cycle of ALI induced by heatstroke and the role of aldehyde dehydrogenase 2 (ALDH2) in breaking this vicious cycle can be attributed to several factors. Heat stress induces inflammation and cell apoptosis through the production of ROS and endogenous active aldehydes. Heat stress activates p38 and NF-κB, leading to the upregulation of NADPH oxidase-1 (NOX-1) overexpression in endothelial cells through NF-κB and p38 activation [85]. ROS produced by NOX causes a decrease in intracellular potential ($\Delta\Psi m$), leading to an increase in ROS produced by mitochondria, which further activates NOX, forming a vicious cycle [86]. Research has found that mitochondrial ALDH2, combined with the ALDH2 activator Alda-1, can inhibit this process, reduce ROS accumulation, and prevent heatstroke-induced ALI [87]. Therefore, Alda-1 can be used as an adjuvant therapy for heatstroke-induced ALI.

Heatstroke may cause ferroptosis in pulmonary tissue. This process involves divalent iron or lipoxygenase catalyzing the high expression of unsaturated fatty acids on the cell membrane, leading to lipid peroxidation and subsequent cell death [88]. Additionally, studies have found that increased acetylation levels of p53 can promote ferroptosis of pulmonary epithelial cells in heatstroke-induced ALI [89]. Research has shown that overexpressing the plasmid of silent information regulator 1 (SIRT1) can reduce the acetylation level of p53 and inhibit ferroptosis in heatstroke-induced mouse lung epithelial-2 cells, indicating that SIRT1-mediated deacetylation of p53 can reverse this process to alleviate ferroptosis [83]. Furthermore, heat stress can induce receptor-interacting protein kinase-dependent necroptosis in pulmonary vascular endothelial cells, which may lead to or exacerbate heatstroke-induced ALI.

Skin damages

The impact of ultraviolet radiation on skin health is a significant area of research. Numerous studies have demonstrated that exposure to ultraviolet radiation accelerates skin aging and carcinogenesis. The specific mechanisms include the formation of ROS, DNA damage, and chronic photodamage [90]. Additionally, while keratinocytes and fibroblasts do not predominantly contribute to the production of cytokines and prostaglandins in cases of heatstroke (< 44 ℃), they may play a significant role in evaporative cooling failure, focal hotspots, or systemic reactions [91].

Endocrine damages

Ischemic, hypoxic, and oxidative damage to the hypothalamus during heatstroke can lead to multi-organ dysfunction or failure via a hypothalamic–pituitary–adrenal axis mechanism. Rodents subjected to heatstroke exhibited elevated hypothalamic cell ischemia values and markers of injury, including pro-oxidant enzymes, pro-inflammatory cytokines, inducible nitric oxide synthase-dependent nitric oxide, and polymorphonuclear leukocyte accumulation [92]. Furthermore, these animals demonstrated neuronal injury post-heatstroke compared to

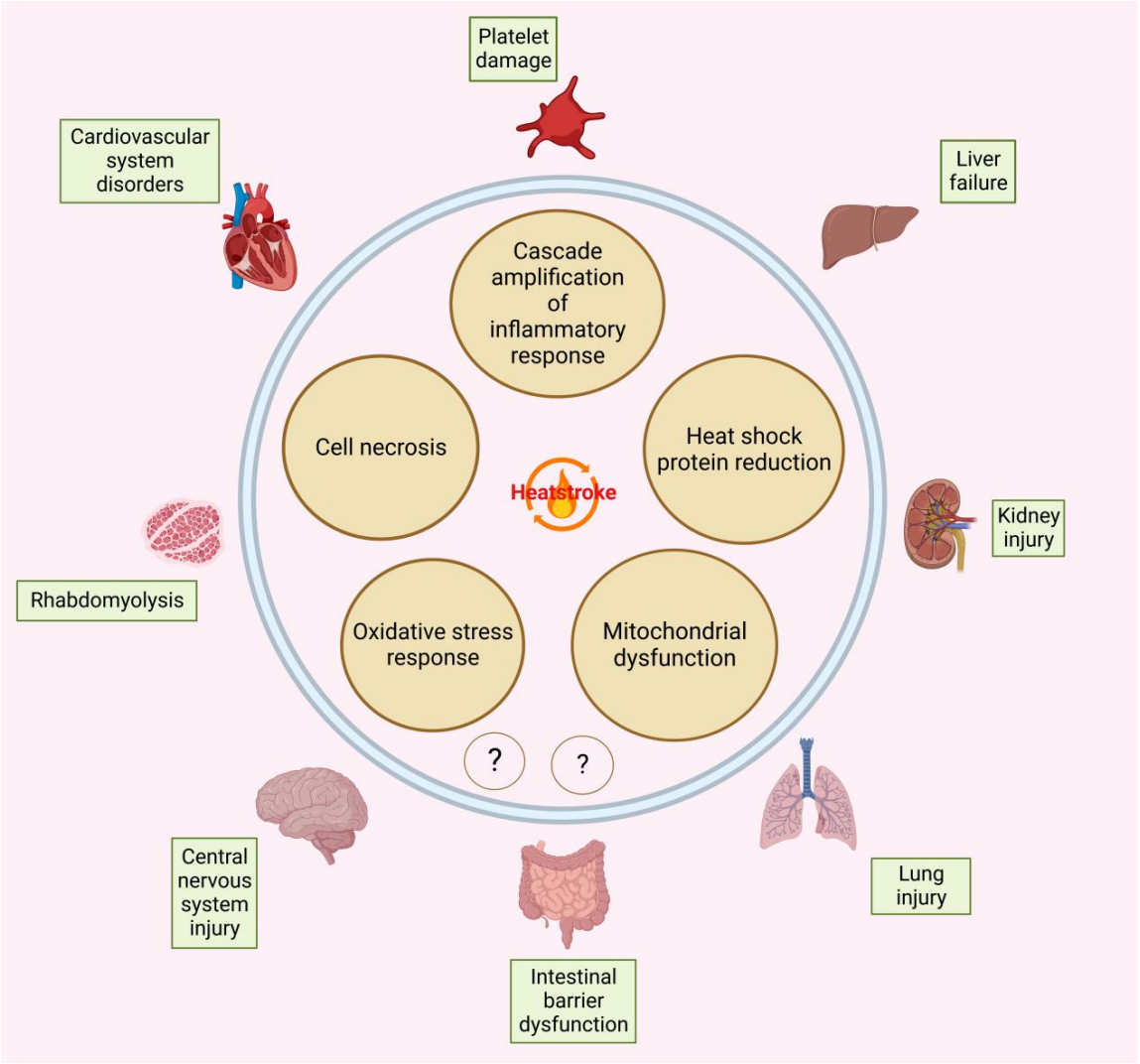

Figure 3. Heatstroke patients suffer from multiple organ injuries involving various molecular mechanisms. The molecular mechanisms of heatstroke include: elevated body temperature inducing oxidative stress, culminating in the generation of reactive oxygen species and subsequent tissue damage; hyperthermia facilitating the penetration of cell cytochrome C through the mitochondrial membrane, resulting in decreased mitochondrial cytochrome C levels, heightened reactive oxygen production, and disruption of mitochondrial membrane integrity; hyperthermia diminishing the permeability of the intestinal wall, enabling the escape of a significant amount of endotoxin, which activates Toll-like receptors, triggering the production of inflammatory factors and subsequently activating Kupffer cells, leading to a "sepsis-like response"; hyperthermia inducing misfolding of cytoplasmic proteins, reducing heat shock proteins, and attenuating the inhibition of the pro-inflammatory pathway; heat stress inducing MLKL and Caspase-8-dependent RIPK3-induced necroptosis through ZBP1. The consequential impact of heatstroke includes a spectrum of symptoms, encompassing liver, kidney, and lung damage, along with compromised intestinal barrier function. MLKL, mixed lineage kinase domain-like pseudokinase; RIPK3, receptor-interacting protein kinase 3; ZBP1, Z-DNA binding protein 1.

their normothermic counterparts. EHS-induced erectile dysfunction was observed in these rats. Additionally, testicular temperature disturbances were noted, along with poor seminiferous tubule differentiation, impaired sperm quality, and atrophy of various testicular tissue cells, such as interstitial mesenchymal cells, supporting cells, and peritubular cells. This was accompanied by spermatozoa azotemia, ruptured spermatozoa, and prostatic inflammation [93].

Molecular mechanisms of organ damage due to heatstroke

Heatstroke, a critical illness characterized by elevated body temperature and neurological manifestations, poses a significant threat to multiorgan function [2]. The pathophysiology of heatstroke involves a cascade of intricate molecular mechanisms, including oxidative stress response, mitochondrial dysfunction, inflammatory amplification, HSP insufficiency, and induction of cell necrosis. These interconnected pathways collectively contribute to the

progression of organ damage and dysfunction during heatstroke, highlighting the need for a comprehensive understanding of the underlying molecular processes for effective therapeutic interventions (**Figure 3**).

Oxidative stress response

Oxidative stress is a type of cellular damage and death that can promote the development and progression of heatstroke through various pathways, such as upregulating the function and expression of the antioxidant system, inducing lipid peroxidation, and activating cell apoptosis [94]. High temperatures can induce the body to produce a large amount of ROS [95]. Several mechanisms may be involved in this process:

1. After entering the irreversible stage, the decrease in cardiac output causes local hypoxia, which induces the production of ROS [67, 94, 95].

2. High heat can adversely affect the integrity of the mitochondrial membrane and its electron transport chain, resulting in the production of ROS. Additionally, high heat can stimulate the production of ROS by inducing mitochondrial fission or inhibiting the activity of mitochondrial complex I [96, 97].

3. Heat stress can induce the production of ROS by upregulating angiotensin II and its receptor (angiotensin receptor 1) [95].

4. Heat stress can promote the activation of the p38-MK2 signaling pathway, which promotes cell apoptosis by regulating the accumulation of ROS [98].

5. Heat stress can activate the Z-DNA binding protein 1 (ZBP1)- receptor-interacting protein kinase 3 (RIPK3) signaling pathway, which may be related to the production of ROS [99].

The high reactivity of ROS can modify several large cellular molecules, such as nucleic acids, proteins, and lipids. Heat stress is an effective inducer of ROS production. Once the cellular redox defense system, which consists of glutathione, glutathione peroxidase, superoxide dismutase, and heme oxygenase 1, is depleted, it can induce cell apoptosis by promoting ERK and Bcl-2 signaling and the release of apoptotic factors, eventually leading to tissue damage [100, 101].

Mitochondrial dysfunction

About ten years ago, the "lysosome-mitochondria axis" cell apoptosis signaling pathway was proposed, revealing the interaction between lysosomes and mitochondria in cell apoptosis. In this process, lysosomal membrane permeabilization is considered a key step, as tissue cysteine cathepsin is released from the lysosome into the cytoplasm and found to be involved in cell apoptosis. Specifically, tissue cysteine cathepsin B cleaves Bid and degrades the anti-apoptotic Bcl-2 protein in the cytoplasm, leading to the activation of caspases and subsequent mitochondrial depolarization, thereby triggering the mitochondrial pathway of cell apoptosis [102]. Recent studies have shown that when SW480 cells and intestinal tissues are exposed to heat stress, lysosomal membrane permeabilization occurs, releasing tissue cysteine cathepsin B into the cytoplasm [4]. This mediates the downstream lysosome-mitochondria apoptosis pathway in intestinal tissues and cultured epithelial cells [4]. Additionally, ROS induced by heat stress acts as an upstream signal in the cell's lysosomal damage and mitochondrial apoptosis pathways through various stimuli. It regulates the lysosome-mitochondria pathway and promotes cell apoptosis induced by heat stress in intestinal tissues and epithelial cells [4, 103].

Furthermore, some studies suggest that heat stress causes a sharp decrease in glutathione levels [104]. The combination of glutathione depletion and increased ROS production is considered an early event in heat-induced cell apoptosis. Due to the heat sensitivity of the respiratory chain, the energy activity of mitochondria changes under heat shock. Heat stress causes the inactivation of complex I in the respiratory chain and its degradation into smaller components, thereby reducing the flow rate of electrons in the electron transfer chain, leading to increased ROS production. Subsequently, ROS may cause the accumulation of secondary mtDNA mutations, leading to increased ROS leakage in the electron transfer chain, further exacerbating mitochondrial respiratory defects and increasing mitochondrial ROS production and lipid peroxidation [105].

High temperatures cause heatstroke, leading to an increase in the expression of the Bcl protein family in liver cells, making it easier for cytochrome C (Cyt-c) to be released from the mitochondrial membrane into the cytoplasm [68]. Once Cyt-c is released into the cytoplasm, it produces two main effects. First, it can activate enzymes of the Caspase family, thereby initiating apoptosis signal pathways and inducing liver cell apoptosis. Secondly, due to the inhibi-

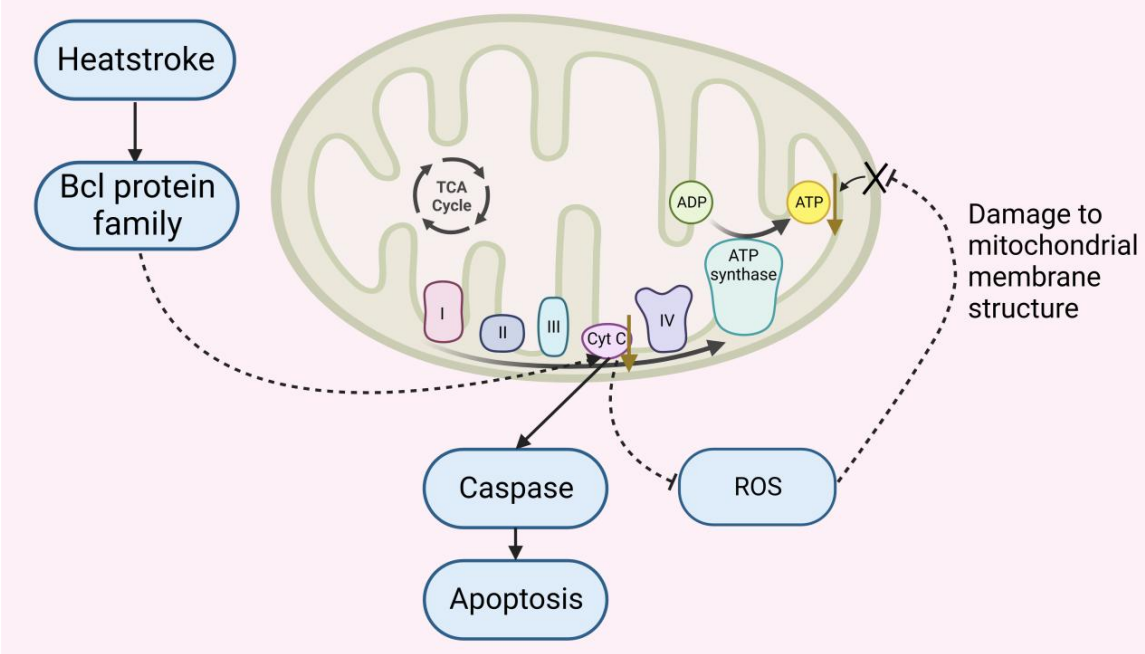

Figure 4. Heat stress leads to mitochondrial dysfunction. Heat stress triggers the expression of the Bcl protein family in mitochondria, facilitating the movement of Cyt-c through the mitochondrial membrane. This dual effect involves Cyt-c entering the cytosol, initiating the apoptosis signaling pathway, and inducing hepatocyte apoptosis. Simultaneously, the reduction of mitochondrial Cyt-c inhibits the electron transport in the oxidative respiratory chain, leading to an accumulation of reactive oxygen species. Elevated ROS levels further compromise the mitochondrial membrane structure, resulting in decreased ATP production and subsequent release of Cyt-c into the cytosol. Cyt-c, cytochrome C; ROS, reactive oxygen species; TCA cycle, tricarboxylic acid cycle.

tion of electron transfer in the oxidative respiratory chain by the decrease of mitochondrial Cyt-c, ROS production increases. Excessive ROS further disrupts the mitochondrial membrane structure, leading to ATP depletion and more Cyt-c release into the cytoplasm (**Figure 4**).

Cascading amplification of inflammatory response

When heatstroke occurs, a large number of endotoxins enter the liver through the portal vein and activate the TLR signaling pathway. These endotoxins bind to lipopolysaccharide binding protein in the blood. Subsequently, they are recognized and bound to TLR4 on the Kupffer cell membrane, forming a complex that interacts with CD14 and MD2 subunits on the membrane. This complex activates intracellular signal transduction through MyD88-dependent and MyD88-independent pathways, leading to the activation of NF-κB. Consequently, this upregulates the expression and release of inflammatory factors such as TNF-α and IL-1β [106]. This process activates Kupffer cells, resulting in a "sepsis-like response."

Insufficient HSP

Heat sickness induces the misfolding and aggregation of proteins within the cytoplasm. This triggers the release of HSPs from inactive monomeric HSF1, initiating the heat shock response. Activated transcription factors then enter the nucleus, forming trimers that activate the gene expression of inducible HSPs. Inducible HSPs, in turn, activate more HSF, triggering the unfolded protein response. This pathway enhances the protein's ability to fold correctly and, in extreme cases, reduces the synthesis of new proteins or induces apoptosis [107]. Additionally, inducible HSPs can bind to misfolded proteins, facilitating their refolding or degradation by proteases to inhibit apoptosis.

The duration and magnitude of the heat shock response are influenced by individual age, genetic and epigenetic regulation, and the degree of adaptation to heat. HSPs, particularly HSP70, play a crucial role in mitigating the onset and development of heat stress disorders. Acting as a molecular chaperone, HSP70 forms protein aggregates and degrades damaged proteins while aiding in the correct refolding of newly synthesized proteins. Furthermore, HSP70 exhibits a potent anti-inflammatory function within cells. In summary, HSPs exert cytoprotective and anti-inflammatory effects by inhibiting multiple pro-inflammatory pathways. Most stress adaptation responses require increased HSP levels, and a reduction or insufficiency in HSP expression may heighten sensi-

tivity to stress.

Cell necrosis induced by heat stress

ZBP1, initially identified as an IFN-induced tumor-associated protein, has been implicated in the pathogenesis of heatstroke. Research indicates that heat stress elevates ZBP1 expression by enhancing the activation and occupancy of HSF1 binding sites in the ZBP1 promoter [108]. ZBP1 activation occurs through a nucleic acid sensing-independent mechanism. Positioned upstream of mixed lineage kinase domain-like pseudokinase (MLKL) and Caspase-8, ZBP1, upon activation, triggers the phosphorylation-dependent activation of MLKL by RIPK3, leading to programmed necrosis [99]. Furthermore, ZBP1 and RIPK3 activation may instigate thrombin activation, fibrosis deposition, and platelet adhesion in microvessels. In summary, heat stress, by mediating MLKL and Caspase-8-dependent RIPK3-induced necroptosis through ZBP1, may contribute to circulatory failure, organ damage, and, in severe cases, heatstroke-related fatalities [108].

Conclusion

This review provides a comprehensive overview of recent advancements in understanding multiple organ damage and the molecular mechanisms of heatstroke. Although existing research indicates that the intricate interplay between heat-related cytotoxicity, inflammatory response, coagulopathy, RM, and gastrointestinal disruption contributes to multiple organ damage in heatstroke patients, the specific mechanisms remain incompletely elucidated. Future investigations should explore high-temperature-induced metabolic changes, tissue cell dysfunction during the cooling process, and the utilization of animal models to delve deeper into the pathophysiological processes and the development and progression mechanisms of heatstroke. Such endeavors will aid clinicians in more accurately assessing the severity and prognosis of patients, facilitating the development and implementation of improved treatment plans.

Authors contributions: Ruilong Li, Dezhi Guo, and Tianying Li wrote the main manuscript text. Tianying Xu and Panpan Hu revised and edited the manuscript. All authors reviewed the manuscript. All authors contributed to the article and approved the submitted version.

References

[1] Bouchama A, Knochel JP. Heat stroke. N Engl J Med 2002;346(25):1978-1988.

[2] Yeo TP. Heat stroke: a comprehensive review. AACN Clin Issues 2004;15(2):280-293.

[3] Argaud L, Ferry T, Le QH, et al. Short- and long-term outcomes of heatstroke following the 2003 heat wave in Lyon, France. Arch Intern Med 2007;167(20):2177-2183.

[4] Yi G, Li L, Luo M, et al. Heat stress induces intestinal injury through lysosome- and mitochondria-dependent pathway in vivo and in vitro. Oncotarget 2017;8(25):40741-40755.

[5] Lucas RA, Epstein Y, Kjellstrom T. Excessive occupational heat exposure: a significant ergonomic challenge and health risk for current and future workers. Extrem Physiol Med 2014;3:14.

[6] Periasamy M, Herrera JL, Reis FCG. Skeletal Muscle Thermogenesis and Its Role in Whole Body Energy Metabolism. Diabetes Metab J 2017;41(5):327-336.

[7] Ainsworth BE, Haskell WL, Herrmann SD, et al. 2011 Compendium of Physical Activities: a second update of codes and MET values. Med Sci Sports Exerc 2011;43(8):1575-1581.

[8] Marty I, Fauré J. Excitation-Contraction Coupling Alterations in Myopathies. J Neuromuscul Dis 2016;3(4):443-453.

[9] Lin BL, Li A, Mun JY, et al. Skeletal myosin binding protein-C isoforms regulate thin filament activity in a Ca(2+)-dependent manner. Sci Rep 2018;8(1):2604.

[10] Calderón JC, Bolaños P, Caputo C. The excitation-contraction coupling mechanism in skeletal muscle. Biophys Rev 2014;6(1):133-160.

[11] van der Poel C, Stephenson DG. Effects of elevated physiological temperatures on sarcoplasmic reticulum function in mechanically skinned muscle fibers of the rat. Am J Physiol Cell Physiol 2007;293(1):C133-C141.

[12] Smith CJ, Johnson JM. Responses to hyperthermia. Optimizing heat dissipation by convection and evaporation: Neural control of skin blood flow and sweating in humans. Auton Neurosci 2016;196:25-36.

[13] Angilletta MJ, Jr., Cooper BS, Schuler MS, et al. The evolution of thermal physiology in endotherms. Front Biosci (Elite Ed) 2010;2(3):861-881.

[14] Goto M, Okazaki K, Kamijo Y, et al. Protein and carbohydrate supplementation during 5-day aerobic training enhanced plasma volume expansion and thermoregulatory adaptation in young men. J Appl Physiol (1985) 2010;109(4):1247-1255.

[15] Horowitz M. Heat acclimation, epigenetics, and cytoprotection memory. Compr Physiol 2014;4(1):199-230.

[16] Taylor NAS, Notley SR, Lindinger MI. Heat

adaptation in humans: extrapolating from basic to applied science. Eur J Appl Physiol 2021;121(4):1237-1238.
[17] Laitano O, Leon LR, Roberts WO, et al. Controversies in exertional heat stroke diagnosis, prevention, and treatment. J Appl Physiol (1985) 2019;127(5):1338-1348.
[18] Lin XJ, Li YJ, Li ZL, et al. Pre-existing lipopolysaccharide may increase the risk of heatstroke in rats. Am J Med Sci 2009;337(4):265-270.
[19] Abello PA, Buchman TG. Heat shock-induced cell death in murine microvascular endothelial cells depends on priming with tumor necrosis factor-alpha or interferon-gamma. Shock 1994;2(5):320-323.
[20] Carter R 3rd, Cheuvront SN, Sawka MN. A case report of idiosyncratic hyperthermia and review of U.S. Army heat stroke hospitalizations. J Sport Rehabil 2007;16(3):238-243.
[21] Dineen SM, Ward JA, Leon LR. Prior viral illness increases heat stroke severity in mice. Exp Physiol 2021;106(1):244-257.
[22] Murray KO, Brant JO, Iwaniec JD, et al. Exertional heat stroke leads to concurrent long-term epigenetic memory, immunosuppression and altered heat shock response in female mice. J Physiol 2021;599(1):119-141.
[23] Yamazawa T, Kobayashi T, Kurebayashi N, et al. A novel RyR1-selective inhibitor prevents and rescues sudden death in mouse models of malignant hyperthermia and heat stroke. Nat Commun 2021;12(1):4293.
[24] Poussel M, Guerci P, Kaminsky P, et al. Exertional Heat Stroke and Susceptibility to Malignant Hyperthermia in an Athlete: Evidence for a Link? J Athl Train 2015;50(11):1212-1214.
[25] Sun Z, Wang L, Han L, et al. Functional Calsequestrin-1 Is Expressed in the Heart and Its Deficiency Is Causally Related to Malignant Hyperthermia-Like Arrhythmia. Circulation 2021;144(10):788-804.
[26] Gibson OR, Tuttle JA, Watt PW, et al. Hsp72 and Hsp90α mRNA transcription is characterised by large, sustained changes in core temperature during heat acclimation. Cell Stress Chaperones 2016;21(6):1021-1035.
[27] Alele FO, Otto JR, Malau-Aduli BS, et al. Next Generation Sequencing of Genotype Variants and Genetic Association between Heat Shock Proteins HSPA1B Single Nucleotide Polymorphism at the g.31829044 Locus and Heat Tolerance: A Pilot Quasi-Experimental Study. Biomolecules 2022;12(10):1465.
[28] Dehbi M, Baturcam E, Eldali A, et al. Hsp-72, a candidate prognostic indicator of heatstroke. Cell Stress Chaperones 2010;15(5):593-603.
[29] Sonna LA, Wenger CB, Flinn S, et al. Exertional heat injury and gene expression changes: a DNA microarray analysis study. J Appl Physiol (1985) 2004;96(5):1943-1953.
[30] Bazille C, Megarbane B, Bensimhon D, et al. Brain damage after heat stroke. J Neuropathol Exp Neurol 2005;64(11):970-975.
[31] Leon LR, Bouchama A. Heat stroke. Compr Physiol 2015;5(2):611-647.
[32] Kao TY, Lin MT. Brain serotonin depletion attenuates heatstroke-induced cerebral ischemia and cell death in rats. J Appl Physiol (1985) 1996;80(2):680-684.
[33] Wang L, Deng Z, Zhao Y, et al. Mesenchymal stem cells regulate activation of microglia cells to improve hippocampal injury of heat stroke rats. J Therm Biol 2021;101:103081.
[34] Burke S, Hanani M. The actions of hyperthermia on the autonomic nervous system: central and peripheral mechanisms and clinical implications. Auton Neurosci 2012;168(1-2):4-13.
[35] Hirayama I, Inokuchi R, Ueda Y, et al. Heat Stroke Lesions in the Globus Pallidus. Intern Med 2020;59(7):1015-1016.
[36] Siegel JS, Snyder AZ, Metcalf NV, et al. The circuitry of abulia: insights from functional connectivity MRI. Neuroimage Clin 2014;6:320-326.
[37] Nelson S, Toma H, LaMonica H, et al. Major Cognitive Changes and Micrographia following Globus Pallidus Infarct. Case Rep Neurol Med 2014;2014:252486.
[38] Knapik JJ, Epstein Y. Exertional Heat Stroke: Pathophysiology, Epidemiology, Diagnosis, Treatment, and Prevention. J Spec Oper Med 2019;19(2):108-116.
[39] Hsu YD, Lee WH, Chang MK, et al. Blood lactate threshold and type II fibre predominance in patients with exertional heatstroke. J Neurol Neurosurg Psychiatry 1997;62(2):182-187.
[40] Deguchi H, Morla S, Griffin JH. Novel blood coagulation molecules: Skeletal muscle myosin and cardiac myosin. J Thromb Haemost 2021;19(1):7-19.
[41] Keuter M, Dharmana E, Kullberg BJ, et al. Phospholipase A2 is a circulating mediator in typhoid fever. J Infect Dis 1995;172(1):305-308.
[42] Schlader ZJ, Davis MS, Bouchama A. Biomarkers of heatstroke-induced organ injury and repair. Exp Physiol 2022;107(10):1159-1171.
[43] He S, Li R, Peng Y, et al. ACSL4 contributes to ferroptosis-mediated rhabdomyolysis in exertional heat stroke. J Cachexia Sarcopenia Muscle 2022;13(3):1717-1730.
[44] Leon LR, Helwig BG. Heat stroke: role of

the systemic inflammatory response. J Appl Physiol (1985) 2010;109(6):1980-1988.
[45] Neves AL, Coelho J, Couto L, et al. Metabolic endotoxemia: a molecular link between obesity and cardiovascular risk. J Mol Endocrinol 2013;51(2):R51-R64.
[46] Hall DM, Buettner GR, Oberley LW, et al. Mechanisms of circulatory and intestinal barrier dysfunction during whole body hyperthermia. Am J Physiol Heart Circ Physiol 2001;280(2):H509-H521.
[47] Lambert GP, Gisolfi CV, Berg DJ, et al. Selected contribution: Hyperthermia-induced intestinal permeability and the role of oxidative and nitrosative stress. J Appl Physiol (1985) 2002;92(4):1750-1761;discussion 1749.
[48] Wells JM, Brummer RJ, Derrien M, et al. Homeostasis of the gut barrier and potential biomarkers. Am J Physiol Gastrointest Liver Physiol 2017;312(3):G171-G193.
[49] Zhang ZT, Gu XL, Zhao X, et al. NLRP3 ablation enhances tolerance in heat stroke pathology by inhibiting IL-1β-mediated neuroinflammation. J Neuroinflammation 2021;18(1):128.
[50] Kawasaki T, Okamoto K, Kawasaki C, et al. Thrombomodulin improved liver injury, coagulopathy, and mortality in an experimental heatstroke model in mice. Anesth Analg 2014;118(5):956-963.
[51] Blatteis CM. The onset of fever: new insights into its mechanism. Prog Brain Res 2007;162:3-14.
[52] Marchbank T, Davison G, Oakes JR, et al. The nutriceutical bovine colostrum truncates the increase in gut permeability caused by heavy exercise in athletes. Am J Physiol Gastrointest Liver Physiol 2011;300(3):G477-G484.
[53] Cao Y, Fan M, Pei Y, et al. CCAAT/Enhancer-Binding Protein Homologous Protein (CHOP) Deficiency Attenuates Heatstroke-Induced Intestinal Injury. Inflammation 2022;45(2):695-711.
[54] Deitch EA. Gut-origin sepsis: evolution of a concept. Surgeon 2012;10(6):350-356.
[55] Munford RS. Detoxifying endotoxin: time, place and person. J Endotoxin Res 2005;11(2):69-84.
[56] Fukui H. Endotoxin and Other Microbial Translocation Markers in the Blood: A Clue to Understand Leaky Gut Syndrome. Cell Mol Med 2016;2:3.
[57] Liu J, Varghese BM, Hansen A, et al. Heat exposure and cardiovascular health outcomes: a systematic review and meta-analysis. Lancet Planet Health 2022;6(6):e484-e495.
[58] Marchand M, Gin K. The Cardiovascular System in Heat Stroke. CJC Open 2022;4(2):158-163.
[59] Chen F, Li H, Zhu G, et al. Sodium tanshinone IIA sulfonate improves inflammation, aortic endothelial cell apoptosis, disseminated intravascular coagulation and multiple organ damage in a rat heat stroke model. Mol Med Rep 2017;16(1):87-94.
[60] Wang JC, Chien WC, Chu P, et al. The association between heat stroke and subsequent cardiovascular diseases. PLoS One 2019;14(2):e0211386.
[61] Huisse MG, Pease S, Hurtado-Nedelec M, et al. Leukocyte activation: the link between inflammation and coagulation during heatstroke. A study of patients during the 2003 heat wave in Paris. Crit Care Med 2008;36(8):2288-2295.
[62] Proctor EA, Dineen SM, Van Nostrand SC, et al. Coagulopathy signature precedes and predicts severity of end-organ heat stroke pathology in a mouse model. J Thromb Haemost 2020;18(8):1900-1910.
[63] Majeed EN. Effects of heat on camel platelet structure and function--a comparative study with humans. Platelets 2009;20(7):528.
[64] Yin H, Wu M, Lu Y, et al. HMGB1-activatied NLRP3 inflammasome induces thrombocytopenia in heatstroke rat. PeerJ 2022;10:e13799.
[65] Wang F, Zhang Y, Li J, et al. The pathogenesis and therapeutic strategies of heat stroke-induced liver injury. Crit Care 2022;26(1):391.
[66] Salathé C, Pellaton C, Carron PN, et al. Acute liver failure complicating exertional heat stroke: possible role of hypophosphatemia. Curr Sports Med Rep 2015;14(1):49-50.
[67] Lian P, Braber S, Garssen J, et al. Beyond Heat Stress: Intestinal Integrity Disruption and Mechanism-Based Intervention Strategies. Nutrients 2020;12(3):734.
[68] Huang W, Xie W, Zhong H, Cai S, Huang Q, Liu Y, Zeng Z and Liu Y. Cytosolic p53 Inhibits Parkin-Mediated Mitophagy and Promotes Acute Liver Injury Induced by Heat Stroke. Front Immunol 2022;13:859231.
[69] Chen Y, Yu T. Involvement of p53 in the Responses of Cardiac Muscle Cells to Heat Shock Exposure and Heat Acclimation. J Cardiovasc Transl Res 2020;13(6):928-937.
[70] Zhang M, Zhu X, Tong H, et al. AVE 0991 Attenuates Pyroptosis and Liver Damage after Heatstroke by Inhibiting the ROS-NLRP3 Inflammatory Signalling Pathway. Biomed Res Int 2019;2019:1806234.
[71] Sorensen C, Garcia-Trabanino R. A New Era of Climate Medicine - Addressing Heat-Triggered Renal Disease. N Engl J Med 2019;381(8):693-696.
[72] Wu M, Wang C, Zhong L, et al. Serum myoglobin as predictor of acute kidney injury and 90-day mortality in patients with rhabdomyolysis after exertional heatstroke:

an over 10-year intensive care survey. Int J Hyperthermia 2022;39(1):446-454.
[73] Thongprayoon C, Qureshi F, Petnak T, et al. Impact of Acute Kidney Injury on Outcomes of Hospitalizations for Heat Stroke in the United States. Diseases 2020;8(3):28.
[74] Mozzini C, Xotta G, Garbin U, et al. Non-Exertional Heatstroke: A Case Report and Review of the Literature. Am J Case Rep 2017;18:1058-1065.
[75] Wang C, Yu B, Chen R, et al. Association of D-dimer and acute kidney injury associated with rhabdomyolysis in patients with exertional heatstroke: an over 10-year intensive care survey. Ren Fail 2021;43(1):1561-1568.
[76] Qin N, Cai T, Ke Q, et al. UCP2-dependent improvement of mitochondrial dynamics protects against acute kidney injury. J Pathol 2019;247(3):392-405.
[77] Goto H, Kinoshita M, Oshima N. Heatstroke-induced acute kidney injury and the innate immune system. Front Med (Lausanne) 2023;10:1250457.
[78] Hu J, Kang H, Liu C, et al. Acute immune responses are involved in liver and kidney injury in heat stroke. Eur J Inflamm 2019;17(9):2058739219838709.
[79] Wu M, Wang C, Liu Z, et al. Clinical Characteristics and Risk Factors Associated With Acute Kidney Injury Inpatient With Exertional Heatstroke: An Over 10-Year Intensive Care Survey. Front Med (Lausanne) 2021;8:678434.
[80] Ji J, Su P, Lin W, et al. Immune Cells Characteristics and Their Prognostic Effects in Exertional Heatstroke Patients: A Retrospective Cohort Study. Front Med (Lausanne) 2022;9:867774.
[81] Junglee NA, Di Felice U, Dolci A, et al. Exercising in a hot environment with muscle damage: effects on acute kidney injury biomarkers and kidney function. Am J Physiol Renal Physiol 2013;305(6):F813-F820.
[82] Luan Y, Huang E, Huang J, et al. Serum myoglobin modulates kidney injury via inducing ferroptosis after exertional heatstroke. J Transl Int Med 2023;11(2):178-188.
[83] Chen H, Lin X, Yi X, et al. SIRT1-mediated p53 deacetylation inhibits ferroptosis and alleviates heat stress-induced lung epithelial cells injury. Int J Hyperthermia 2022;39(1):977-986.
[84] Mokrá D. Acute lung injury - from pathophysiology to treatment. Physiol Res 2020;69(Suppl 3):S353-S366.
[85] Song W, Wei L, Du Y, et al. Protective effect of ginsenoside metabolite compound K against diabetic nephropathy by inhibiting NLRP3 inflammasome activation and NF-κB/p38 signaling pathway in high-fat diet/streptozotocin-induced diabetic mice. Int Immunopharmacol 2018;63:227-238.
[86] Masselli E, Pozzi G, Vaccarezza M, et al. ROS in Platelet Biology: Functional Aspects and Methodological Insights. Int J Mol Sci 2020;21(14):4866.
[87] Tsai HY, Hsu YJ, Lu CY, et al. Pharmacological Activation Of Aldehyde Dehydrogenase 2 Protects Against Heatstroke-Induced Acute Lung Injury by Modulating Oxidative Stress and Endothelial Dysfunction. Front Immunol 2021;12:740562.
[88] Yu T, Sun S. Role and mechanism of ferroptosis in acute lung injury. Cell Cycle 2023;22(19):2119-2129.
[89] Chen H, Xie W, Peng Z, et al. Nobiletin ameliorates heatstroke-induced acute lung injury by inhibiting ferroptosis via p53/slc7a11 pathway. Shock 2024;61(1):105-111.
[90] Mohania D, Chandel S, Kumar P, et al. Ultraviolet Radiations: Skin Defense-Damage Mechanism. Adv Exp Med Biol 2017;996:71-87.
[91] Bowers W, Blaha M, Alkhyyat A, et al. Artificial human skin: cytokine, prostaglandin, Hsp70 and histological responses to heat exposure. J Dermatol Sci 1999;20(3):172-182.
[92] Chen SH, Lin MT, Chang CP. Ischemic and oxidative damage to the hypothalamus may be responsible for heat stroke. Curr Neuropharmacol 2013;11(2):129-140.
[93] Lin PH, Huang KH, Tian YF, et al. Exertional heat stroke on fertility, erectile function, and testicular morphology in male rats. Sci Rep 2021;11(1):3539.
[94] Ni XX, Nie J, Xie QY, et al. Protective Effects of Hyperbaric Oxygen Therapy on Brain Injury by Regulating the Phosphorylation of Drp1 Through ROS/PKC Pathway in Heatstroke Rats. Cell Mol Neurobiol 2020;40(8):1253-1269.
[95] Wang X, Yuan B, Dong W, et al. Humid heat exposure induced oxidative stress and apoptosis in cardiomyocytes through the angiotensin II signaling pathway. Heart Vessels 2015;30(3):396-405.
[96] Yu T, Ferdjallah I, Elenberg F, et al. Mitochondrial fission contributes to heat-induced oxidative stress in skeletal muscle but not hyperthermia in mice. Life Sci 2018;200:6-14.
[97] Huang C, Jiao H, Song Z, et al. Heat stress impairs mitochondria functions and induces oxidative injury in broiler chickens. J Anim Sci 2015;93(5):2144-2153.
[98] Li H, Liu Y, Gu Z, et al. p38 MAPK-MK2 pathway regulates the heat-stress-induced accumulation of reactive oxygen species that

mediates apoptotic cell death in glial cells. Oncol Lett 2018;15(1):775-782.
[99] Li F, Deng J, He Q, et al. ZBP1 and heatstroke. Front Immunol 2023;14:1091766.
[100] Li L, Tan H, Yang H, et al. Reactive oxygen species mediate heat stress-induced apoptosis via ERK dephosphorylation and Bcl-2 ubiquitination in human umbilical vein endothelial cells. Oncotarget 2017;8(8):12902-12916.
[101] Tajeddine N. How do reactive oxygen species and calcium trigger mitochondrial membrane permeabilisation? Biochim Biophys Acta 2016;1860(6):1079-1088.
[102] Chen F, Deng Z, Xiong Z, et al. A ROS-mediated lysosomal-mitochondrial pathway is induced by ginsenoside Rh2 in hepatoma HepG2 cells. Food Funct 2015;6(12):3828-3837.
[103] Ding Y, Wang H, Niu J, et al. Induction of ROS Overload by Alantolactone Prompts Oxidative DNA Damage and Apoptosis in Colorectal Cancer Cells. Int J Mol Sci 2016;17(4):558.
[104] Ohtsuka Y, Yabunaka N, Fujisawa H, et al. Effect of thermal stress on glutathione metabolism in human erythrocytes. Eur J Appl Physiol Occup Physiol 1994;68(1):87-91.
[105] Kirkinezos IG, Moraes CT. Reactive oxygen species and mitochondrial diseases. Semin Cell Dev Biol 2001;12(6):449-457.
[106] Chen XJ, Tang ZZ, Zhu GG, et al JNK signaling is required for the MIP-1α-associated regulation of Kupffer cells in the heat stroke response. Mol Med Rep 2017;16(3):2389-2396.
[107] Morimoto RI. The heat shock response: systems biology of proteotoxic stress in aging and disease. Cold Spring Harb Symp Quant Biol 2011;76:91-99.
[108] Yuan F, Cai J, Wu J, et al. Z-DNA binding protein 1 promotes heatstroke-induced cell death. Science 2022;376(6593):609-615.

Perioperative Precision Medicine
ISSN: 2957-5443

Zentime

Review Article https://doi.org/10.61189/768941essmpc

Ultrasound-guided forearm selective nerve block: A bright future on the horizon

Ziwei Xia[1,2], Guangkuo Ma[1,2], Huanjia Xue[1,2], Hui Wu[1,2], Liwei Wang[1,2], Kai Wang[1,2]

[1]Graduate School, Xuzhou Medical University, Xuzhou 221009, Jiangsu Province, China. [2]Department of Anesthesiology, Xuzhou Central Hospital, Xuzhou 221009, Jiangsu Province, China.

Corresponding author: Kai Wang.

Acknowledgement: This work was supported by the Department of Anesthesiology of Xuzhou Central Hospital. The authors would like to thank all the guest editors and anonymous reviewers for their constructive comments.

Declaration of conflict of interest: None.

Received January 25, 2024; Accepted April 2, 2024; Published September 30, 2024

Highlights

- In the realm of forearm, wrist, and hand surgeries, ultrasound-guided forearm selective nerve block techniques offer distinct advantages over alternative methods such as Bier's block, brachial plexus block, and wrist block. These advantages include reduced anesthesia-related time, prolonged duration of analgesia, and minimal interference with upper extremity motor function.
- Ultrasound-guided forearm selective nerve block stands as a straightforward and conducive anesthesia method ideally suited for distal upper limb surgeries. This approach harmonizes seamlessly with the principles of fast surgical recovery and enhances patient comfort during both diagnostic and therapeutic procedures.
- Supplementation of dexmedetomidine or dexamethasone in ultrasound-guided selective nerve blocks of the forearm has been shown to significantly prolong the duration of analgesia.

Abstract

Objective: In light of the advancement of modern medicine, anesthesiologists and surgeons are increasingly prioritizing patient comfort in diagnostic and therapeutic procedures. A growing body of research revolves around the utilization of ultrasound-guided forearm selective nerve blocks for surgeries involving the distal upper limb. This review aims to provide an overview of regional anesthesia techniques in forearm, hand, and wrist surgeries, laying a theoretical foundation for the prospects of ultrasound-guided forearm selective nerve blocks in optimizing comfort during diagnostic and therapeutic procedures. **Methods:** A retrospective review of literature sourced from the PubMed database was conducted to comprehensively evaluate and elucidate the advantages and drawbacks of ultrasound-guided forearm selective nerve blocks, brachial plexus blocks, Bier blocks, and wrist blocks. Additionally, a summary was provided regarding the selection of local anesthetics for ultrasound-guided forearm selective nerve blocks. **Results:** Overall, ultrasound-guided forearm selective nerve block techniques exhibit several advantages over Bier's block, brachial plexus block, and wrist block for the majority of forearm, wrist, and hand surgeries. These advantages include reduced anesthesia-related time, prolonged duration of analgesia, and minimal impairment of upper extremity motor function. Consequently, these techniques enhance surgical safety and facilitate postoperative recovery. Furthermore, the addition of dexmedetomidine or dexamethasone to ultrasound-guided selective nerve blocks of the forearm could extend the duration of analgesia. **Conclusion:** Ultrasound-guided forearm selective nerve block is a straightforward and conducive anesthesia method for distal upper limb surgeries, aligning with the principles of fast surgical recovery and enhanced patient comfort during diagnostic and therapeutic procedures. Given its manifold benefits, widespread promotion and adoption of this technique in clinical practice are warranted.

Keywords: Ultrasound; distal peripheral forearm block; brachial plexus block; dexmedetomidine; dexamethasone

Address correspondence to: Kai Wang, Department of Anesthesiology, Xuzhou Central Hospital, No. 199 Jiefang South Road, Quanshan District, Xuzhou 221009, Jiangsu Province, China. Tel: +86-18112012729; E-mail: wangkaistream99@sina.com or 760020230115@xzhmu.edu.cn.

Introduction

In the early stages of anesthesia development, even routine upper limb surgeries required general anesthesia. However, perioperative pain management for upper limb procedures has undergone a paradigm shift, with regional anesthesia now assuming a pivotal role and often preferred over general anesthesia [1, 2]. Various regional anesthesia techniques, such as Bier block, brachial plexus block, and wrist block, have been widely employed in surgeries involving the forearm, hand, and wrist. However, each method carries its own set of drawbacks: Bier block often results in postoperative tourniquet pain; brachial plexus block may induce prolonged motor paralysis leading to the phenomenon of "dead arm"; wrist block often entails multiple puncture attempts. Therefore, there has been a collective call within the field to identify an anesthesia approach that offers precise analgesia without compromising postoperative upper limb motor function. Within this context, ultrasound-guided forearm selective nerve block has emerged as a viable option. This article will chronologically review and compare anesthesia methods for forearm, hand, and wrist surgeries, aiming to provide valuable insights and guidance for future clinical anesthesia work. (**Figure 1**)

Traditional regional anesthesia techniques for forearm, hand, and wrist surgeries

Bier block

In 1908, German surgeon August Gustav Bier introduced the technique of Intravenous Regional Anesthesia (IVRA), commonly known as the Bier block technique. This method relies on the application of tourniquets and bandages to achieve regional anesthesia by slowly injecting anesthetic agents through a venous catheter [3, 4]. It is a simple procedure that allows for adequate muscle relaxation [5]. Upper limb IVRA encompasses both traditional upper arm IVRA and forearm IVRA techniques. Traditional IVRA typically requires the administration of 40 ml of 0.5% lidocaine, whereas forearm IVRA achieves comparable anesthesia blockade with a reduced volume of 25 ml of 0.5% lidocaine, thereby lowering the incidence of tourniquet related discomfort [6]. However, a notable limitation of the Bier block technique, when compared to ultrasound-guided nerve blocks, is the occurrence of tourniquet pain. The most severe complications associated with Bier block involve inadvertent release of the tourniquet, leading to rapid systemic toxicity due to the sudden release of local anesthetic [5]. Additionally, Bier block carries risks such as arterial puncture injury and the development of ventricular septal syndrome [7].

Brachial plexus nerve block

Brachial plexus block is a commonly used regional anesthesia technique for upper limb surgeries [8]. Common approaches for brachial plexus nerve block include the interscalene, supraclavicular, infraclavicular, and axillary routes, with additional variations such as posterior clavicular brachial plexus nerve block and selective proximal and distal brachial plexus nerve block within the plexus itself [9, 10]. Despite its widespread utilization, brachial plexus nerve block is associated with several potential complications, including pneumothorax, arterial puncture, hematoma formation, Horner's syndrome, and phrenic nerve block, among others [11]. Furthermore, the use of long-acting local anesthetics in proximal brachial plexus blocks can result in prolonged motor paralysis, commonly termed as the "dead arm", which extends the patient's postoperative recovery period and reduces patient satisfaction [12]. Despite the efficacy of ultrasound-guided brachial plexus block for most upper limb surgical anesthesia requirements, instances of incomplete anesthesia or block failure with isolated brachial plexus nerve blocks have been reported, necessitating additional local anesthetics or adjunctive intravenous medication [13].

Wrist block

Wrist block, performed in the proximal forearm near the wrist, represents a distal peripheral nerve block when compared to forearm selective nerve block. This technique entails the blockade of six nerves, including the median nerve, ulnar nerve, superficial branch of the radial nerve, dorsal branch of the ulnar nerve, posterior interosseous nerve, and anterior interosseous nerve, in addition to the primary nerves [14, 15]. Wrist block serves as a standalone method during surgery or as an adjunct to general anesthesia, such as in wrist release procedures [16]. However, it requires six punctures, heightening the risk of infection and potentially influencing patient satisfaction, in contrast to ultrasound-guided selective nerve blocks of the forearm, which require a maximum of four punctures. Moreover, in cases of tendon and nerve damage or severe compression injuries, an upper arm tourniquet may be indispensable to ensure bloodless surgery and prevent ischemic necrosis in the distal limb. However, the use of an upper arm tourniquet is contraindicated in wrist block procedures,

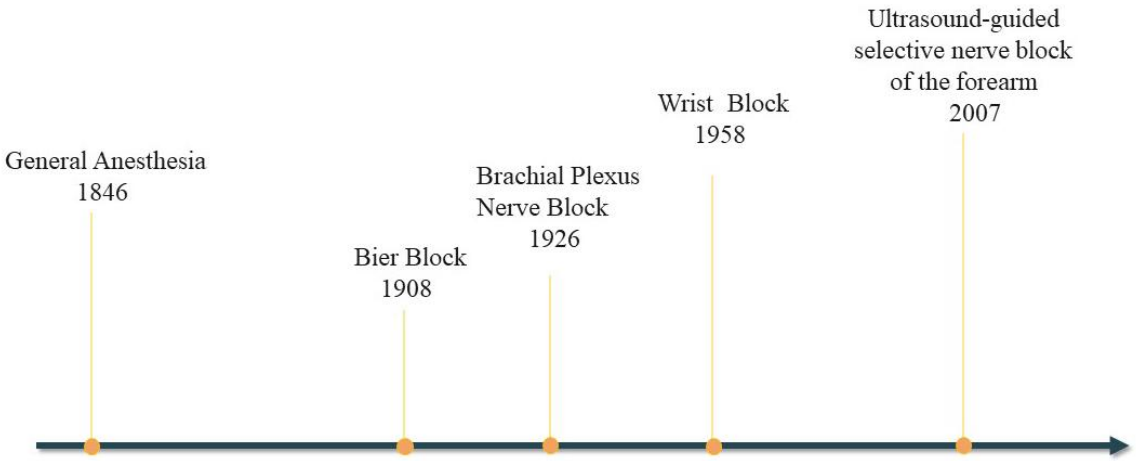

Figure 1. Historical development of anesthesia methods for forearm, hand, and wrist surgeries.

which limits its applicability [17]. Consequently, ultrasound-guided forearm selective nerve blocks have a wider range of applications than wrist blocks [18].

Ultrasound-guided forearm selective nerve block

Currently, with increasing policy demands and higher patient expectations regarding postoperative outcomes, anesthesiologists are facing growing pressures throughout the perioperative period [19]. There is a growing awareness of the benefits associated with ultrasound-guided forearm selective nerve blocks within the context of comfort diagnostic and therapeutic procedures. It is becoming increasingly apparent that proficiency in this technique is a crucial skill that anesthesiologists ought to possess.

Ultrasound-guided forearm selective nerve block technique

Ultrasound technology serves as a pivotal tool in the practice of regional anesthesia, facilitating precise administration of anesthesia while mitigating associated risks [20]. The sensory and motor functions of the forearm, hand, and wrist are predominantly governed by the radial nerve, ulnar nerve, median nerve, and musculocutaneous nerve, along with their respective branches. With the guidance of ultrasound, anesthesiologists can selectively or concurrently block various nerves as required by the surgical procedure, ensuring anesthesia coverage for diverse regions of the forearm, hand, and wrist [21].

The procedure for ultrasound-guided forearm nerve block is relatively straightforward. The ultrasound probe is positioned horizontally in the mid-forearm, and the injection of local anesthetics is performed in three stages, targeting the ulnar nerve, superficial branch of the radial nerve, and median nerve, sequentially. In forearm surgeries, it is often imperative to perform selective nerve blocks of the radial nerve, ulnar nerve, and median nerve concurrently with a musculocutaneous nerve block in the upper arm [22]. In contrast, wrist surgeries typically require selective blockage of the ulnar nerve, superficial branch of the radial nerve, and median nerve [23]. To reduce the number of needle insertions, NC Lam et al. introduced a technique for simultaneously blocking the median nerve and ulnar nerve with a single needle insertion [24]. The ultrasound probe is positioned 5 cm proximal to the wrist fold on the inner side of the forearm and then shifted towards the ulnar side to visualize the ulnar nerve adjacent to the ulnar artery [24]. Once these structures are identified, subcutaneous local anesthesia is administered at the inner edge of the ultrasound probe, followed by needle insertion from the inner side to the outer side, reaching the vicinity of the ulnar nerve for ulnar nerve blockade [24]. At the same horizontal level as the ulnar nerve injection site, the median nerve becomes visible [24].

Employing an in-plane approach, the needle is advanced from the ulnar side towards the median nerve for median nerve blockade [24]. Similarly, I. Ince et al. proposed a method for simultaneous blockade of the radial nerve and median nerve [25]. The ultrasound is positioned in the middle or slightly above the forearm, where the superficial branch of the radial nerve can be clearly observed [25]. After blocking the superficial branch of the radial nerve, the ultrasound probe is shifted from the outer side to the inner side to visualize the median nerve [25]. Subsequently, the needle is advanced towards the median nerve to perform median nerve blockade [25]. It is important to note that these techniques, involving the simul-

taneous blocking of two nerves in one needle insertion, may require a high level of expertise from the anesthesiologist, and further research is needed as no additional studies on this technique have been conducted to date.

Comparison and advantages of ultrasound-guided forearm selective nerve block technique over others

Firstly, in comparison to ultrasound-guided axillary brachial plexus nerve block, ultrasound-guided forearm selective nerve block offers the advantages of simplicity and safety, leading to a potential reduction in anesthesia-related time [26]. It is associated with fewer severe complications, such as phrenic nerve block and pneumothorax, making it a technique that even junior residents can relatively easily master and perform [27]. The study also demonstrated that ultrasound-guided forearm selective nerve blocks, when compared to ultrasound-guided brachial plexus nerve blocks, could reduce the incidence of moderate to severe postoperative wrist pain and provide superior anesthesia and analgesia [27].

Secondly, when compared to forearm Bier block, ultrasound-guided forearm nerve block in patients undergoing outpatient hand surgeries results in only 10% of cases requiring additional analgesics due to incomplete block, whereas this proportion can be as high as 31% in Bier block procedures in the operating room [4, 28]. Research also indicates that ultrasound-guided forearm nerve block can reduce the incidence of moderate to severe postoperative wrist pain, providing superior anesthesia and analgesia outcomes [12, 28].

Finally, ultrasound-guide forearm selective nerve block also proves to be cost-effective. According to a survey, the cost of operating room time in the United States averages $15 per minute, with each forearm selective nerve block procedure saving approximately 20 minutes of anesthesia time [29]. This efficiency allows patient pathways to transition from a serial to a “parallel processing mode,” wherein surgeries can be performed simultaneously, saving approximately $300 per nerve block procedure [29]. This not only significantly reduces resource and financial costs but also has the potential to enhance patient satisfaction [30, 31]. Overall, the primary advantages of peripheral nerve blocks in the forearm over other anesthetic methods include maximizing the preservation of finger and distal muscle function, requiring fewer local anesthetics, reducing anesthesia-related time, prolonging the duration of analgesia, and expediting postoperative recovery. These advantages collectively contribute to improving the patient’s prognosis [32-34] (**Table 1**).

Currently, ultrasound-guided forearm nerve block has emerged as a reliable method for providing precise analgesic effects and has become a method for anesthesia and analgesia in acute pain management of hand and wrist injuries [35]. It can be employed in outpatient settings and emergency department surgeries [28, 36, 37]. Furthermore, ultrasound-guided forearm selective nerve block has demonstrated remarkable efficacy across various orthopedic surgeries [35, 38]. For example, in the United States, it has proven successful in interventions such as finger reduction, upper limb fractures, dislocations, and abscess drainage [39, 40]. In addition, it serves as a valuable tool for postoperative pain management, aligning with the growing trend of employing peripheral nerve blocks for adult postoperative pain control, which has proven to be both well-tolerated and effective [41]. Following surgery, the implementation of forearm selective nerve block not only enhances pain management but also reduces the need for opioid medications and mitigates associated side effects such as vomiting [42].

Selection of local anesthetics and adjuvant medications for ultrasound-guided forearm selective nerve block

Long-acting local anesthetics, such as ropivacaine or bupivacaine, play a pivotal role in enhancing postoperative pain management. Ropivacaine is a long-acting amide-type local anesthetic that exhibits superior selectivity for A δ and C nerve fibers over A β nerve fibers, resulting in sensory-motor separation [43, 44]. While high doses of ropivacaine can effectively block both sensory and motor fibers, forearm nerve block procedures typically utilize lower doses. However, when local anesthetics are used alone, there may arise situations where the duration of block is insufficient, making it challenging to avoid the use of opioid medications postoperatively. Therefore, the addition of adjuvant medications to local anesthetics is often considered to enhance the analgesic effects of the local anesthetic [45, 46]. This approach proves beneficial for patients in overcoming postoperative pain-related obstacles, facilitating early hand function exercises, and expediting postoperative recovery [47]. Adjuvant medications for local anesthesia encompass a wide array of options, among which adrenaline, clonidine, opioid medications, ket-

Table 1. Comparison of common regional anesthesia methods for hand and wrist surgeries

Methods of regional anesthesia	Punctures	Motor block	Sensory block	Contraindication	Complications	Advantages	Major shortcomings
Ultrasound-guided forearm selective nerve block	1, 2, 3, 4, (depending on the needs of the surgical site)	Little motor block	1. Compared to brachial plexus nerve block, it prolongs the duration of sensory blockade. 2. It accelerates the onset of sensory blockade.	1. Patient declined multiple needle punctures. 2. Local anesthetic allergy. 3. Infection at the puncture site. 4. Coagulation abnormalities. 5. Distorted or absent anatomical landmarks.	1. Peripheral nerve injury. 2. Local anesthetic toxicity. 3. Vascular damage. 4. Infection.	1. Smaller local anesthetic doses. 2. Shorter anesthesia-related times. 3. Prolonged postoperative analgesic effects. 4. Higher safety profile. 5. Most studies indicate no need for additional rescue anesthesia measures [32-34]. 6. Cost-effective. 7. Preserving motor function, and aiding in postoperative recovery. 8. Successfully employed in a variety of surgical procedures.	Multiple punctures
Brachial plexus nerve block	1	Prolonged motor block	Prolonged sensory block	1. Anatomical deformity. 2. Infection at the puncture site. 3. Coagulation abnormalities. 4. Allergic reaction to local anesthetics.	1. Intercostal space approach: ipsilateral diaphragmatic paralysis, etc. 2. Supraclavicular approach: pneumothorax, etc. 3. Infraclavicular approach: pneumothorax, diaphragmatic paralysis, etc. 4. Axillary approach: local anesthetic toxicity reactions and arterial puncture, etc.	1. Brachial plexus nerve block is a clinically proven and reliable anesthesia method. 2. Brachial plexus nerve block has multiple approaches that can be selected based on the specific patient's condition.	"Dead arm"
Bier block	1	Adequate muscle relaxation	Compared to general anesthesia, forearm Bier block can enhance the anesthetic and analgesic effect.	1. Patients requiring prolonged use of tourniquets. 2. Infection at the puncture site.	1. Relatively higher risk of compartment syndrome. 2. Systemic toxicity (potential cardiac and neurological toxicity). 3. Arterial puncture.	1. Compared to traditional upper arm Bier block, forearm Bier block requires a shorter tourniquet time. 2. It has a broad spectrum of applications and is suitable for various surgeries. 3. Compared to traditional upper arm Bier block, forearm Bier block has a lower incidence of tourniquet pain.	Tourniquet pain
Wrist block	6	Elbow joint immobility	Adequate sensory block	1. Consistency with ultrasound-guided selective nerve block in the forearm. 2. Patients requiring upper arm tourniquet.	Consistency with ultrasound-guided selective nerve block in the forearm.	1. Smaller local anesthetic doses. 2. Higher safety profile. 3. Cost-effective.	Multiple punctures

amine, and midazolam, when co-administered with local anesthetics around the nerves, have been shown to have limited effectiveness [48]. However, dexamethasone and dexmedetomidine have demonstrated efficacy in enhancing the effects of peripheral nerve blocks, including those performed for hand and wrist surgeries [49, 50]. Overall, the use of adjuvant medications can prolong the duration of analgesia, speed up the onset of action, and mitigate complications or risks.

Dexmedetomidine, an α-2 agonist with an affinity approximately 8 times greater than that of clonidine, is frequently utilized as an adjunct medication in various regional anesthesia procedures [51]. While the precise mechanisms underlying the analgesic and sedative effects of α-2 adrenergic agonists remain not fully understood, they are believed to involve multiple factors. Peripherally, α-2 agonists can diminish norepinephrine release and exert an inhibitory effect on nerve fiber action potentials, independent of α-2 receptors. They also directly

block the Ih cation current activated during hyperpolarization, thereby producing analgesic effects [52]. Dexmedetomidine has been demonstrated to reduce postoperative pain and opioid consumption [53]. Studies indicate that supplementing lidocaine with dexmedetomidine in selective forearm nerve blockade can extend the duration of analgesia by 364 minutes, in contrast to a mere 21-minute extension with systemic administration of dexmedetomidine [54]. It's worth noting that the addition of dexmedetomidine to local anesthetics does not significantly prolong the duration of motor blockade [55]. Additionally, research indicates that both peripheral and systemic use of dexmedetomidine can effectively enhance analgesic effects, which is advantageous for patients' postoperative recovery [56]. This further underscores the effectiveness of dexmedetomidine as an adjunct medication in regional anesthesia.

Dexamethasone, a synthetic corticosteroid, is one of the most extensively studied adjuvant medications in anesthesia [57]. It boasts analgesic, antiemetic, and anti-inflammatory properties, effectively alleviating tissue inflammation and inflammation-related pain. When compared to clonidine or dexmedetomidine, the addition of dexamethasone to ropivacaine has been shown to prolong analgesia without inducing rebound pain [58, 59]. Furthermore, dexamethasone extends the duration of analgesia when combined with local anesthetics while concurrently reducing the onset time for sensory and motor blockade [60]. A meta-analysis revealed that both peripheral administration and intravenous infusion of dexamethasone prolonged the duration of supraclavicular brachial plexus block, with intravenous administration extending analgesia by 76.4 minutes and peripheral administration by 11.4 minutes [46]. However, peripheral use of dexamethasone is associated with fewer adverse reactions compared to intravenous administration. Additionally, an animal study indicated that combining nerve blockade with dexamethasone did not increase neurotoxicity, underscoring its safety and reliability [61, 62]. Nevertheless, conflicting findings were reported in a study where researchers supplemented a standard peripheral nerve blockade model with dexamethasone, concluding that its impact on sensory blockade with ropivacaine lacked clinical or statistical significance [57]. This discrepancy highlights the necessity for further experimental studies to clarify this issue.

Conclusion

In summary, ultrasound-guided forearm selective nerve block represents a promising and straightforward anesthesia technique for forearm, hand, and wrist surgeries. It holds the potential to expedite anesthesia onset, prolong analgesia duration, mitigate patient discomfort, foster postoperative recovery, and improve patient outcomes. Furthermore, the duration of analgesia can be extended when ultrasound-guided selective nerve blocks of the forearm are supplemented with dexmedetomidine or dexamethasone. Future research should focus on refining puncture approaches, minimizing the number of puncture attempts, and highlighting the benefits of preserving motor function. This focus aims to meet the requirements of surgical anesthesia while further enhancing patient outcomes and satisfaction. Additionally, in thumb surgery, further research could explore the blockage of branches of the musculocutaneous nerve on the lateral forearm. This approach circumvents the impact on elbow joint motor function while meeting the anesthesia requirements of thumb surgery. Future studies in this direction could provide a more comprehensive theoretical framework and guidance for selective forearm nerve blocks

Author Contributions: Ziwei Xia: essay writing, form preparation. Guangkuo Ma: collection of information, organizing the literature. Huanjia Xue: collection of information, organizing the literature. Hui Wu: collection of information, organizing the literature. Liwei Wang: dissertation guidance. Kai Wang: dissertation guidance, proposing the topic, thesis revision.

References

[1] Turbitt LR, Mariano ER, El-Boghdadly K. Future directions in regional anaesthesia: not just for the cognoscenti. Anaesthesia 2020;75(3):293-297.

[2] Vietor R 3rd, Buckenmaier C 3rd. Regional Anesthesia in the Field for Trauma Victims. Anesthesiol Clin 2021;39(2):337-351.

[3] van Zundert A, Helmstädter A, Goerig M, et al. Centennial of intravenous regional anesthesia. Bier's Block (1908-2008). Reg Anesth Pain Med 2008;33(5):483-489.

[4] Nijs K, Lismont A, De Wachter G, et al. The analgesic efficacy of forearm versus upper arm intravenous regional anesthesia (Bier's block): A randomized controlled non-inferiority trial. J Clin Anesth 2021;73:110329.

[5] Löser B, Petzoldt M, Löser A, et al. Intravenous Regional Anesthesia: A Historical Overview and Clinical Review. J Anesth Hist 2019;5(3):99-108.

[6] Ghaderi K, Rahmani K, Rahmanpanah N, et al. Comparison of lidocaine-dexmedetomidine and lidocaine-saline on the characteristics of the modified forearm bier block: A clinical trial. J Anaesthesiol Clin Pharmacol 2021;37(4):610-615.
[7] Teunkens A, Vermeulen K, Belmans A, et al. Patient satisfaction with intravenous regional anaesthesia or an axillary block for minor ambulatory hand surgery: A randomised controlled study. Eur J Anaesthesiol 2020;37(10):847-856.
[8] Grape S, Pawa A, Weber E, et al. Retroclavicular vs supraclavicular brachial plexus block for distal upper limb surgery: a randomised, controlled, single-blinded trial. Br J Anaesth 2019;122(4):518-524.
[9] Georgiadis PL, Vlassakov KV, Patton ME, et al. Ultrasound-guided supraclavicular vs. retroclavicular block of the brachial plexus: comparison of ipsilateral diaphragmatic function: A randomised clinical trial. Eur J Anaesthesiol 2021;38(1):64-72.
[10] Zhang J, Li M, Jia HB, et al. Clinical application of ultrasound-guided selective proximal and distal brachial plexus block in rapid rehabilitation surgery for hand trauma. World J Clin Cases 2020;8(11):2137-2143.
[11] Xing T, Ge L. Ultrasound-Guided Brachial Plexus Block by Costoclavicular Space Approach: A Narrative Review. Med Sci Monit 2023;29:e939920.
[12] Bao N, Chen L, Xia Y, et al. Effect of Ultrasound-guided Nerve Block With 0.75% Ropivacaine at the Mid-forearm on the Prevalence of Moderate to Severe Pain After Hand Surgery. Clin Ther 2018;40(6):1014-1022.
[13] Gunjiyal MS, Mohammed S, Bhatia P, et al. Effect of combined versus sequential injection of 2% lidocaine and 0.5% bupivacaine on the onset and duration of supraclavicular brachial plexus block: A double blinded randomised controlled trial. J Clin Anesth 2021;72:110313.
[14] Kocheta A, Agrawal Y. Landmark Technique for a Wrist Block. JBJS Essent Surg Tech 2018;8(1):e7.
[15] Bloc S, Mercadal L, Cadas H. Distal Block for Wrist Bone Analgesia: The Anterior and Posterior Interosseous Nerves Must Be Blocked. J Hand Surg Am 2015;40(10):2114-2115.
[16] Sallum Y, Fodor L, Mărginean G, et al. Combined distal median nerve block and local anesthesia with lidocaine:epinephrine for carpal tunnel release. Heliyon 2022;8(3):e09119.
[17] Burnham PJ. Regional block at the wrist of the great nerves of the hand. J Am Med Assoc 1958;167(7):847-850.
[18] Sohoni A, Nagdev A, Takhar S, et al. Forearm ultrasound-guided nerve blocks vs landmark-based wrist blocks for hand anesthesia in healthy volunteers. Am J Emerg Med 2016;34(4):730-734.
[19] Sun EC, Memtsoudis SG, Mariano ER. Regional Anesthesia: A Silver Bullet, Red Herring, or Neither? Anesthesiology 2019;131(6):1205-1206.
[20] O'Donnell BD, Loughnane F. Novel nerve imaging and regional anesthesia, bio-impedance and the future. Best Pract Res Clin Anaesthesiol 2019;33(1):23-35.
[21] Chandrasoma J, Harrison TK, Ching H, et al. Peripheral Nerve Blocks for Hand Procedures. N Engl J Med 2018;379(10):e15.
[22] Kawase S, Horiuchi T, Nagahata T. Use of Ultrasound-Guided Selective Sensory Nerve Blocks to Provide Satisfactory Postoperative Analgesia Without Motor Paralysis in Bilateral Distal Radius Fracture Fixation: A Case Report. A A Pract 2021;15(8):e01514.
[23] Mori T, Nomura O, Ihara T. Ultrasound-guided peripheral forearm nerve block for digit fractures in a pediatric emergency department. Am J Emerg Med 2019;37(3):489-493.
[24] Lam NC, Charles M, Mercer D, et al. A triple-masked, randomized controlled trial comparing ultrasound-guided brachial plexus and distal peripheral nerve block anesthesia for outpatient hand surgery. Anesthesiol Res Pract 2014;2014:324083.
[25] Ince I, Aksoy M, Celik M. Can We Perform Distal Nerve Block Instead of Brachial Plexus Nerve Block Under Ultrasound Guidance for Hand Surgery? Eurasian J Med 2016;48(3):167-171.
[26] Nijs K, Van Rossum M, Ory JP, et al. Ultrasound-guided axillary brachial plexus block versus distal peripheral forearm nerve block for hand and wrist surgery: a randomised controlled trial. Br J Anaesth 2023;131(1):e20-e22.
[27] Winter J, McLeod G, Quaife T, et al. Surgeon-administered Ultrasound-guided Peripheral Nerve Blocks in Outpatient Procedures of the Upper Extremity. Plast Reconstr Surg Glob Open 2020;8(11):e3227.
[28] Snyman J, Goldstein LN. Nervous breakdown! A registry of nerve blocks from a South African emergency centre. Afr J Emerg Med 2019;9(4):177-179.
[29] Macachor JD, Kumar CM, Seet E, et al. Peripheral Nerve Blocks in a Regional Anesthesia Block Area: An Economic Model. Reg Anesth Pain Med 2018;43(4):448-449.
[30] Chazapis M, Kaur N, Kamming D. Improving the Peri-operative care of Patients by

instituting a 'Block Room' for Regional Anaesthesia. BMJ Qual Improv Rep 2014;3(1):u204061.
[31] Guay J, Rosenblatt MA. Peripheral nerve blocks for elective primary total hip arthroplasty: Have we yet found the optimal solution? J Clin Anesth 2020;67:109964.
[32] Sehmbi H, Madjdpour C, Shah UJ, et al. Ultrasound guided distal peripheral nerve block of the upper limb: A technical review. J Anaesthesiol Clin Pharmacol 2015;31(3):296-307.
[33] Marhofer P, Harrop-Griffiths W, Kettner SC, et al. Fifteen years of ultrasound guidance in regional anaesthesia: part 1. Br J Anaesth 2010;104(5):538-546.
[34] Jalil H, Polfliet F, Nijs K, et al. Efficacy of ultrasound-guided forearm nerve block versus forearm intravenous regional anaesthesia in patients undergoing carpal tunnel release: A randomized controlled trial. PLoS One 2021;16(2):e0246863.
[35] Wiederhold BD, Garmon EH, Peterson E, et al. Nerve Block Anesthesia. In: editors. StatPearls. Treasure Island (FL) ineligible companies. Disclosure: Emily Garmon declares no relevant financial relationships with ineligible companies. Disclosure: Elisha Peterson declares no relevant financial relationships with ineligible companies. Disclosure: Joshua Stevens declares no relevant financial relationships with ineligible companies. Disclosure: Maria O'Rourke declares no relevant financial relationships with ineligible companies. StatPearls Publishing Copyright © 2024, StatPearls Publishing LLC., 2024. p.
[36] Wheelock M, Petropolis C, Lalonde DH. The Canadian Model for Instituting Wide-Awake Hand Surgery in Our Hospitals. Hand Clin 2019;35(1):21-27.
[37] Vrablik M, Akhavan A, Murphy D, et al. Ultrasound-Guided Nerve Blocks for Painful Hand Injuries: A Randomized Control Trial. Cureus 2021;13(10):e18978.
[38] Divella M, Vetrugno L, Orso D, et al. Which regional anesthesia technique is the best for arthroscopic shoulder surgery in terms of postoperative outcomes? A comprehensive literature review. Eur Rev Med Pharmacol Sci 2021;25(2):985-998.
[39] Amini R, Patricia Javedani P, Amini A, et al. Ultrasound-Guided Forearm Nerve Blocks: A Novel Application for Pain Control in Adult Patients with Digit Injuries. Case Rep Emerg Med 2016;2016:2518596.
[40] Stone MB, Price DD, Wang R. Ultrasound-guided supraclavicular block for the treatment of upper extremity fractures, dislocations, and abscesses in the ED. Am J Emerg Med 2007;25(4):472-475.
[41] De Windt AC, Asehnoune K, Roquilly A, et al. An opioid-free anaesthetic using nerve blocks enhances rapid recovery after minor hand surgery in children. Eur J Anaesthesiol 2010;27(6):521-525.
[42] Campoy L. Locoregional Anesthesia for Hind Limbs. Vet Clin North Am Small Anim Pract 2019;49(6):1085-1094.
[43] Fang G, Wan L, Mei W, et al. The minimum effective concentration (MEC90) of ropivacaine for ultrasound-guided supraclavicular brachial plexus block. Anaesthesia 2016;71(6):700-705.
[44] Huang R, Zhu J, Zhao Z, et al. The effect of programmed intermittent epidural bolus compared with continuous epidural infusion in labor analgesia with ropivacaine: a meta-analysis of randomized controlled trials. Ann Palliat Med 2021;10(3):2408-2420.
[45] Sehmbi H, Brull R, Ceballos KR, et al. Perineural and intravenous dexamethasone and dexmedetomidine: network meta-analysis of adjunctive effects on supraclavicular brachial plexus block. Anaesthesia 2021;76(7):974-990.
[46] Imani F, Farahmand Rad R, Salehi R, et al. Evaluation of Adding Dexmedetomidine to Ropivacaine in Pediatric Caudal Epidural Block: A Randomized, Double-blinded Clinical Trial. Anesth Pain Med 2021;11(1):e112880.
[47] Hade AD, Okano S, Pelecanos A, et al. Factors associated with low levels of patient satisfaction following peripheral nerve block. Anaesth Intensive Care 2021;49(2):125-132.
[48] Cummings KC 3rd, Napierkowski DE, Parra-Sanchez I, et al. Effect of dexamethasone on the duration of interscalene nerve blocks with ropivacaine or bupivacaine. Br J Anaesth 2011;107(3):446-453.
[49] Xuan C, Yan W, Wang D, et al. The Facilitatory Effects of Adjuvant Pharmaceutics to Prolong the Duration of Local Anesthetic for Peripheral Nerve Block: A Systematic Review and Network Meta-analysis. Anesth Analg 2021;133(3):620-629.
[50] Hashemi N, Modir H, Moshiri E, et al. Effects of adding dexmedetomidine, fentanyl, and verapamil to 0.5% ropivacaine on onset and duration of sensory and motor block in forearm surgeries: a randomized controlled trial. Med Gas Res 2021;11(2):47-52.
[51] Edinoff AN, Houk GM, Patil S, et al. Adjuvant Drugs for Peripheral Nerve Blocks: The Role of Alpha-2 Agonists, Dexamethasone, Midazolam, and Non-steroidal Anti-inflammatory Drugs. Anesth Pain Med 2021;11(3):e117197.
[52] Lu TL, Lu TJ, Wu SN. Effectiveness in Block by Dexmedetomidine of Hyperpolarization-

Activated Cation Current, Independent of Its Agonistic Effect on α(2)-Adrenergic Receptors. Int J Mol Sci 2020;21(23):9110.

[53] Zha J, Ji S, Wang C, et al. Thoracic Paravertebral Nerve Block with Ropivacaine and Adjuvant Dexmedetomidine Produced Longer Analgesia in Patients Undergoing Video-Assisted Thoracoscopic Lobectomy: A Randomized Trial. J Healthc Eng 2021;2021:1846886.

[54] Bao N, Shi K, Wu Y, et al. Dexmedetomidine prolongs the duration of local anesthetics when used as an adjuvant through both perineural and systemic mechanisms: a prospective randomized double-blinded trial. BMC Anesthesiol 2022;22(1):176.

[55] Abdallah FW, Dwyer T, Chan VW, et al. IV and Perineural Dexmedetomidine Similarly Prolong the Duration of Analgesia after Interscalene Brachial Plexus Block: A Randomized, Three-arm, Triple-masked, Placebo-controlled Trial. Anesthesiology 2016;124(3):683-695.

[56] Motaghi E, Ghasemi Pirbalooti M, Bozorgi H, et al. Safety and Efficacy of Dexmedetomidine in Breast Surgeries: A Systematic Review and Meta-Analysis. J Perianesth Nurs 2021;36(2):179-186.

[57] Marhofer P, Columb M, Hopkins PM, et al. Dexamethasone as an adjuvant for peripheral nerve blockade: a randomised, triple-blinded crossover study in volunteers. Br J Anaesth 2019;122(4):525-531.

[58] Dong X, Wu CL, YaDeau JT. Clinical care pathways for ambulatory total shoulder arthroplasty. Curr Opin Anaesthesiol 2022;35(5):634-640.

[59] Maagaard M, Stormholt ER, Nielsen LF, et al. Perineural and Systemic Dexamethasone and Ulnar Nerve Block Duration: A Randomized, Blinded, Placebo-controlled Trial in Healthy Volunteers. Anesthesiology 2023;138(6):625-633.

[60] Ahmed NA, Altaei AH, Jasim MA. COMPARISON OF THE ONSET OF SENSORY BLOCK USING LIDOCAINE 1.5% WITH ADRENALINE OR LIDOCAINE 1.5% WITH ADRENALINE AND DEXAMETHASONE IN ULTRASOUND GUIDED AXILLARY NERVE BLOCK FOR BELOW ELBOW SURGERIES. Wiad Lek 2021;74(9 cz 2):2337.

[61] Marty P, Bennis M, Legaillard B, et al. A New Step Toward Evidence of In Vivo Perineural Dexamethasone Safety: An Animal Study. Reg Anesth Pain Med 2018;43(2):180-185.

[62] Duggan NM, Nagdev A, Hayes BD, et al. Perineural Dexamethasone as a Peripheral Nerve Block Adjuvant in the Emergency Department: A Case Series. J Emerg Med 2021;61(5):574-580.

Perioperative Precision Medicine
ISSN: 2957-5443

Zentime

Review Article https://doi.org/10.61189/275419wdddvs

Artificial intelligence in perioperative pain management: A review

Yan Liao[1*], Zhanheng Chen[1*],Wangzheqi Zhang[1*], Lindong Cheng[2], Yanchen Lin[2], Ping Li[3], Miao Zhou[4], Mi Li[1], ChunHua Liao[1]

[1]School of Anesthesiology, Naval Medical University, Shanghai 200433, China. [2]Graduate School, Hebei North University, Zhangjiakou 075000, China. [3]Graduate School, Wannan Medical College, Wuhu 241000, China. [4]Department of Anesthesiology, the Affiliated Cancer Hospital of Nanjing Medical University, Jiangsu Cancer Hospital, Jiangsu Institute of Cancer Research, Nanjing Medical University, Nanjing 210009, China.
[*]The authors contribute equally.

Corresponding authors: Miao Zhou, Mi Li and ChunHua Liao.

Acknowledgement: This work was supported by the National Natural Science Foundation of China under Grants 62002297, 62073225, and 61836005, the Science and Technology Commission of Shanghai Municipality under Grant 20XD1434400, talent Development Fund of Shanghai under Grant 2020075, Medical-Engineering Cross Fund of Shanghai Jiao Tong University under Grant YG2022QN043, and the Guangxi Science and Technology Base and Talent Special Project under Grant 2021AC19394. The authors would like to thank all the guest editors and anonymous reviewers for their constructive advice.

Declaration of conflict of interest: None.

Received February 21, 2024; Accepted March 25, 2024; Published September 30, 2024

Highlights

- Artificial intelligence (AI) is lauded for its capacity to resolve intricate problems with unwavering efficiency, devoid of fatigue. To elucidate the potential of AI in perioperative pain management, we have meticulously surveyed a vast array of scholarly works to discern the landscape of research in this multifaceted domain.
- Conventional perioperative pain studies have primarily confined their scope to clinical aspects. However, this review delves into the amalgamation of AI and perioperative pain, heralding a diverse methodology for pain control.
- AI's applicability in medical domains, particularly anesthesia, has spawned numerous inquiries into its synergy with perioperative pain. Yet, a dearth of comprehensive reviews encapsulating the current research milieu, pinpointing hurdles, and envisioning future directions in this sphere necessitated the present discourse.
- We herein offer horizontal and vertical assessments of diverse models and algorithms employed in perioperative pain management, encapsulated in diagrammatic form for reader accessibility. The compilation of this review draws from a spectrum of online scholarly repositories, thus ensuring a thorough and relevant assembly of insights.

Abstract

Artificial intelligence (AI) leverages its swift, precise, and fatigue-resistant problem-solving abilities to significantly influence anesthetic practices, ranging from monitoring the depth of anesthesia to controlling its delivery and predicting events. Within the domain of anesthesia, pain management plays a pivotal role. This review examines the promises and challenges of integrating AI into perioperative pain management, offering an in-depth analysis of their converging interfaces. Given the breadth of research in perioperative pain management, the review centers on the quality of training datasets, the integrity of experimental outcomes, and the diversity of algorithmic approaches. We conducted a thorough examination of studies from electronic databases, grouping them into three core themes: pain assessment, therapeutic interventions, and the forecasting of pain management-related adverse effects. Subsequently, we addressed the limitations of AI application, such as the need for enhanced predic-

Address correspondence to: Miao Zhou, The Affiliated Cancer Hospital of Nanjing Medical University, Department of Anesthesiology, Jiangsu Cancer Hospital, Jiangsu Institute of Cancer Research, Nanjing Medical University, Nanjing 210009, China. E-mail: zhoumiao2613@163.com; Tel: +86 18217567295. **Mi Li**, School of Anesthesiology, Naval Medical University, 800 Xiangyin Road, Yangpu District, Shanghai 200433, China. E-mail: limi@smmu.edu.cn; Tel: +86-21-81872033. **Chunhua Liao**, School of Anesthesiology, Naval Medical University, 800 Xiangyin Road, Yangpu District. Shanghai 200433, China. E-mail: Liaochh7@smmu.edu.cn; Tel: +86 21 81872025.

tive accuracy, privacy concerns, and the development of a robust database. Building upon these considerations, we propose avenues for future research that harness the potential of AI to effectively contribute to perioperative pain management, aiming to refine the clinical utility of this technology.

Keywords: Artificial intelligence, pain management, perioperative pain, acute pain

Introduction

Artificial intelligence (AI)

AI is characterized by the "science and engineering of creating intelligent machines," as conceptualized in prior research. In 1950, the seminal work of Alan Turing, a mathematician and AI's progenitor, proposed the notion of machines emulating human cognitive processes [1]. Over the past several decades, AI has burgeoned into a multifaceted discipline, encompassing specialized areas such as machine learning, deep learning, neural networks, computer vision, among others [1, 2]. Numerous taxonomies have been proposed to categorize AI. Primordially, AI is bifurcated into Artificial Narrow Intelligence, which predominates in specific domains, Artificial General Intelligence, which approximates human-level intelligence, and Artificial Superintelligence, which surpasses human capabilities by fostering innovation and social interaction [3].

The advent of advanced technology has propelled AI into a multitude of sectors, including robotics, natural language processing, simulation, learning systems, problem-solving methodologies, and gaming. As depicted in **Figure 1**, each of these sectors is further subdivided into a tapestry of specialized fields, reflecting the intricate taxonomy that arises from AI's diverse applications [4]. Machine learning, a subset of AI algorithms, is particularly adept at addressing challenges through classification and regression techniques, capable of parsing and interpreting diverse data formats, ranging from text and numerical datasets to visual and auditory information [5]. Drawing inspiration from the complexities of the nervous system, deep neural networks represent a class of models that bridge the gap between those informed by the workings of biological neurons and those that delve into the cognitive aspects of human information processing. These intricate networks are capable of processing limited inputs and producing high-quality outputs by efficiently leveraging the scarce data contained within their hidden layers [6]. Computer vision is a critical component of AI, empowering machines with the ability to comprehend and decipher visual information, encompassing images and videos. This field extracts salient features from visual data, such as hue, form, and texture. AI has achieved substantial advancement and is extensively applied across various domains, each with its subset of specializations and areas of emphasis [5].

AI's paramount advantage over human cognition lies in its capacity for predictive analytics when confronting extensive explanatory variables or intricate interdependencies among features. In the face of complex challenges, the human mind can laboriously parse through pertinent experiences, resulting in a taxing process. In contrast, AI leverages data-driven methodologies and extensive datasets, affording it a distinctive edge in managing such complexities. The technology can seamlessly compute the most nuanced computations and tenaciously pursue solutions without fatigue [7]. For instance, AI can encapsulate a multitude of variables, referred to as 'model features,' and thereafter elucidate intricate correlations among these features [8]. Subsequently, AI-based algorithms and models are being implemented across a spectrum of medical disciplines, including anesthesiology. AI is augmenting the oversight of anesthetic depth, forecasting the likelihood of deleterious events throughout anesthesia, supporting ultrasound-guided interventions, and assisting in the prediction and administration of pain phenotypes. Across all these domains, the amalgamation of AI is demonstrating enhanced efficacy when compared to conventional approaches [5, 9].

Perioperative pain management

What is pain? Extensive research on pain has been conducted from perspectives of molecules, cells, etc. [10]. The prevalent conceptualization of pain characterizes it as an "unpleasant sensory and emotional experience linked to real or potential tissue harm, or articulated in terms of such harm [11]." Prevalence of perioperative pain is considerable, particularly in the postoperative phase. Data indicate that roughly half of all surgical patients report moderate to severe pain levels within two weeks post-operation, with over 10% experiencing severe to extreme pain intensity [12]. This phenomenon extends beyond major surgical procedures, being a widespread occurrence across various types of surgery [13]. Effective pain management thus constitutes a critical component of the an-

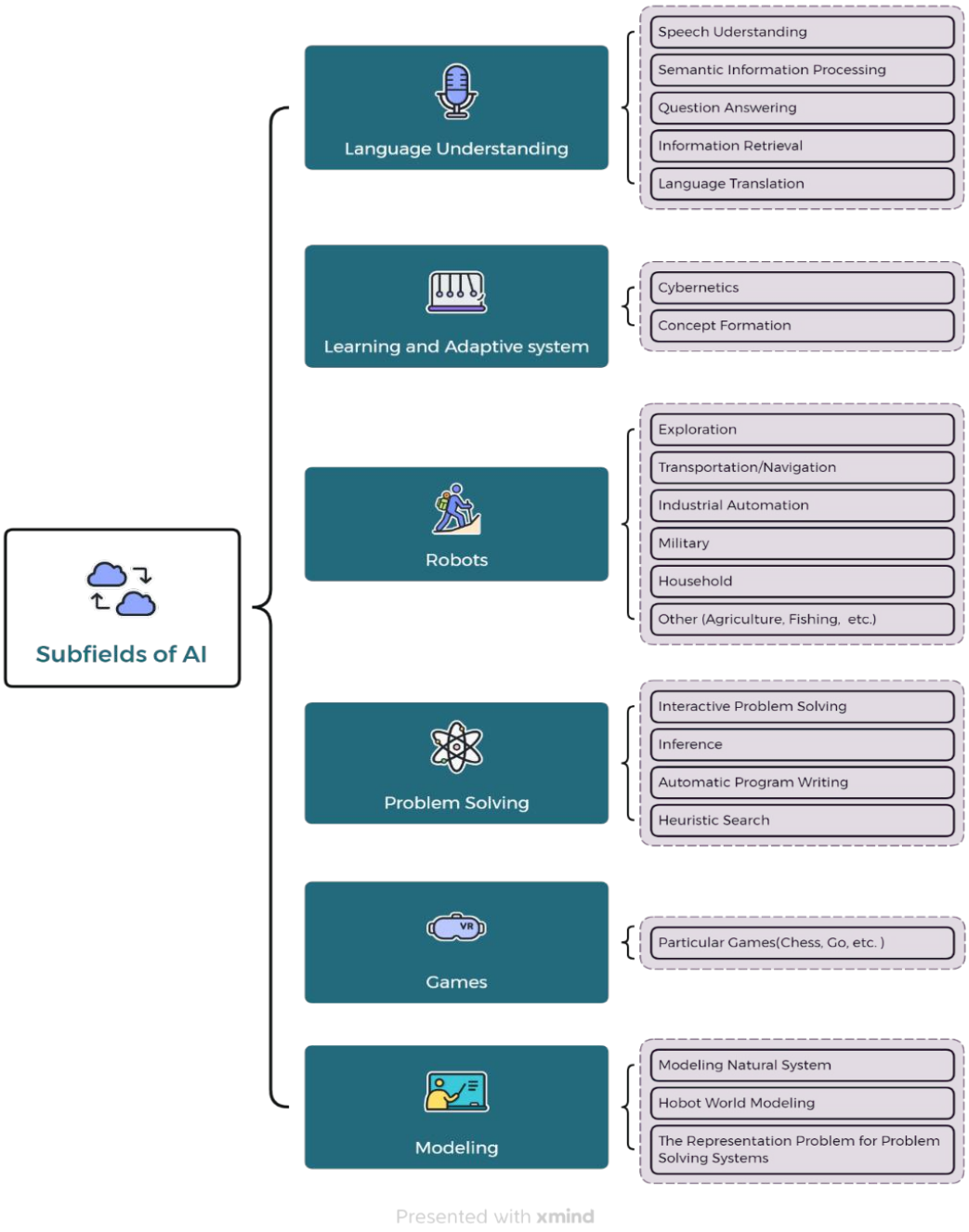

Figure 1. Subfields of AI. AI, artificial intelligence.

esthetic process. In alignment with the Perioperative Surgical Home objectives set forth by the American Society of Anesthesiologists (ASA), optimized perioperative pain control is shown to enhance patient recovery while also conferring societal and economic benefits [14]. However, conventional methods often struggle to achieve optimal pain management outcomes. Inadequate pain control can precipitate a myriad of issues for patients, encompassing both physical and mental health challenges. These may include increased susceptibility to morbidity across various organ systems, the development of depression and anxiety, prolonged pain hypersensitivity potentially progressing to chronic pain, the use of opioids and its associated adverse effects, elevated medical expenses, and a diminution in life quality [13-15].

Overcoming these obstacles and refining perioperative pain management are paramount to bolstering patient recovery and optimizing healthcare provision. In response to the potential issues outlined, medical professionals such as surgeons and anesthesiologists have endeavored to implement improvements. Over the past few decades, there has been a significant evolution in the conceptual frameworks and methodologies underpinning perioperative pain management [16, 17]. The ASA-hosted Pain

Table 1. Summary of works on "Pain Assessment"

Author/Year	Data Type	Patients/ Datasets	Target	Results	Model(best)
2015, Sikka [28]	Videos	50	Pain detection, pain intensity classification	AUC = 0.84-0.94	CVML
2022, Fontaine [29]	Images	2,180 facial expressions	Pain intensity classification (pain intensity>4/10 and >7/10)	ACC = 53% Sensitivity = 89.7%, 77.5%	ResNet-18 CNN
2022, Chen [30]	Images, videos	UNBC-Mc-Master Dataset, Wilkie's Video Dataset	Pain intensity classification	ACC = 87% AUC = 0.94	MIL, MCIL
2019, Hu [31]	Functional near-infrared spectroscopy	21	Pain detection and localization	ACC = 80.37%	3-layer NN
2021, Han [32]	EEG	67	Pain intensity classification	ACC = 92.54%	LDA
2015, Gruss [33]	Bio-potentials	85	Classification (baseline vs. pain tolerance threshold), (baseline vs. pain threshold)	Identification rate = 90.94%, 79.29%	SVM
2013, Ben-Israel [34]	Physiological parameters	25	NoL (nociception level) development and validation	AUC = 0.97 R = 0.88	Non-linear Random Forest regression
2021, Gao [35]	Clinical data	300	Pain intensity classification	ACC = 95.6%	BP
2023, Pinzon-Arenas [36]	EDA	36	Pain intensity classification	ACC = 91.5%	1D-CNN, LSTM, CNN-LSTM
2024, Carlini [37]	Facial expression	73	Pain intensity classification	ACC = 77.1% F1 = 80.8% AUC = 76.0%	CNN
2021, Salekin [38]	Visual and vocal signals	Neonatal Pain Dataset	Pain intensity classification	ACC = 79% AUC = 0.87	VGG-Net, LSTM
2021, Choi [39]	PPG	120	Pain intensity classification	ACC = 71.4% AUC = 0.76 Sensitivity = 68.3% Specificity = 73.8%	CNN
2021, Baharloo [40]	Pain intensity measured manually	218	Assess pain's slow/fast dynamics	F score = 0.79 AUC = 0.704	MLP
2016, Nickerson [41]	Clinical data	26,090	Pain intensity classification	MSE = 5.54, 4.96, 5.14, 6.09 Correlation Coefficient = 0.604, 0.606, 0.593, 0.545	Several NN models (Elastic Net)
2015, Tighe [42]	Clinical data	8,071	Pain detection	AUC = 0.643-0.727	Several ML models (LASSO)
2021, Tan [43]	Clinical data	20,716	Pain detection	AUC = 0.763-0.772 Sensitivity = 67.0-69.4% Specificity = 70.9-76.2% PPV = 28.3-31.8% NPV = 93.3-93.5%	Several ML models (Logistic regression)
2023, Llorián-Salvador [44]	Radiomics, semantic and clinical features	261	Pain intensity classification	AUROC = 0.62±0.01	ML
2024，Berg [45]	Clinical data	22,707	Pain detection	C statistic (back pain and leg pain) = 0.78(95% CI, 0.77-0.78), 0.76 (95% CI, 0.76-0.77)	ML

Note: If more than one structure/task were investigated in a study, the corresponding information are reported in the same order in which the structures are presented in the "Target"/ "Results"/"Model" columns. ACC, accuracy; AUC, area under curve; CVML, computer vision and machine-learning; MIL, multiple instance learning; MCIL, multiple clustered instance learning; NN, neural network; EEG, electroencephalography; LDA, linear discriminant analysis; SVM, support vector machine; BP, back propagation; EDA, electrodermal activity; PPG, photoplethysmogram; MLP, multilayer perceptron; LSTM, long short term memory; CNN, convolutional neural network; MSE, Mean Squared Error; PPV, Positive predictive values; NPV, negative predictive values; LASSO, least absolute shrinkage and selection operator; ML, machine learning; Clinical data, it refers to risk factors that may influence patients' cognitive of pain intensity.

Summit in 2019 reached a consensus on foundational principles for the acute management of perioperative pain [18]. These principles include integral preoperative assessment, the adoption of multimodal analgesia, personalized treatment plans, and the necessity for adaptable modifications to care strategies.

Reliable data are derived from clinical registries, administrative databases and so on. Based on the development of AI and the anxious desire for improving the status quo of perioperative pain management in order to follow advanced theories and guidelines, big data analysis has been applied in many fields of perioperative pain management, for example, assessing postoperative pain outcomes, forecasting opioid utilization, evaluating the efficiency of multimodal pain management strategies, and predicting the adverse effect caused by inaccurate pain [19].

In an era marked by the burgeoning individualization, predictability, and complexity in perioperative pain management, AI stands as a powerful tool for navigating and interpreting the intricate tapestry of data relationships. AI's capabilities are particularly well-aligned with the evolving needs of perioperative pain care, which is increasingly reliant on precise, data-driven strategies. This review delves into the synergy between AI and perioperative pain management, examining its integration in the realms of pain assessment, therapeutic interventions, and the prevention of adverse effects associated with suboptimal pain control. At the outset of each section, we provide a concise overview of the field's current landscape. Furthermore, we critically appraise the limitations of this field and speculate on its future trajectory, highlighting the potential of AI to revolutionize perioperative pain care.

AI in perioperative pain assessment

Up to now, most forms of pain assessing instruments applied in the clinical are rating scales, checklists or questionnaires, psychological screening or observational (behavioral) measures. For example, visual analogue scale, verbal rating scale, numerical rating scale and face pain scale are the most frequent tools used for pain assessment, which rely on patients' own appraisal of pain sensory [20-22]. Current methods to measure pain in the clinic are almost restricted to these classical but unidimensional tools while evidence shows there exists some bias. These unidimensional tools cannot always reflect the real reception of pain due to their subjective attributes [23-25].

In addition, the existing pain assessing tools have trouble with infants, critical patients or narcose patients who are unable to speak up, and patients with intellectual disability or dementia who cannot express themselves clearly. Apart from that, inconsistency, slowness and discontinuation of pain prediction are problems to be solved, too.

The use of AI in perioperative pain assessment

Only there is an accurate outcome for pain assessment, can doctors carry out better schemes and adjust plans of drug administration or technique implementation timely for an optimum analgesia [26]. Advantages of AI can help achieve this goal. There has already been a concept called automated pain recognition (APR). APR is an external observation method into which hardware and software components with AI are integrated. Through data collected from diverse parts of human body shown in **Figure 2**, such as facial expression, vocal information, body language, physiological data and so forth, APR can detect, locate, and classify pain [27]. As for the perioperative pain with AI, we divide the current research directions into three parts: facial expression, neural system signals and biopotential and multidimensional factors, combined with AI respectively to measure pain. In this review, 14 papers were identified to be combinations of AI and perioperative pain assessment, and their main features are presented in the **Table 1**.

Facial expression

To explore the secrets between facial expression and pain intensity, researchers have made great efforts, including animal research [46]. Even with high precision in animal experiments, algorithms for human have a long way to go since the quantity of human's facial muscles is too large to locate and analyze. In 2015, Sikka and team introduced a method for evaluating postoperative pain in children using computer vision and machine learning [28]. Their model, trained on facial expressions from 50 patients aged 5 to 18 after laparoscopic appendectomy, showed accurate pain detection and quantification with an area under the curve (AUC) of 0.84 to 0.94. While slightly outperforming nurses and matching parents' assessments, the model's accuracy was the highest under static conditions and was limited to pediatric use. Subsequent research has expanded the use of AI in pain assessment, contributing to a growing body of evidence in this field [28]. Fontaine and colleagues developed a convolutional

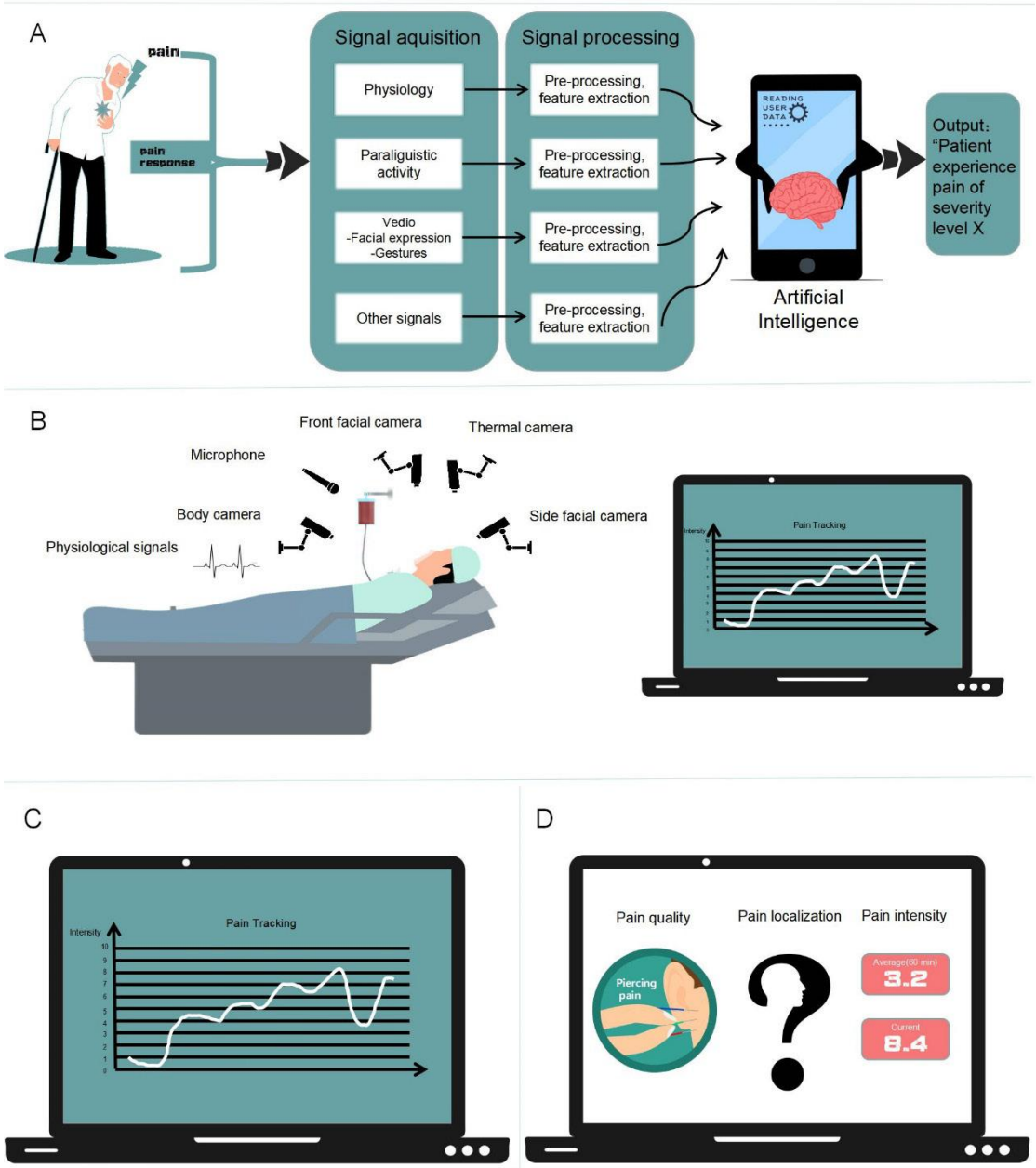

Figure 2. Basis and objectives of automated pain recognition. (A) Data processing in automated pain recognition; (B) Technical infrastructure of multimodality; (C) Monitoring of pain intensity; (D) Proposed monitoring of pain intensity, pain localization and quality.

neural network to analyze facial expressions from 1,189 patients, including 2,810 pre- and postoperative images, to assess pain intensity using the numeric rating scale. The model's performance exceeded that of nurses, with higher sensitivity in detecting moderate (> 4/10) and severe (> 7/10) pain, at 89.7% and 77.5%, respectively, compared to 44.9% and 17.0% in nurses.

However, the overall accuracy of AI (53%) and nurses (14.9%) highlight areas for technological advancement in pain assessment [29]. Chen and team in China created novel data structures to encode facial muscle action units from individual video frames and sequences [30]. Their model achieved 87% precision and an AUC of 0.94 in pain recognition, validated against the UNBC-McMaster Shoulder Pain Expression dataset [30]. In a meticulous analysis, Carlini and collaborators have isolated facial expression features unique to newborns to construct VGG-face and N-CNN deep learning models for the assessment of pain. The study records an accuracy of 77.1%, an F1 score of 80.8%, and an AUC of 76.0% [37]. Pain perception is a profoundly personal affair, and individuals often exhibit alterations in their facial expressions when experiencing intense discomfort. Consequently, the discerning observation of these nuanced changes in expression can serve as a clever means to gauge an individu-

al's state of distress. This approach is particularly beneficial when assessing neonates who are unable to articulate their own feelings, yet its utility among adults with intact language capabilities is comparatively limited.

Neural system signals and biopotentials

As deep researches carried out, certain brain areas have been scoped to be relevant to pain location, severity, duration, and other characters [47]. More and more researchers cast their attention on neural system signals and biopotentials to measure pain. Different stimuli elicit different pain responses, and they are detected by neural imaging instruments combined with given experimental variable as input. For example, on the basis of multivariate pattern analysis, functional magnetic resonance image was used to detect if there are special signals in certain brain areas while positron emission tomography and arterial spin labeling were applied to examine the cerebral blood flow to infer the presence of pain [48]. Electroencephalography derived from cortical activity is a commonly electronical approach to detect pain. In 2019, Hu et al. measured patients' cortical activity during acute pain and used neural network-based AI algorithm to analyze pain diction and location [31]. The data were collected and transmitted into visual images by Augmented Reality devices, in which they achieved an accuracy of 80.37% for pain or no pain discrimination. Neural oscillations combined with AI to predict pain also gained a high precision of 92.54%. Restrained by the limited sample, this study didn't testify the specificality of electroencephalography oscillations to acute pain which may limit clinical localization diagnostics [32]. Beyond neural activity, various biopotentials such as electromyography, skin conductance, and electrocardiography are employed to train algorithms that gauge pain intensity, tolerance, and onset. Our research yielded a 90.94% classification accuracy for distinguishing baseline from pain tolerance, and a 79.29% accuracy for differentiating baseline from pain onset [33]. A predictive model leveraging electrodermal activity as a biomarker for pain has been refined, demonstrating superior performance in detecting severe pain with a precision of 91.5%. Additionally, the model has pioneered continuous pain detection, representing substantial advancement [36].

Other factors

Pain assessment has traditionally relied on unidimensional tools, which are inadequate due to the multifaceted nature of pain [23]. Advances in multidimensional assessments incorporating AI, such as machine learning techniques, have emerged to improve accuracy. Machine learning algorithms have been engineered to analyze data from various parameters, such as plethysmograph waveforms and heart rate, in pre-operative patients, significantly improving the assessment of nociceptive responses. This is evidenced by an AUC of 0.97, markedly superior to the AUCs of individual parameters, which ranged from 0.56 to 0.74. Nonetheless, this method is currently applicable only to patients with ASA physical statuses I-II [34]. In addition, to predict postoperative pain after root canal treatment, Gao et al. collected data from 300 patients undergoing root canal treatment [35]. They established relationships between postoperative pain and 13 biophysical parameters (personal, inflammatory reaction, operative procedure factors) via building neural network models using MATLAB 7.0 neural network toolbox and obtained an accuracy of 95.60%.

Furthermore, data of the pain intensity on early postoperative days, multimodal spatial-temporal approach including signals of vision and hearing, manually measured pain intensity ratings and photolethysmogram spectrograms were exploited to be indicators applied in assessing pain intensity with AUC = 0.87, 0.76, 0.74, respectively. In conclusion, such indicators and algorithms still show space for improvement. As the data mentioned aforesaid in this paragraph, though AUC of machine learning model has achieved 0.97, its application is very limited. So future work may concentrate on indicators which are more easily to capture and analyze. Also, optimizing algorithm for pain prediction or even specified location is deserving expectation [38-40]. Utilizing data from a cohort of 261 volunteers, including radiomics, semantic, and clinical features, researchers have developed a machine learning model capable of predicting the pain response in patients suffering from painful spinal bone metastases. Specifically, the model predicts the comprehensive pain response following palliative radiotherapy [44].

Research indicates that while methods to assess pain generally exhibit good accuracy, those utilizing neural signals and biopotentials as biomarkers achieve higher averages of precision or sensitivity. However, the cost associated with these methods can limit their widespread patient adoption. In response, researchers have focused on enhancing systems by refining algorithms. For example, in a recent prospective multicenter study, a machine learning model was developed to predict postoperative pain

following lumbar disc herniation surgery, involving a total of 22,707 participants. The model yielded C statistics ranging from 0.75 to 0.80 for back pain and 0.74 to 0.77 for leg pain predictions [45]. Nickerson et al. built 4 models to evaluate accuracy of pain intensity and found that the Elastic Net performed the best to predict pain intensity with mean squared error of 4.96 and correlation coefficient of 0.606 [41].

Besides, Tighe et al. developed five models to assess their efficacy in predicting severe postoperative pain, with the least absolute shrinkage and selection operator model emerging as the most effective, boasting an AUC of 0.704 [42]. When comparing regression methods to machine learning models for predicting breakthrough pain during labor neuraxial analgesia, the machine learning models edged out the competition slightly. In practical terms, the two approaches exhibited similar performance, with AUCs ranging from 0.763 to 0.772, sensitivities from 67.0 to 69.4%, specificities from 70.9 to 76.2%, positive predictive values from 28.3 to 31.8%, and negative predictive values from 93.3 to 93.5%. These results suggest that further research and algorithmic refinement are necessary to enhance current prediction capabilities [43].

Moreover, each independent study has introduced distinct algorithms for comparative analysis, utilizing a heterogeneous array of data. Consequently, the optimal results from these disparate investigations offer limited utility for cross-comparison. As efforts to refine accuracy persist, relentless exploration remains an imperative. Clinical data, such as vital signs, are relatively accessible, making it objectively informative to learn from these vital signs to predict pain. However, the majority of current studies are retrospective, thereby suffering from a considerable degree of lag.

AI in perioperative pain treatment

In terms of perioperative analgesia, patients hold high expectations on comfortableness, and the requirements of analgesia vary among different patients [49]. To meet patient needs, opioid drug was prescribed beyond their real needs, leading to opioid epidemic, which induced thousands of citizens' addiction and death [50, 51]. Consequently, more flexible and secure techniques are in urgent needs due to the contradiction between patients' ever-growing expectation for better pain management and inadequate antalgic development. To solve this problem, scientists have made unremitting efforts. Thus, patient-controlled analgesia (PCA), a medical device applied in analgesia, which is used for patients to adjust dosage of drugs according to the sensory of pain based on the prescription, was invented [52]. With the development of technology, there are a few types of PCA, from traditional PCA, wireless PCA to AI-assisted PCA which is discussed in this article [53].

Although PCA is one of the most popular technologies applied in analgesia, anesthesiologists also use nerve block in intraoperative general anesthetic or postoperative analgesia courses [14]. Nerve block owns its unique advantages in perioperative pain management, such as a decrease in the opioid use, shortening the length of stay, and a more agreement with enhanced recovery after surgery protocols [16]. However, some problems in the nerve block field remain to be solved. For example, it's hard to precisely localize a nerve, or it may damage important anatomical structures near the target nerve like arteries or other nerves [54, 55]. In this review, we identified a total of 8 articles investigated combinations of AI and perioperative pain treatment, and their main characteristics are reported in the **Table 2**.

AI in pain treatment

As mentioned above, when combined with AI, many things change. In the next paragraphs, we'll discuss how AI is applied in PCA and nerve block.

PCA

Back to 2012, on the premise of having learned 280 attributes of 1,099 patients, Hu et al. developed a predictive model for analgesic dosing [56]. They utilized a decision tree-based algorithm to forecast both total and PCA drug requirements based on the initial two-hour consumption. Their model achieved an accuracy of 80.9% for total dosage and 73.1% for PCA dosage predictions. Despite the labor-intensive process of manually collecting data at the time, another study employed a multi-model regression tree (MRT) approach to analyze the profiles of 3,052 IV-PCA patients, aiming to predict analgesic usage. MRT outperformed their proposed algorithms, human expert predictions, and traditional methods like linear regression and F-text, with the lowest root mean square error. The researchers intentioned to enhance the model by integrating expert knowledge into the MRT system, moving towards a model that is both data-driven and knowledge-driven [57]. Research has suggested that the analgesia nociception index correlates with pain medication

Table 2. Summary of works on "Pain Treatment"

Author/Year	Data Type	Patients/ Dataset	Target	Results	Model(best)
2012, Hu [56]	PCA usage	1,099	Strategies of drug infusion (Total Analgesic Consumption and PCA Analgesic Requirement)	ACC = 80.9% ACC = 71.3%	Decision tree-based learning
2018, Hu [57]	Clinical data	3,052	Strategies of drug infusion	The least RMSE (compared with human experts)	MRT
2018, Gonzalez [58]	ANI signal	15	Strategies of drug infusion	ACC = 81%	Several ML models (SVM)
2020, Nair [59]	Clinical data	13,700	Prediction on drug dosage	ACC = 72%	Several ML models (Random Forest)
2011, Tighe [60]	Clinical data	349	Predict needs for nerve block	AUC = 0.7	Several ML models (AD Tree)
2021, Liu [61]	Ultrasound images	100	Assist nerve block	ACC enhancement = 0.5-12.5%	SegNet Model
2022, Yang [62]	Ultrasound images	1,126	Assist nerve block	ACC = 96% Sensitivity = 97.7% Specificity = 84.6%	CNN
2016, Smistad [63]	CT images	48 ultrasound image sequences	Locate anatomic markers	Average DSC = 0.91	Kalman filter

Note: If more than one structure/task were investigated in a study, the corresponding results are reported in the same order in which the structures are presented in the "Target"/"Results"/"Model" columns. PCA, patient controlled analgesia; ACC, accuracy; AUC, area under curve; RMSE, root mean square error; MRT, multimodal regression tree; SVM, support vector machine; ANI, analgesia nociception index; ML, machine learning; CNN, convolutional neural network; CT, computed tomography; AD Tree, alternating decision tree; DSC, dice similarity coefficient; Clinical data, it refers to risk factors that may influence the dosage of drug or the likelihood one needs nerve block.

dosage, potentially enabling the prediction of drug consumption using AI [64]. By employing various machine learning models, investigators explored the relationship between analgesia nociception index and the administration of intravenous remifentanil. Analysis of data from 15 patients undergoing cholecystectomy surgery at specific time points revealed that the support vector machines (SVM) model yielded the highest accuracy of 81%. However, the small sample size limits the generalizability of these findings [58].

In contrast, Nair et al. analyzed pre-operative data from 13,700 adult patients, including patient characteristics, procedures, and other factors that could influence post-operative pain and opioid consumption [59]. These data were split into training and validation sets for model training and testing. The researchers observed outcomes throughout both the pre-operative and post-operative phases and found only a minimal difference in prediction accuracy between the two periods, suggesting that AI algorithms can effectively predict post-operative opioid usage based on pre-operative data. However, as opioid usage increased, accuracy rates declined from 89% to 43%. It is important to note that this study was conducted at a single center and focused solely on outpatients, which may introduce bias into the results.

AI has indeed enhanced the precision of PCA by improving drug infusion accuracy. However, there are limitations to its application. For instance, the role of genetic and psychological factors in the efficacy of analgesic drugs, as reported in some studies, has not been fully integrated into AI models due to a lack of comprehensive research in these areas and the absence of detailed genomic and psychological patient data [65- 68]. Furthermore, the quality of the data sources could be improved; many studies have been confined to single centers or have utilized datasets that are too limited in scope.

Nerve block

As early as 2011, Tighe et al. gathered perioperative data from 349 patients to develop prediction algorithms [60]. Five different algorithms—

BayesNet, multilayer perceptron, SVM, ADTree, and simple logistic regression—were used to forecast the need for femoral nerve block after anterior cruciate ligament surgery. The ADTree algorithm emerged as the most effective, with an AUC of 0.7 in cross-validation. However, the complexity of machine learning algorithms and the limited understanding among clinical physicians at the time posed a challenge. The study's limitations include a small sample size and the absence of single-unit predictors. Subsequent reports have shown that AI-assisted ultrasound nerve block outperforms traditional methods in terms of accuracy and reduced operation time. The AI model's accuracy enhancement ranged from 0.5% to 12.5%, suggesting more efficient anesthesia and a reduction in post-operative complications, particularly in scapular fracture surgeries [61]. In the realm of nerve localization, AI has shown remarkable prowess. By utilizing AI algorithms, anatomical markers specific to nerves were learned and translated into sonography guidance, facilitating procedures such as inter-scalene, supraclavicular, and infraclavicular blocks. The AI-assisted system significantly enhanced the accuracy of nerve location for anesthesiologists, achieving a 96% accuracy rate, with 97.7% sensitivity and 84.6% specificity [62]. The integration of ultrasound with AI is marked by the attribute of real-time functionality. A real-time 3D vessel reconstruction algorithm, derived from an extended Kalman filter, was employed to locate, allocate, and reconstruct the 3D model of the femoral artery during ultrasound-guided femoral nerve block procedures. This tracking algorithm demonstrated high precision and rapid processing in identifying the anatomical position of the femoral artery, yielding an average dice similarity coefficient of 0.91 [63].

While AI has significantly streamlined nerve block procedures, particularly by improving precision in nerve location, there is ongoing need for advancements. The challenges in nerve block are not confined to the identification of anatomical markers; there are also discrepancies between ultrasound anatomical recognition and the coordination of the needle and probe. Aspects such as the initial scan location, pressure, tilt, rotation, and angulation of the probe needle remain under the control of practitioners. These areas could represent future directions for AI development to enhance its capabilities in nerve block procedures.

Risk prediction of adverse effects associated with pain management

Many factors and reasons contribute to challenges in the process of perioperative pain management, including anesthesia, patients, and surgeries, which give rise to intraoperative hypotension and bradycardia, postoperative urinary retention (POUR) and so on [69]. Among all these factors, opioid use matters a lot. Although multimodal analgesia has been advocated to optimize effects of analgesia and to reduce opioid side effects, opioid usage still plays an important part in pain management and it can bring many side effects like nausea and vomiting, constipation, respiratory depression and so forth [70, 71]. Since adverse effects caused by nerve block could mainly be avoided through locating precisely, details on which are not introduced here. Common and severe adverse reactions resulted from analgesic medications are mainly discussed in the **Table 3**.

AI in adverse event prediction

Overdose of opioid use

Chronic opioid use, previously encapsulated by the term "opioid extended use," is now further complicated by evidence that surgery can become a risk factor [86]. The critical nature of identifying and forecasting opioid overdose looms large. Investigations, such as those led by Karhade, have tested the application of AI in predicting continued opioid prescriptions post-surgery. These trials focused on preoperative data and biophysical patient characteristics from various surgical procedures. Utilizing a dataset of 5,413 patients with lumbar disc herniation, a study evaluated the efficacy of five machine learning models in predicting continued opioid use. Findings highlighted that 7.7% of patients experienced extended opioid prescription, with the Elastic-net Penalized Logistic Regression model exhibiting the least bias and a commendable calibration rate (c-statistic = 0.81), thus emerging as the most effective among the models tested [72]. Subsequent research by Karhade et al. exploring the postoperative opioid use in patients following total hip arthroplasty and anterior cervical discectomy and fusion corroborated the utility of the Elastic-net Penalized Logistic Regression and Stochastic Gradient Boosting algorithms, with c-statistics of 0.77 and 0.81, respectively [73, 74]. In addition, Klemt et al. developed five machine learning models to analyze clinical data and forecast the risk of prolonged opioid use, achieving high accuracy in predictions (AUC > 80%) [75]. These models not only predicted risk but also identified the relative importance of each risk factor, enabling more objective decision-making than subjective expert judgment. Klemt's work highlighted that a preoperative

Table 3. Summary of works on "Adverse Effects Associated with Pain Management"

Author/Year	Data Type	Patients/ Datasets	Target	Results	Model(best)
2019, Karhade [72]	Clinical data	5,413	Predict prolonged opioid use	c-statistic = 0.81	Several ML models (Elastic Net Penalized Logistic)
2019, Karhade [73]	Clinical data	5,507	Predict prolonged opioid use	c-statistic = 0.77	Several ML models (Elastic Net Penalized Logistic)
2019, Karhade [74]	Clinical data	2,737	Predict prolonged opioid use	c-statistic = 0.81	Several ML models (Stochastic Gradient Boosting)
2022, Klemt [75]	Clinical data	8,873	Predict prolonged opioid use	AUC > 80%	Several ML models (ANN)
2006, Peng [76]	Clinical data	1,086	Predict occurrence of PONV	ACC = 83.3% Specificity = 85.0% Sensitivity = 77.9% AUC = 0.814	Several classifiers (ANN)
2012, Bassanezi [77]	Clinical data	198	Predict occurrence of PONV	AUC = 0.72	Fuzzy logic
2014, Gong [78]	Clinical data	195	Predict occurrence of PONV	AUC = 0.761 AUC = 0.900	LR, ANN
2016, Wu [79]	Clinical data	195	Predict occurrence of PONV	AUC = 0.734 AUC = 0.929	LR, SVM
2016, Nickerson [41]	Clinical data	26,090 clinical records	Predict occurrence of POUR	ACC = 66.0%	Several ML models (SVM)
2022, Porche [80]	Clinical data	891	Predict occurrence of POUR	AUC = 0.753 Specificity = 68.2% Sensitivity = 72.9% PPV = 43.4% NPV = 88.2%	Combination of binomial logistic model and MLP
2018, Hatib [81]	Arterial waveform	1,334	Predict occurrence of hypotension (before 15min, 10min, 5min respectively)	AUC = 0.95, 0.95, 0.97 Specificity = 88%, 89%, 92% Sensitivity = 90%, 92%, 97%	LR
2021, Lee [82]	Bio-signal waveforms	3,301	Predict occurrence of hypotension (invasive and non-invasive groups)	AUC = 0.897, 0.762 less MAE than non-AI method	CNN
2020, Solomon [83]	Clinical data	62,182	Predict occurrence of bradycardia (3 phases during the procedure)	AUC = 0.81, 0.87, 0.89 PPV at 95% specificity = 0.30, 0.29, 0.15	GBM
2020, Chou [84]	ABP	83,905 ABP waves	Predict occurrence of bradycardia	Specificity = 99.74 ± 0.07% Sensitivity = 93.12 ± 1.24% ACC = 99.37 ± 0.10% Kappa coefficient = 93.92 ± 0.92%.	Several classifiers (DT)
2019, Jungquist [85]	Electronic monitoring biomedical data	60	Predict occurrence of OIRD	ACC = 80%	SVM

Note: If more than one structure/task were investigated in a study, the corresponding results are reported in the same order in which the structures are presented in the "Target"/"Results"/"Model" columns. ACC, accuracy; AUC, area under curve; ML, machine learning; PONV, postoperative nausea and vomiting; LR, logistic regression; ANN, artificial neural network; SVM, support vector machine, POUR, post-operative urinary retention; PPV, Positive predictive values; NPV, negative predictive values; MLP, multilayer perceptron; CNN, convolutional neural network; GBM, gradient boosting machine; DT, decision tree; OIRD, opined-induced respiratory depression; ABP, arterial blood pressure; MAE, mean absolute error; Clinical data, it refers to risk factors that may contribute to an occurrence of a clinical event.

opioid use duration of more than 90 days was a potent predictor of extended postoperative opioid prescription.

The aforementioned studies, while rich in sample size, are limited by their retrospective design, which lacks diverse experimental classification. Furthermore, the samples were drawn from a tertiary referral center, thus potentially lacking broader population representation.

Nausea and vomiting

Postoperative nausea and vomiting (PONV), as one of the most common complications after surgeries, often leads to patient dissatisfaction. Many well-established and potential risk factors were detected or supposed to cause PONV among which intraoperative and postoperative opioid use plays a significant role [87].

In exploring the intersection of AI and prediction of PONV, researchers initiated studies as early as 2006. They constructed an artificial neural network (ANN) from a dataset of 1,086 patient profiles to predict PONV based on multiple risk factors. Concurrently, four alternative algorithms—Naive Bayesian classifier, logistic regression, Koivuranta score, and simplified Apfel score—were developed for comparative analysis. The ANN demonstrated superior performance, with an accuracy of 83.3%, an AUC of 0.814, a sensitivity of 85.0%, and a specificity of 77.9%, asserting its dominance among the five models tested [76].

In a 2012 study, the Eberhart score was extensively utilized to predict PONV in pediatric patients. However, its efficacy has been questioned by the emergence of fuzzy logic systems, which offer enhanced predictive capabilities by analyzing preoperative risk factors. The findings revealed that the Eberhart score achieved an AUC of 0.62, in contrast to the fuzzy logic model, which attained an AUC of 0.72 [77]. But at that time, it remained unknown how much does every risk factor contributes to the occurrence of PONV. Later, new methods were introduced by Wu and Gong et al. in the prediction work looking for better ways of predicting the PONV during the patient-controlled epidural analgesia [78, 79]. Logistic regression model, ANN, SVM obtained great results, with fairly high accuracy and AUC of 0.734, 0.900, 0.929, respectively. Also, they found female sex is the strongest risk factor in patient-controlled epidural analgesia [78, 79]. Pity is that only small samples were collected and were from single center, so deeper research is needed to validate the outcomes.

Urinary retention

POUR affects 5-70% of patients, prolonging hospital stays and raising the risk of urinary tract infections. Anesthesia and analgesic use are key factors contributing to POUR development [88].

In 2016, on the basis of stacked neural network, Nickerson et al. updated the classification neural network, by setting an upper limit on neuron weight vector norms and rectifying linear unit activation functions [41]. They used an updated algorithm to estimate the risk of complications of POUR and obtained an accuracy of 66.0% using classifiers to predict risks of POUR, achieving more powerful results than traditional methods. However, the algorithm could not determine the exact time of POUR onset. Porche et al. developed a model combining a binomial logistic model and a multilayer perceptron, trained on preoperative data including pain and opioid use, to predict POUR incidence [80]. While achieving an AUC of 0.753, the model's specificity and sensitivity for prediction were only 68.2% and 72.9%, respectively.

Hypotension and bradycardia

When conducting epidural analgesia, hypotension is a very common side effect due to physiological principles of this technique, whose incidence ranks from 0 to 50% [89]. There is an even higher incidence of hypotension of spinal-epidural analgesia than epidural analgesia [90]. Intraoperative blood pressure changes in an imperceptible way, so identifying it early helps predict hypotension which may lead to unfavorable patient outcomes like malignant bradycardia, issue hypoperfusion, and organ dysfunction [91].

In 2018, Hatib et al. utilized invasive arterial waveforms to create algorithms capable of predicting intraoperative hypotension with high accuracy [81]. The algorithm accurately predicted hypotension 15, 10, and 5 minutes before it occurred, achieving AUC values of 0.95, 0.95, and 0.97, respectively, with specificities of 88%, 89%, and 92%, and sensitivities of 90%, 92%, and 97%. The precision of the predictions increased as the time of occurrence approached [81]. But it's an invasive approach. If it's non-invasive, it will be more acceptable for it takes safety into account. In 2021, Lee et al. developed algorithms capable of predicting real-time intraoperative hypotension from multiple bio-signals, including arterial pressure waveforms, capnography, photoplethysmography, and electrocardiography [82]. The study

compared invasive and noninvasive methods, revealing that multichannel models outperformed single bio-signal models in terms of accuracy and mean absolute error, with AUC values of 0.897 and 0.762, respectively. Nonetheless, the extent of blood pressure decrease and the timing of appropriate medical interventions remain uncertain.

Bradycardia may happen during the epidural or spinal analgesia, and it can also be a subsequence of hypotension [92]. Solomon et al. constructed logistic regression models using preoperative and real-time intraoperative data to predict the occurrence of severe bradycardia following hypotension at various stages of surgery, achieving AUC values of 0.81, 0.87, and 0.89 for induction (TP1), procedure start (TP2), and 30 minutes post-procedure (TP3), respectively [83]. They identified the most significant risk factors for each surgical phase and confirmed the effectiveness of their models. However, by raising the threshold for vital signs, the true incidence of toxic events may be higher than reported. In another research, Chou et al. used arterial blood pressure waves to develop a neural network and decision tree to detect changes predictive of extreme bradycardia, finding the decision tree model to be the most accurate with 99% specificity and accuracy, and a sensitivity of 93.12% [84].

Respiratory depression

Despite the fact that opioid-induced respiratory depression (OIRD) is rare, aftermath of it can be severe, even fatal [93]. Jungquist et al. enrolled 60 patients who underwent surgery, monitoring their respiratory parameters like SpO_2 and end-tidal CO_2 levels on the first day of their surgery [85]. Further, they constructed machine learning models to analyze these data to predict OIRD. With an 80% accuracy rate, their models can predict an OIRD before a real event happens. But this is observational research, lacking higher level of evidence.

Limitations of the current AI techniques

Nowadays, human is at a stage called artificial narrow intelligence, which allows the completion of single task but with narrow border application. Away from superintelligence, there is still a long distance to trek [94].

Firstly, there is significant scope for enhancing the predictive accuracy of AI. Present-day AI systems lack foolproof precision, and even the most rudimentary algorithms can exhibit biases. This is particularly pertinent in the field of medicine, and particularly in anesthesia, where all interventions involve the human body, leaving little room for errors. In the context of pain assessment, as previously mentioned, studies have seldom reported accuracy rates exceeding 90%. Furthermore, the data utilized as input for AI are, at best, historical; this implies that AI learning may be compromised by flawed clinical judgments or the exclusion of certain scenarios [19].

Second, on most occasions, AI technology could only calculate an outcome but is not able to trace the root cause. It seems that what AI probed is the surface of a huge iceberg, but the rest of it hides under the sea level. The practice of anesthesiology needs not only the high sense of accuracy but also detailed analysis of problems detected during surgeries, including the original etiological factors, the whole process of pathophysiology, and at last, the optimum solutions to the problem. It may exist a circumstance that the machine obtains a certain outcome through the database constructed by the clinical data all over the world, but it's hard for the clinicians to determine whether the outcome is true or false according to his or her own clinical experience, let alone to analyze the etiological factors [7]. As discussed above, AI can predict hypotension and PONV, but it remains confusing whether clinicians should carry out measures to change the situation when the alarm is on.

Additionally, systematical and united databases are waited to construct, while this contradicts personal privacy protection to some extent, which presents a large challenge in linking big biomedical data [95]. In the realm of AI applications, a pressing concern has been the ethical dilemmas previously identified in extant research. These encompass a spectrum of principles, including prudence, equity, privacy, responsibility, democratic participation, and solidarity [96]. For instance, AI algorithms exhibit formidable prowess in language and graphical processing, facilitating significant advancements in clinical robotics capable of interacting with patients. Nonetheless, trust remains a paramount issue, encroaching upon the patient-provider relationship and the interface between patients and AI systems [97]. Another case in point is the globally captivating AI chatbot, ChatGPT, which generates convincingly coherent sentences by mimicking linguistic statistical patterns gleaned from vast text databases culled from the internet. However, this convenience has been disruptive to various domains, including academia, prompting numerous publishers to withhold recognition

of AI-generated manuscript editing. The implications of such developments are far-reaching and demand rigorous contemplation and regulatory oversight to navigate the complex ethical landscape of AI deployment [98].

Conclusions

In summary, although current AI technologies have their limitations, the potential of AI to tackle complex challenges and to rapidly illuminate complex relationships is evident. This has led to its successful integration into perioperative pain management, enhancing our understanding and paving the way for future developments. This review presents a curated forecast of future research directions in this domain.

Current literature highlights that existing models and algorithms often fall short due to low accuracy and insufficient reliability, usually stemming from single-center or retrospective observational design. Future endeavors may overcome these hurdles by continually refining algorithms to bolster clinical tools for perioperative pain management. As AI and pain management progress swiftly, current research predominantly focuses on integrating AI with mainstream pain management techniques, albeit with limited functionalities. The trend is shifting towards multifaceted pain management strategies to optimize therapeutic outcomes. AI's potential role in the clinic is poised to evolve into a multifunctional entity, possibly encompassing pain assessment, treatment, and prediction of adverse effects in the future.

The future trajectory of each field is discussed, identifying potential opportunities to address current shortcomings. In pain assessment, researchers may identify additional indicators to refine pain intensity measurements, with the advent of next-generation devices expected to offer real-time monitoring during surgeries. Pain treatment may see the development of AI-integrated devices that assist clinicians in drug selection and dosing. AI's role in nerve block procedures could expand to ultrasound guidance, anatomical localization, and precise needle insertion. Predicting adverse effects could be enhanced with future techniques that provide comprehensive analyses and actionable recommendations for practitioners. These envisioned advancements promise to refine the precision and effectiveness of pain management in perioperative care, justifying further research to explore these promising avenues.

Author Contributions: Yan Liao, Wangzheqi Zhang, Zhanheng Chen: Conceptualization, Writing - original draft. LinDong Chen, Yanchen Lin, Ping Li: Writing - review & editing. Miao Zhou: Supervision. Mi Li, Chunhua Liao: Conceptualization & Writing - review & editing.

References

[1] Kaul V, Enslin S, Gross SA. History of artificial intelligence in medicine. Gastrointest Endosc 2020;92(4):807-812.

[2] Ramesh A, Kambhampati C, Monson J, et al. Artificial intelligence in medicine. Ann R Coll Surg Engl 2004;86(5):334-338.

[3] Meskó B, Hetényi G, Győrffy Z. Will artificial intelligence solve the human resource crisis in healthcare? BMC Health Serv Res 2018;18(1):1-4.

[4] Pannu A. Artificial Intelligence and its Application in Different Areas. Comput Sci 2015;4(10).

[5] Hashimoto DA, Witkowski E, Gao L, et al. Artificial Intelligence in Anesthesiology: Current Techniques, Clinical Applications, and Limitations. Anesthesiology 2020;132(2):379-394.

[6] Kriegeskorte N, Golan T. Neural network models and deep learning. Curr Biol 2019;29(7):R231-R236.

[7] Connor CW. Artificial Intelligence and Machine Learning in Anesthesiology. Anesthesiology 2019;131(6):1346-1359.

[8] Mathis MR, Kheterpal S, Najarian K. Artificial Intelligence for Anesthesia: What the Practicing Clinician Needs to Know: More than Black Magic for the Art of the Dark. Anesthesiology 2018;129(4):619-622.

[9] Lötsch J, Ultsch A. Machine learning in pain research. Pain 2018;159(4):623-630.

[10] Woolf CJ. What is this thing called pain? J Clin Invest 2010;120(11):3742-3744.

[11] Raja SN, Carr DB, Cohen M, et al. The Revised IASP definition of pain: concepts, challenges, and compromises. Pain 2020;161(9):1976-1982.

[12] Buvanendran A, Fiala J, Patel KA, et al. The Incidence and Severity of Postoperative Pain following Inpatient Surgery. Pain Med 2015;16(12):2277-2283.

[13] Gan TJ. Poorly controlled postoperative pain: prevalence, consequences, and prevention. J Pain Res 2017;10:2287-2298.

[14] Pozek JPJ, De Ruyter M, Khan TW. Comprehensive Acute Pain Management in the Perioperative Surgical Home. Anesthesiol Clin 2018;36(2):295-307.

[15] Glare P, Aubrey KR, Myles PS. Transition from acute to chronic pain after surgery. Lancet 2019;393(10180):1537-1546.

[16] Mitra S, Carlyle D, Kodumudi G, et al. New Advances in Acute Postoperative Pain Management. Curr Pain Headache Rep

2018;22(5):35.
[17] Hyland SJ, Brockhaus KK, Vincent WR, et al. Perioperative Pain Management and Opioid Stewardship: A Practical Guide. Healthcare 2021;9(3):333.
[18] Mariano ER, Dickerson DM, Szokol JW, et al. A multisociety organizational consensus process to define guiding principles for acute perioperative pain management. Reg Anesth Pain Med 2022;47(2):118-127.
[19] Müller-Wirtz LM, Volk T. Big Data in Studying Acute Pain and Regional Anesthesia. J Clin Med 2021;10(7):1425.
[20] Hadjileontiadis LJ. EEG-Based Tonic Cold Pain Characterization Using Wavelet Higher Order Spectral Features. IEEE Trans Biomed Eng 2015;62(8):1981-1991.
[21] Breivik H, Borchgrevink PC, Allen SM, et al. Assessment of pain. Br J Anaesth 2008;101(1):17-24.
[22] Williamson A, Hoggart B. Pain: a review of three commonly used pain rating scales. J Clin Nurs 2005;14(7):798-804.
[23] Baamer RM, Iqbal A, Lobo DN, et al. Utility of unidimensional and functional pain assessment tools in adult postoperative patients: a systematic review. Br J Anaesth 2022;128(5):874-888.
[24] Pasero C, Quinlan-Colwell A, Rae D, et al. American Society for Pain Management Nursing Position Statement: Prescribing and Administering Opioid Doses Based Solely on Pain Intensity. Pain Manag Nurs 2016;17(5):291-292.
[25] van Dijk JFM, Kappen TH, Schuurmans MJ, et al. The Relation Between Patients' NRS Pain Scores and Their Desire for Additional Opioids after Surgery. Pain Pract 2015;15(7):604-609.
[26] Ravaud P, Keïta H, Porcher R, et al. Randomized clinical trial to assess the effect of an educational programme designed to improve nurses' assessment and recording of postoperative pain. Br J Surg 2004;91(6):692-698.
[27] Walter S, Gruss S, Frisch S, et al. "What About Automated Pain Recognition for Routine Clinical Use?" A Survey of Physicians and Nursing Staff on Expectations, Requirements, and Acceptance. Front Med 2020;7:566278.
[28] Sikka K, Ahmed AA, Diaz D, et al. Automated Assessment of Children's Postoperative Pain Using Computer Vision. Pediatrics 2015;136(1):e124-131.
[29] Fontaine D, Vielzeuf V, Genestier P, et al. Artificial intelligence to evaluate postoperative pain based on facial expression recognition. Eur J Pain 2022;26(6):1282-1291.
[30] Chen Z, Ansari R, Wilkie DJ. Learning Pain from Action Unit Combinations: A Weakly Supervised Approach via Multiple Instance Learning. IEEE Trans Affect Comput 2022;13(1):135-146.
[31] Hu XS, Nascimento TD, Bender MC, et al. Feasibility of a Real-Time Clinical Augmented Reality and Artificial Intelligence Framework for Pain Detection and Localization From the Brain. J Med Internet Res 2019;21(6):e13594.
[32] Han Q, Yue L, Gao F, et al. The Prediction of Acute Postoperative Pain Based on Neural Oscillations Measured before the Surgery. Neural Plast 2021;2021:5543974.
[33] Gruss S, Treister R, Werner P, et al. Pain Intensity Recognition Rates via Biopotential Feature Patterns with Support Vector Machines. PLoS One 2015;10(10):e0140330.
[34] Ben-Israel N, Kliger M, Zuckerman G, et al . Monitoring the nociception level: a multi-parameter approach. J Clin Monit Comput 2013;27(6):659-668.
[35] Gao X, Xin X, Li Z, et al. Predicting postoperative pain following root canal treatment by using artificial neural network evaluation. Sci Rep 2021;11(1):17243.
[36] Pinzon-Arenas JO, Kong Y, Chon KH, et al. Design and Evaluation of Deep Learning Models for Continuous Acute Pain Detection Based on Phasic Electrodermal Activity. IEEE J Biomed Health Inform 2023;27(9):4250-4260.
[37] Carlini LP, Coutrin GAS, Ferreira LA, et al. Human vs machine towards neonatal pain assessment: A comprehensive analysis of the facial features extracted by health professionals, parents, and convolutional neural networks. Artif Intell Med 2024 Jan;147:102724.
[38] Salekin MS, Zamzmi G, Goldgof D, et al. Multimodal spatio-temporal deep learning approach for neonatal postoperative pain assessment. Comput Biol Med 2021;129:104150.
[39] Choi BM, Yim JY, Shin H, et al. Novel Analgesic Index for Postoperative Pain Assessment Based on a Photoplethysmographic Spectrogram and Convolutional Neural Network: Observational Study. J Med Internet Res 2021;23(2):e23920.
[40] Baharloo R, Principe JC, Fillingim RB, et al. Slow Dynamics of Acute Postoperative Pain Intensity Time Series Determined via Wavelet Analysis Are Associated With the Risk of Severe Postoperative Day 30 Pain. Anesth Analg 2021;132(5):1465-1474.
[41] Nickerson P, Tighe P, Shickel B, et al. Deep neural network architectures for forecasting analgesic response. Annu Int Conf IEEE Eng Med Biol Soc 2016;2016:2966-2969.
[42] Tighe PJ, Harle CA, Hurley RW, et al. Teaching a Machine to Feel Postoperative Pain: Combining High-Dimensional Clinical Data with Machine Learning Algorithms to Fore-

cast Acute Postoperative Pain. Pain Med 2015;16(7):1386-1401.
[43] Tan HS, Liu N, Sultana R, et al. Prediction of breakthrough pain during labour neuraxial analgesia: comparison of machine learning and multivariable regression approaches. Int J Obstet Anesth 2021;45:99-110.
[44] Llorián-Salvador Ó, Akhgar J, Pigorsch S, et al. The importance of planning CT-based imaging features for machine learning-based prediction of pain response. Sci Rep 2023;13(1):17427.
[45] Berg B, Gorosito MA, Fjeld O, et al. Machine Learning Models for Predicting Disability and Pain Following Lumbar Disc Herniation Surgery. JAMA Netw Open 2024;7(2):e2355024.
[46] Andresen N, Wöllhaf M, Hohlbaum K, et al. Towards a fully automated surveillance of well-being status in laboratory mice using deep learning: Starting with facial expression analysis. PLoS One 2020;15(4):e0228059.
[47] Schweinhardt P, Bushnell MC. Pain imaging in health and disease--how far have we come? J Clin Invest 2010;120(11):3788-3797.
[48] Davis KD, Flor H, Greely HT, et al. Brain imaging tests for chronic pain: medical, legal and ethical issues and recommendations. Nat Rev Neurol 2017;13(10):624-638.
[49] Zhou Y, Xie CB, Tu WF. Emphasis on promotion and popularization of comprehensive goal-directed perioperative analgesia. Perioper Saf Qual Assur 2017;1(2):55-59.
[50] Gawande AA. It's Time to Adopt Electronic Prescriptions for Opioids. Ann Surg 2017;265(4):693-694.
[51] Skolnick P. The Opioid Epidemic: Crisis and Solutions. Annu Rev Pharmacol Toxicol 2018;58:143-159.
[52] Sechzer PH. Objective Measurement of Pain. Anesthesiology 1968;29(1):209-209.
[53] Wang R, Wang S, Duan N, et al. From Patient-Controlled Analgesia to Artificial Intelligence-Assisted Patient-Controlled Analgesia: Practices and Perspectives. Front Med (Lausanne) 2020;7:145.
[54] Helen L, O'Donnell BD, Moore E. Nerve localization techniques for peripheral nerve block and possible future directions. Acta Anaesthesiol Scand 2015;59(8):962-974.
[55] Strakowski JA. Ultrasound-Guided Peripheral Nerve Procedures. Phys Med Rehabil Clin N Am 2016;27(3):687-715.
[56] Hu YJ, Ku TH, Jan RH, et al. Decision tree-based learning to predict patient controlled analgesia consumption and readjustment. BMC Med Inform Decis Mak 2012;12:131.
[57] Hu YJ, Ku TH, Yang YH, et al. Prediction of Patient-Controlled Analgesic Consumption: A Multimodel Regression Tree Approach. IEEE J Biomed Health Inform 2018;22(1):265-275.
[58] Gonzalez-Cava JM, Arnay R, Méndez Pérez JA, et al. A Machine Learning Based System for Analgesic Drug Delivery. International Joint Conference SOCO'17-CISIS'17-ICEUTE'17 León, Spain, September 6-8, 2017, Springer 2018;461-470.
[59] Nair AA, Velagapudi MA, Lang JA, et al. Machine learning approach to predict postoperative opioid requirements in ambulatory surgery patients. PLoS One. 2020;15(7):e0236833.
[60] Tighe P, Laduzenski S, Edwards D, et al. Use of machine learning theory to predict the need for femoral nerve block following ACL repair. Pain Med 2011;12(10):1566-1575.
[61] Liu Y, Cheng L. Ultrasound Images Guided under Deep Learning in the Anesthesia Effect of the Regional Nerve Block on Scapular Fracture Surgery. J Healthc Eng 2021;2021:6231116.
[62] Yang XY, Wang LT, Li GD, et al . Artificial intelligence using deep neural network learning for automatic location of the interscalene brachial plexus in ultrasound images. Eur J Anaesthesiol 2022;39(9):758-765.
[63] Smistad E, Lindseth F. Real-Time Automatic Artery Segmentation, Reconstruction and Registration for Ultrasound-Guided Regional Anaesthesia of the Femoral Nerve. IEEE Trans Med Imaging 2016;35(3):752-761.
[64] Ledowski T. Objective monitoring of nociception: a review of current commercial solutions. Br J Anaesth 2019;123(2):e312-e321.
[65] Coulbault L, Beaussier M, Verstuyft C, et al . Environmental and genetic factors associated with morphine response in the postoperative period. Clin Pharmacol Ther 2006;79(4):316-324.
[66] Yoshida K, Nishizawa D, Ichinomiya T, et al. Prediction formulas for individual opioid analgesic requirements based on genetic polymorphism analyses. PLoS One 2015;10(1):e0116885.
[67] De Cosmo G, Congedo E, Lai C, et al. Preoperative psychologic and demographic predictors of pain perception and tramadol consumption using intravenous patient-controlled analgesia. Clin J Pain 2008;24(5):399-405.
[68] Pan PH, Coghill R, Houle TT, et al. Multifactorial preoperative predictors for postcesarean section pain and analgesic requirement. Anesthesiology 2006;104(3):417-425.
[69] Lou W, Miao C. Shanghai expert consensus on perioperative analgesia management in general surgery patients (2020 edition). Chin J Pract Surg 2021;41(1):31-37.
[70] Rawal N. Current issues in postoperative pain management. Eur J Anaesthesiol 2016;33(3):160-171.
[71] Paul AK, Smith CM, Rahmatullah M, et al. Opioid Analgesia and Opioid-Induced Adverse Effects: A Review. Pharmaceuticals (Basel)

2021;14(11):1091.
[72] Karhade AV, Ogink PT, Thio QCBS, et al. Development of machine learning algorithms for prediction of prolonged opioid prescription after surgery for lumbar disc herniation. Spine J 2019;19(11):1764-1771.
[73] Karhade AV, Schwab JH, Bedair HS. Development of Machine Learning Algorithms for Prediction of Sustained Postoperative Opioid Prescriptions After Total Hip Arthroplasty. J Arthroplasty 2019;34(10):2272-2277.e1.
[74] Karhade AV, Ogink PT, Thio QCBS, et al. Machine learning for prediction of sustained opioid prescription after anterior cervical discectomy and fusion. Spine J 2019;19(6):976-983.
[75] Klemt C, Harvey MJ, Robinson MG, et al. Machine learning algorithms predict extended postoperative opioid use in primary total knee arthroplasty. Knee Surg Sports Traumatol Arthrosc 2022;30(8):2573-2581.
[76] Peng SY, Wu KC, Wang JJ, et al. Predicting postoperative nausea and vomiting with the application of an artificial neural network. Br J Anaesth 2007;98(1):60-65.
[77] Bassanezi BSB, de Oliveira-Filho AG, Jafelice RSM, et al. Postoperative vomiting in pediatric oncologic patients: prediction by a fuzzy logic model. Paediatr Anaesth 2013;23(1):68-73.
[78] Gong CSA, Yu L, Ting CK, et al. Predicting postoperative vomiting for orthopedic patients receiving patient-controlled epidural analgesia with the application of an artificial neural network. Biomed Res Int 2014;2014:786418.
[79] Wu HY, Gong CSA, Lin SP, et al. Predicting postoperative vomiting among orthopedic patients receiving patient-controlled epidural analgesia using SVM and LR. Sci Rep 2016;6:27041.
[80] Porche K, Maciel CB, Lucke-Wold B, et al. Preoperative prediction of postoperative urinary retention in lumbar surgery: a comparison of regression to multilayer neural network. J Neurosurg Spine 2022;36(1):32-41.
[81] Hatib F, Jian Z, Buddi S, et al. Machine-learning Algorithm to Predict Hypotension Based on High-fidelity Arterial Pressure Waveform Analysis. Anesthesiology 2018;129(4):663-674.
[82] Lee S, Lee HC, Chu YS, et al. Deep learning models for the prediction of intraoperative hypotension. Br J Anaesth 2021;126(4):808-817.
[83] Solomon SC, Saxena RC, Neradilek MB, et al. Forecasting a Crisis: Machine-Learning Models Predict Occurrence of Intraoperative Bradycardia Associated With Hypotension. Anesth Analg 2020;130(5):1201-1210.
[84] Chou Y, Zhang A, Gu J, et al. A recognition method for extreme bradycardia by arterial blood pressure signal modeling with curve fitting. Physiol Meas 2020;41(7):074002.
[85] Jungquist CR, Chandola V, Spulecki C, et al. Identifying Patients Experiencing Opioid-Induced Respiratory Depression During Recovery From Anesthesia: The Application of Electronic Monitoring Devices. Worldviews Evid Based Nurs. 2019;16(3):186-194.
[86] Scully RE, Schoenfeld AJ, Jiang W, et al. Defining Optimal Length of Opioid Pain Medication Prescription After Common Surgical Procedures. JAMA Surg 2018;153(1):37-43.
[87] Pierre S, Whelan R. Nausea and vomiting after surgery. Continuing Education in Anaesthesia Critical Care & Pain 2013;13(1):28-32.
[88] Baldini G, Bagry H, Aprikian A, et al. Postoperative urinary retention: anesthetic and perioperative considerations. Anesthesiology 2009;110(5):1139-1157.
[89] Mayberry LJ, Clemmens D, De A. Epidural analgesia side effects, co-interventions, and care of women during childbirth: a systematic review. Am J Obstet Gynecol 2002;186(5 Suppl Nature):S81-S93.
[90] Grangier L, Martinez de Tejada B, Savoldelli GL, et al. Adverse side effects and route of administration of opioids in combined spinal-epidural analgesia for labour: a meta-analysis of randomised trials. Int J Obstet Anesth 2020;41:83-103.
[91] Saugel B, Kouz K, Hoppe P, et al. Predicting hypotension in perioperative and intensive care medicine. Best Pract Res Clin Anaesthesiol 2019;33(2):189-197.
[92] Watterson LM, Morris RW, Westhorpe RN, et al. Crisis management during anaesthesia: bradycardia. Qual Saf Health Care 2005;14(3):e9.
[93] Sultan P, Gutierrez MC, Carvalho B. Neuraxial morphine and respiratory depression: finding the right balance. Drugs 2011;71(14):1807-1819.
[94] Narain K, Swami A, Srivastava A, et al. Evolution and control of artificial superintelligence (ASI): a management perspective. J Adv Manage Res 2019;16(5):698-714.
[95] Weber GM, Mandl KD, Kohane IS. Finding the missing link for big biomedical data. JAMA 2014;311(24):2479-2480.
[96] Mörch CM, Atsu S, Cai W, et al. Artificial Intelligence and Ethics in Dentistry: A Scoping Review. J Dent Res 2021;100(13):1452-1460.
[97] McGreevey JD, Hanson CW, Koppel R. Clinical, Legal, and Ethical Aspects of Artificial Intelligence-Assisted Conversational Agents in Health Care. JAMA 2020;324(6):552-553.
[98] Stokel-Walker C. ChatGPT listed as author on research papers: many scientists disapprove. Nature 2023;613(7945):620-621.

Perioperative Precision Medicine
ISSN: 2957-5443

Zentime

Research Article https://doi.org/10.61189/031494xruanc

The effectiveness of a novel modified retracting arm for transaxillary endoscopic thyroid surgery to minimize complications: A randomized controlled study

Mingling Wang[1*], Gaolei Jia[2*], Kai Wang[3], Haifeng Zhuang[4], Li Ma[2], Ping Wang[4]

[1]Department of Operating Room, Xuzhou Central Hospital, Xuzhou 221009, China. [2]Department of Thyroid, Xuzhou Central Hospital, Xuzhou 221009, China. [3]Department of Anesthesiology, Xuzhou Central Hospital, Xuzhou 221009, China. [4]Department of Nursing, Xuzhou Central Hospital, Xuzhou 221009, China.
[*]The authors contribute equally.

Corresponding authors: Ping Wang and Li Ma.

Acknowledgement: This study was financially supported by a grant from the Xuzhou City Science and Technology Project (KC22156). We thank International Science Editing (http://www.internationalscienceediting.com) for editing this manuscript.

Declaration of conflict of interest: The authors declare no potential conflicts of interest.

Ethics approval and consent to participate: The study protocol was approved by the Institutional Review Committee of Xuzhou Central Hospital (approval no. XZXY-LJ-20191212-069) and conducted in accordance with the ethical principles for medical research involving human subjects described in the Declaration of Helsinki. Prior to inclusion in this study, informed consent was obtained from all participants. The thyroid pull hook used in this study is an approved medical device (Su Xu, 20210063).

Received May 17, 2024; Accepted August 9, 2024; Published September 30, 2024

Highlights

- A novel modified retracting arm for transaxillary endoscopic thyroid surgery was designed.
- The modified hook better exposed and protected the recurrent laryngeal nerve and parathyroid glands.
- The modified retracting arm achieved better visual analog scale and cosmetic scores.

Abstract

Objective: To evaluate the safety of a novel modified retracting arm for endoscopic thyroidectomy by gasless unilateral axillary approach (ETGUA) and its effectiveness in minimizing complications. **Methods:** A novel retracting arm, which comprises a suspension part, a retracting arm, and a suction tube, was designed for ETGUA. The thyroid pull hook used in this study is an approved medical device: Su Xu, 20210063 (https://scjgj.xz.gov.cn/).The cohort of this randomized controlled study included 84 patients with unilateral thyroid cancer who underwent ETGUA at Xuzhou Central Hospital from February 2021 to March 2023. The patients (n = 42/group) were randomly assigned to a control group (conventional endoscopic retracting arm) or an experimental group (modified endoscopic thyroid retracting arm). Clinical indicators, complication rates, neck pain scores, and cosmetic scores were compared between the two groups. **Results:** There were no significant differences in hospitalization time, surgical duration, intraoperative blood loss, postoperative drainage volume, hypoparathyroidism, or postoperative hematoma between the groups. However, there were significant differences in the incidences of transient recurrent laryngeal nerve injury ($x2 = 6.65$, $p = 0.02$) and transient superior laryngeal nerve injury ($x2 = 4.49$, $p = 0.03$), as well as visual analog scale scores on postoperative day (POD) 1 and 7 ($tPOD1 = 12.66$; $tPOD7 = 10.54$; both, $p < 0.001$), and cosmetic scores ($t = -15.27$, $p < 0.05$). **Conclusion:** The modified retracting arm was safe and effective for ETGUA.

Keywords: Endoscopic thyroidectomy by gasless unilateral axillary approach; modified retracting arm; surgical complications

Address correspondence to: Ping Wang, Department of Nursing, Xuzhou Central Hospital, No. 199 Jiefang South Road, Xuzhou 221009, China. Tel: +86-18952172176; Fax: 0086-0516-83956203; E-mail: wangkaistream99@xzhmu.edu.cn. **Li Ma**, Department of Thyroid, Xuzhou Central Hospital, No. 199 Jiefang South Road, Xuzhou 221009, China. Tel: +86-18112023690; E-mail: 675694863@qq.com.

Introduction

Papillary thyroid carcinoma is the most frequent type of thyroid cancer, accounting for 70%–80% of all cases [1]. Thyroid tumors occur more commonly in female and younger patients. Traditionally, thyroid tumors are removed by an open surgery via a neck incision [2]. However, with the development of minimally invasive techniques, endoscopic thyroidectomy by gasless unilateral axillary approach (ETGUA) has become more popular [3]. ETGUA not only makes full use of the folds of the axillary skin to hide the surgical scar, but also avoids the use of CO_2 gas during surgery to prevent complications associated with CO_2 accumulation [4-7]. However, ETGUA requires the use of a dedicated retracting arm for adequate exposure of thyroid tumors. Conventional retracting arms have a rectangle head approximately 6 cm wide, which leads to a large incision. To reduce postoperative scarring, a structurally simple and easy-to-use modified endoscopic retracting arm was designed and achieved satisfactory results for the resection of thyroid tumors in 42 cases.

Methods

Study approval and patient consent

The study protocol was approved by the Institutional Review Committee of Xuzhou Central Hospital (approval no. XZXY-LJ-20191212-069) and conducted in accordance with the ethical principles for medical research involving human subjects described in the Declaration of Helsinki. Prior to inclusion in this study, informed consent was obtained from all participants. The thyroid pull hook used in this study is an approved medical device (Su Xu, 20210063).

Instrument design

The novel modified endoscopic thyroid retracting arm for the transaxillary approach comprises a suspension part (**Figure 1A**, **Notes 1–3**), a retracting arm (**Figure 1A**, **Notes 4–7**, **9**), and a suction tube (**Figure 1A**, **Note 8**). The suspension part has multiple hooks on both sides. The primary hook (**Figure 1A**, **Note 1**) is used to hang the whole retracting arm on the surgical scaffold, and the height can be adjusted as needed. The main retracting arm is U-shaped, consisting of a vertical part (see **Figure 1A**, **Note 7**), a horizontal part (**Figure 1A**, **Note 6**), and a connecting part (**Figure 1A**, **Note 9**). There are three suspension holes (**Figure 1A**, **Note 3**) on the connecting part to fix the secondary hook of the suspension part (**Figure 2B**). The horizontal part, which is parallel to the connecting part, has a dissection part (**Figure 1A**, **Note 4**) at the distal end with racket-shaped hollowed-out areas (**Figure 1A**, **Note 5**). The suction tube is attached to the other side of the retracting arm, with the distal end bent at 45 ° toward the suspension part. Images of a conventional retracting arm are included for comparison in **Figure 1B**.

Study design

The cohort of this randomized controlled study included 84 patients who underwent unilateral thyroid cancer surgery using the ETGUA at Xuzhou Central Hospital (Xuzhou, China) from February 2021 to March 2023. The patients were randomly assigned to an experimental group or a control group using a computer-based block randomization (block size of 20) method with sealed envelopes.

The inclusion criteria were: (1) preoperative ultrasound indicating unilateral thyroid nodules with a diameter of less than 1 cm; (2) fine-needle aspiration biopsy confirming thyroid microcarcinoma; and (3) availability of complete clinical data. The exclusion criteria were: (1) history of neck surgery; (2) tumor diameter > 1 cm; (3) distant lymph node metastasis; and (4) hepatic or renal function disorders. The primary outcome was the number of injuries to the recurrent laryngeal nerve (RLN) and superior laryngeal nerve (SLN), while the secondary outcomes were clinical indicators, among others. The sample size was calculated based on the primary outcome and adjusted according to research experience. Finally, 48 patients were included in each group. For analysis, the statisticians were not blinded to the type of surgery.

Type of surgery in the control and experimental groups

All procedures were performed by the same surgical team. Patients in the control group underwent ETGUA using a conventional retracting arm (KC-106-01; Hangzhou Kangji Medical Instrument Co, Ltd, Hangzhou, China) (**Figure 2A**). The incision was 5–6 cm long, extending beyond the axilla but not exceeding the anterior axillary line. After incising the skin and subcutaneous tissue, the second assistant exposed the surgical field with the retracting arm, and an electrocautery was used to create the working space. Depending on the depth of dissection, a different retracting arm (shallow, deep, or specialized) was used to create the working space, while a specialized retracting arm was used for left or right axillary ETGUA. The remaining steps were identical to those in the experimental

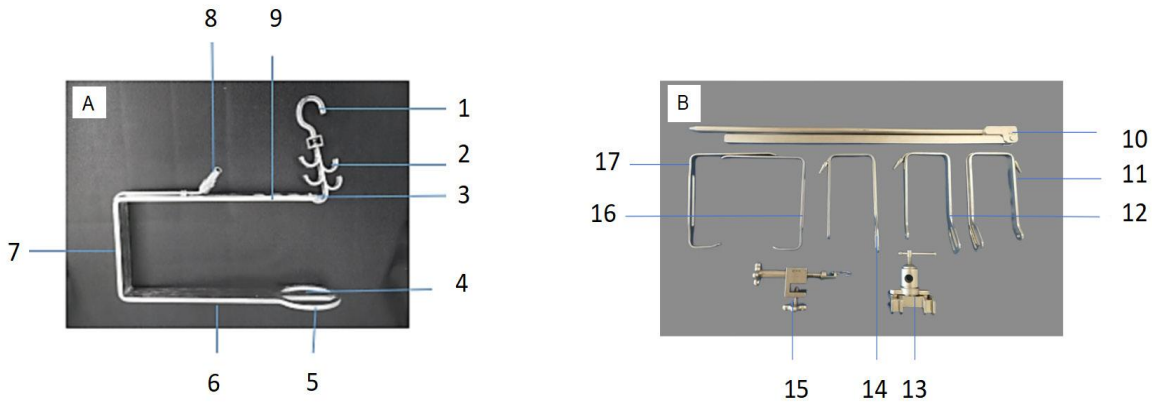

Figure 1. Design of the modified retracting arm for axillary endoscopic thyroid surgery. (A) Modified retracting arm; (B) Conventional retracting arm. Note: 1. Primary suspension hook; 2. Secondary suspension hooks; 3. Suspension hole; 4. Dissection part; 5. Hollowed-out area; 6. Horizontal part; 7. Vertical part; 8. Suction tube; 9. Connecting part; 10. Suspension bar; 11. I type retracting arm (right bending); 12. I type retracting arm (left bending); 13. Suspension device retainer; 14. Type I retracting arm (no bending); 15. Winder of suspension device; 16. Type II retracting arm 1 (simplified version); 17. Type II retracting arm 2 (simplified version).

Figure 2. Two types of retracting arms were used for ETGUA. (A) Conventional retracting arm. (B) Modified retracting arm. (C) Sufficient exposure of the recurrent laryngeal nerve with the modified retracting arm. This figure was derived from Xuzhou Central Hospital. ETGUA: endoscopic thyroidectomy by gasless unilateral axillary approach.

group.

Patients in the experimental group underwent ETGUA using the modified retracting arm. With the patient in the supine position, the collateral arm was abducted to less than 90 °. An incision (-3 cm) was made at the second skin crease of the axilla. After incising the skin and subcutaneous fat tissue, dissection was performed to preserve the fascia of the pectoralis major muscle. The modified retracting arm was inserted and suspended on the anesthesia headframe without additional retracting arms (**Figure 2B**). Tissue dissection was continued, while identifying various anatomical landmarks, including the clavicle, space between the sternocleidomastoid muscle, clavicle, omohyoid muscle, fused part of the deep cervical fascia, and the upper pole plane of the thyroid gland. The dissection extended downwards to the suprasternal notch, exposing the isthmus of the thyroid gland. At the same time, the depth of the retracting arm was adjusted to identify the RLN and parathyroid gland (**Figure 2C**). In the upper pole of the thyroid, the anterior branch of the superior thyroid artery was ligated, while preserving the posterior branch of the superior thyroid artery. Finally, the central compartment lymphatic fat tissue was lifted and cleared. For right-side lesions, the lymph nodes behind the RLN were simultaneously removed. The wound was flushed with distilled water and physiological saline to confirm the absence of injuries to the RLN, parathyroid glands, trachea, and esophagus. A drainage tube was inserted, subcutaneous tissue was sutured, and the skin was closed.

Evaluation criteria

The primary outcome was the incidence of injuries to the RLN and SLN [8, 9]. Injury to the RLN was defined as postoperative hoarseness and/or vocal cord paralysis, while injury to the SLN

Table 1. Comparison of general data between the two groups

Parameters	Experimental group (n=42)	Control group (n=42)	x^2/t	p
Sex, cases (%)			0.21	0.46
Male	15 (32.5)	13 (27.5)		
Female	27 (67.5)	29 (72.5)		
Age, years	45.8±8.2	48.23±11.26	-1.11	0.27
Tumor diameter, mm	7.1±1.6	7.45±2.21	-0.68	0.497
Tumor location, n (%)			0.19	0.65
Left	19 (45.2)	17 (40.5)		
Right	23 (54.8)	25 (59.5)		

Table 2. Comparison of secondary outcomes between the two groups

Parameters	Experimental group (n=42)	Control group (n=42)	t	p
Hospital stays, days	6.4±1.2	6.8±1.5	-1.31	0.19
Surgical duration, min	98.3±16.2	96.2±17.9	0.57	0.57
Intraoperative blood loss, mL	19.2±12.7	16.1±11.3	1.18	0.24
Number of central zone lymph nodes dissected, n	4.0±2.3	5±2.7	1.83	0.07
Postoperative 48-hour drainage, mL	38.6±13.3	41.2±12.4	0.95	0.34

was defined as postoperative external laryngeal branch injury, cricothyroid muscle paralysis, decreased tone, internal laryngeal branch injury, loss of laryngeal mucosa sensation, and/or inability to swallow or choking when eating or drinking. The secondary outcomes included (1) clinical indicators (length of hospital stay, surgical duration, intraoperative blood loss, number of cleared central area lymph nodes, and drainage volume within 48 h after surgery), (2) incidence of complications (decreased parathyroid gland function, and postoperative hematoma), (3) neck pain score using the visual analog scale (VAS) on postoperative day (POD) 1 and 7 using a 10-cm ruler with the scale facing away from the patient for the patient to indicate the degree of pain, where a score of 0 indicated no symptoms and 10 indicated severe symptoms, (4) cosmetic score, which was assessed during a one-month follow-up visit to assess skin appearance, color, and texture on a scale of 0 to 10, where a lower score indicates a more ideal cosmetic effect for the corresponding dimension. The total cosmetic score was calculated to evaluate satisfaction with the surgical incision.

Statistical analysis

Statistical analysis was performed using IBM SPSS Statistics for Windows (version 21.0; IBM Corporation, Armonk, NY, USA). Continuous data were compared using the independent samples t-test and are presented as the mean ± standard deviation, while categorical data were compared using the chi-square test and are presented as numbers and percentages. A probability (p) value < 0.05 was considered statistically significant.

In this study, we hypothesized that the prevalence of injury to the RLN and/or SLN would be lower in the experimental group than in the control group. The primary end point of this study was the prevalence of injury to the RLN and/or SLN. In the preliminary experiment, the prevalence of injury to the RLN and SLN in the experimental and control groups was 0.0% and 12.3% vs. 1.0% and 11.3%, respectively. At an α value of 0.05 and 1-β value of 0.80, the sample size was calculated to be 30 participants using the following formula:

$$n_1 = \frac{[u_\alpha \sqrt{p(1-p)(1+c)/c} + u_\beta \sqrt{p_1(1-p_1)+p_2(1-p_2)/c}]^2}{(p_1-p_2)^2}$$

Results

Comparison of general data

As shown in **Table 1**, there were no statistically significant differences in sex, age, tumor size, or location between the two groups (p > 0.05).

Comparison of clinical indicators

As shown in **Table 2**, there were no significant

Table 3. Incidences of SLN injury, RLN injury, postoperative hematoma, and parathyroid function decline between the two groups

Parameters	Experimental group (n=42)	Control group (n=42)	x^2	p
Superior laryngeal nerve injury, cases (%)	1 (2.4)	7 (16.7)	4.49	0.03
Recurrent laryngeal nerve injury, cases (%)	0 (0.0)	6 (14.3)	6.65	0.03
Postoperative hematoma, cases (%)	0 (0.0)	1 (2.4)	1.10	0.99
Parathyroid function decline, cases (%)	0 (0.0)	0 (0.0)	---	---

Table 4. Comparison of the VAS score on POD 1 and 7 and cosmetic score between the two groups

Parameters	Experimental Group (n=40)	Control Group (n=40)	t	p
VAS score on POD 1	3.3±1.7	7.3±1.4	12.66	<0.001
VAS score on POD 7	1.7±0.9	4.2±1.2	10.54	<0.001
Cosmetic score	2.6±1.8	8.1±1.4	-15.27	<0.001

Note: VAS: visual analog scale; POD: postoperative day.

difference in hospitalization stay, surgical duration, intraoperative blood, number of dissected central zone lymph nodes, or postoperative 48-hour drainage between the two groups ($p > 0.05$).

Comparison of postoperative complications

As shown in **Table 3**, there were significant differences in the incidences of SLN injury ($x^2 = 4.49$, $p = 0.03$) and RLN injury ($x^2 = 6.65$, $p = 0.02$) between the groups, but not in postoperative hematoma and hypoparathyroidism ($p > 0.05$). All instances of nerve injury in this study were transient and fully recovered within the 6-month follow-up period.

Comparison of postoperative VAS and cosmetic scores

As shown in **Table 4**, there were significant differences in the cosmetic score, and the VAS score on POD 1 and 7 ($t_{POD1} = 12.66$; $t_{POD7} = 10.54$; both, $p < 0.05$).

Discussion

Following the widespread use of ETGUA in clinical practice, various approaches have been developed, such as transoral, areolar, axillary, and various combinations. The advantages and disadvantages of each of these surgical approaches remain controversial. ETGUA is reported to achieve good results in terms of both surgical safety and cosmetic outcomes [10-13]. Regardless of the approach, an adequate surgical space must be established [14-17]. The traditional cavity-building model relies on the use of CO_2 at a certain pressure to maintain the surgical space. However, this approach is limited by the risks of intraoperative hypercapnia, obstruction of blood flow from the brain to the heart, unstable maintenance of the surgical space, interference of smoke, and waste of medical resources [18]. In contrast, gasless ETGUA has many advantages, including stability of the surgical space, clear visualization, flexible adjustment, less environmental pollution in the operating room, and minimal waste of resources [19]. However, gasless procedures often require specific surgical instruments, which can easily lead to medical waste and hinder widespread applications. Consequently, cavity-building instruments that are compatible with multiple gasless procedures are urgently needed to meet clinical requirements.

ETGUA is a side neck approach [20]. As compared to open surgery, ETGUA involves an axillary incision and uses the anatomical natural space of the neck to build the cavity, which is convenient, feasible, safe, and can ensure good cosmetic outcomes. Exposure of the RLN and central regional lymph nodes during ETGUA can be problematic [21, 22]. Hence, safe and effective access to the thyroid is key to ETGUA with the distal neck approach [23, 24]. In this study, a novel retracting arm, consisting of a suspension device, a main hook, and a suction tube, was developed for ETGUA. The stripping part of the pull hook is a racket type. Gently moving the pull hook can achieve surgical exposure and improved access to the tissue gap to avoid secondary damage. The hollow design of the stripping part can reduce pressure on the tissue and protect the neck muscles. The suction tube facing the joint bend allows for cleaning and dredging of the blockage. The suspension device with adjustable height can help reduce the incidence of nerve injury and postoperative pain, while improving cosmetic outcomes.

The inflatable posterior axillary approach for ETGUA with a pull hook can be complicated and involve the entire surgical space. At present, the pull hook used in thyroid surgery requires the use of a special frame, and different types of pull hooks must be adjusted during different steps of the procedure. The square head design of the hook with the modified retracting arm can adequately expose the surgical space. The modified retracting arm, including the suspension device, main hook, and suction tube, is easy to assemble and operate, without requiring exchange midway through the procedure, which can shorten the surgical duration and reduce the workload of the operating room nurse.

With the rear approach, the lens hook must be fully exposed to open the central area and the posterior surface of the vertebral fascia in order to transit to the tracheal esophageal ditch until the anterior tracheal gap, and access the central lymphoadipose tissue from behind [25]. At this point, the thyroid and central area lymph nodes remain on the ceiling of the cavity space, fully exposing the posterior boundary of the lymph nodes in the central area, while reducing the omission of cleaning and minimalizing lymph node dissection required with open surgery [26].

The modified retracting arm reduced the incidence of nerve injury. Recent studies have primarily focused on the ability to expose the surgical area, shorten the surgical duration, and reduce blood loss [27, 28]. As the most common complication of ETGUA, nerve injury was the primary outcome in the present study [29]. The rate of nerve injury was relatively high in the control group, which may be attributed to the type of retracting arm and the surgery team being less aware of the importance of protecting the nerves. The conventional retracting arm used in the control group had a wide rectangle dissection part, which can easily stretch the nerves. Since nerve injury is usually transient, the surgical team may be less concerned about protecting the nerve from injury. The modified retracting arm was used in the experimental group to create the surgical space and reduce the incidence of nerve injury.

The novel design of the mirror hook allows creation of a surgical space, while avoiding muscle damage and local trauma. The lateral approach with the thyroid suspension hook allows for continuous negative pressure, maintenance of field clarity to protect the parathyroid gland and SLN, and minimal exposure of the RLN to avoid injury. In addition, the dissection part of modified retracting arm is designed to be hollow to minimize damage to local tissues and reduce nerve stimulation. In this study, ETGUA was conducted with the lateral approach, and the thyroid gland was suspended to create a natural, well-exposed working space. The suction tube of the modified retracting arm helped to maintain clarity of the surgical field. These factors allowed total exposure of the nerves and reduced the risk of nerve injury.

The modified retracting arm improved cosmetic outcomes. The conventional laparoscopic retracting arm has a head width of 6 cm, which results in a longer scar in the fold from the armpit to the anterior axillary line. Although the surgical incision is relatively concealed and does not exceed the anterior axillary line, the scar is noticeable. Comparatively, the modified retracting arm has a racket-shaped design at the front end with a head width of 4 cm. Due to the elasticity and laxity of the armpit skin, the incision is limited to only 3 cm and remains concealed within the armpit, resulting a greater satisfaction with postoperative cosmetic outcomes.

The modified retracting arm has a simple design, is easy to transport, and can be reused after sterilization. The height can be adjusted as needed during the procedure to provide better exposure of the limited space for laparoscopic surgery. In addition, reducing the flap detachment time facilitates tumor dissection, especially for large nodules close to the capsule. The retracting arm also helps to separate the tissues and better protect the RLN to reduce the risks of postoperative complications and shorten the surgical duration. Additionally, the modified retracting arm leads to small concealed surgical incisions and satisfactory cosmetic outcomes.

Conclusion

The safety and efficacy of the modified laparoscopic retracting arm were confirmed for ETGUA, resulting in satisfactory cosmetic outcomes. However, the present study was limited by the relatively small sample size and short follow-up period.

Author Contributions: Mingling Wang contributed to the conception of the study; Mingling Wang and Gaolei Jia performed the experiment; Kai Wang and Haifeng Zhuang contributed significantly to analysis and manuscript preparation; Mingling Wang performed the data analyses and wrote the manuscript; Li Ma and Ping Wang helped perform the analysis with constructive discussions.

References

[1] Aryanpour Z, Asban A, Boyd C, et al. A single institution experience with papillary thyroid cancer: Are outcomes better at comprehensive cancer centers? Am J Surg 2021;222(4):802-805.

[2] Kurumety SK, Helenowski IB, Goswami S, et al. Post-thyroidectomy neck appearance and impact on quality of life in thyroid cancer survivors. Surgery 2019;165(6):1217-1221.

[3] Tae K, Ji YB, Song CM, et al. Robotic and Endoscopic Thyroid Surgery: Evolution and Advances. Clin Exp Otorhinolaryngol 2019;12(1):1-11.

[4] Liu Z, Li Y, Wang Y, et al. Comparison of the transoral endoscopic thyroidectomy vestibular approach and open thyroidectomy: A propensity score-matched analysis of surgical outcomes and safety in the treatment of papillary thyroid carcinoma. Surgery 2021;170(6):1680-1686.

[5] Luo JH, Xiang C, Wang P, et al. The Learning Curve for Transoral Endoscopic Thyroid Surgery: A Single Surgeon's 204 Case Experience. J Laparoendosc Adv Surg Tech A 2020;30(2):163-169.

[6] Qu R, Li J, Yang J, et al. Treatment of differentiated thyroid cancer: can endoscopic thyroidectomy via a chest-breast approach achieve similar therapeutic effects as open surgery? Surg Endosc 2018; 32: 4749-4756.

[7] Lewis CM, Chung WY, Holsinger FC. Feasibility and surgical approach of transaxillary robotic thyroidectomy without CO(2) insufflation. Head Neck 2010;32(1):121-126.

[8] Karpathiotakis M, D'Orazi V, Ortensi A, et al. Intraoperative Neuromonitoring and Optical Magnification in the Prevention of Recurrent Laryngeal Nerve Injuries during Total Thyroidectomy. Medicina (Kaunas) 2022;58(11):1560.

[9] Iwata AJ, Liddy W, Barczyński M, et al. Superior Laryngeal Nerve Signal Attenuation Influences Voice Outcomes in Thyroid Surgery. Laryngoscope 2021;131(6):1436-1442.

[10] Meng K, Chen X, Shen W, et al. Gasless transaxillary endoscopic surgery for papillary thyroid carcinoma in a patient with thyroid hemiagenesis: An appropriate choice or not? Asian J Surg 2023;46(10):4545-4546.

[11] Jasaitis K, Skimelyte M, Maleckas A, et al. Transaxillary gasless endoscopic hemithyroidectomy versus conventional open hemithyroidectomy: early single-centre experience. Updates Surg 2022;74(3):917-925.

[12] Chen XL, Li C, Zhou YQ, et al. [A comparative study for the efficacies of transaxillary non-inflatable endoscopic surgery versus traditional surgery for papillary thyroid carcinoma]. Zhonghua Er Bi Yan Hou Tou Jing Wai Ke Za Zhi 2023;58(4):351-357.

[13] Lee H, Lee J, Sung K Y. Comparative study comparing endoscopic thyroidectomy using the axillary approach and open thyroidectomy for papillary thyroid microcarcinoma. World J Surg Oncol 2012;10:269.

[14] Cong R, Li X, Ouyang H, et al. Gasless, endoscopic trans-axillary thyroid surgery: our series of the first 51 human cases. World J Surg Oncol 2022;20(1):9.

[15] Hu B, Chen Y, Jin Y, et al. Clinical analysis of a new multifunctional instrument set for gasless endoscopic thyroidectomy with two different approaches. Surg Endosc 2024;38(4):1958-1968.

[16] Dhoomun DK, Cai H, Li N, et al. Comparison of health-related quality of life and cosmetic outcome between traditional gasless trans-axillary endoscopic thyroidectomy and modified gasless trans-axillary endoscopic thyroidectomy for patients with papillary thyroid microcarcinoma. Cancer Med 2023;12(15):16604-16614.

[17] Xu T, Qin X, Zhang Y, et al. A prospective study comparing the gasless endoscopic thyroidectomy trans-axillary approach to conventional open thyroidectomy: health and quality of life outcomes. Surg Endosc 2024;38(4):1995-2009.

[18] Kang YJ, Cho JH, Stybayeva G, et al. Safety and Efficacy of Transoral Robotic Thyroidectomy for Thyroid Tumor: A Systematic Review and Meta-Analysis. Cancers (Basel) 2022;14(17):4230.

[19] Bhandarwar A, Wagh A, Tandur A, et al. Endoscopic Thyroidectomy: A 6-Year Experience from a Tertiary Care Teaching Hospital in Western India. J Laparoendosc Adv Surg Tech A 2023;33(8):728-737.

[20] Li SL, Du P, Lv T, et al. Quantitative comparison of three thyroidectomy approaches in neck muscles, voice, and swallowing functions. Asian J Surg 2024;47(4):1734-1739.

[21] Liu YC, Shen CL, Fu ZY, et al. Effectiveness of the recurrent laryngeal nerve monitoring during endoscopic thyroid surgery: systematic review and meta-analysis. Int J Surg 2023;109(7):2070-2081.

[22] Biswas SS, Hossain MM, Mahbub S, et al. Routine Exposure Versus Non-Exposure of Recurrent Laryngeal Nerve during Thyroid Surgery: Our Experience of 300 Cases. Mymensingh Med J 2022;31(1):154-160.

[23] Torky RA, Abdel-Tawab M, Hussein MM. Short term Outcomes of Routine Exposure Versus non Exposure of the Recurrent Laryngeal Nerve During Thyroidectomy for Benign Thyroid Diseases. Indian J Otolaryngol Head

Neck Surg 2023;75(3):1974-1980.
[24] Pandey AK, Varma A, Bansal C, et al. An Exposition on Surgical Experiences in Identification, Exposure, and Injuries of Recurrent Laryngeal Nerve (RLN) During Thyroid Operations: Gleanings, Narrative, and the Reflections. Indian J Otolaryngol Head Neck Surg 2023;75(3):1363-1369.
[25] Min Y, Huang Y, Wei M, et al. Preoperatively Predicting the Central Lymph Node Metastasis for Papillary Thyroid Cancer Patients With Hashimoto's Thyroiditis. Front Endocrinol (Lausanne) 2021;12:713475.
[26] Sun P, Zhan J, Chong TH, et al. Endoscopic central lymph node dissection of thyroid cancer via chest-breast approach: results, indications, and strategies. Surg Endosc 2022;36(6):4239-4247.
[27] Darbandi A, Pujari A, Lin C. Evaluation of a novel C-Arm draping technique to minimize surgical field contamination and surgery time. ANZ J Surg 2021;91(7-8):1455-1461.
[28] Pisapia JM, Nayak NR, Salinas RD, et al. Navigated odontoid screw placement using the O-arm: technical note and case series. J Neurosurg Spine 2017;26(1):10-18.
[29] Dionigi G, Bacuzzi A, Boni L, et al. Influence of new technologies on thyroid surgery: state of the art. Expert Rev Med Devices 2005;2(5):547-557.